WING IN GROUND EFFECT VEHICLE: MODELLING AND CONTROL

A THESIS SUBMITTED TO
THE GRADUATE SCHOOL OF NATURAL AND APPLIED SCIENCES
OF
MIDDLE EAST TECHNICAL UNIVERSITY

BY

ABDUL GHAFOOR

IN PARTIAL FULFILLMENT OF THE REQUIREMENTS
FOR
THE DEGREE OF MASTER OF SCIENCE
IN
ELECTRICAL AND ELECTRONICS ENGINEERING

SEPTEMBER 2015

Approval of the thesis:

WING IN GROUND EFFECT VEHICLE: MODELLING AND CONTROL

submitted by **ABDUL GHAFOOR** in partial fulfillment of the requirements for the degree of **Master of Science in Electrical and Electronics Engineering Department, Middle East Technical University** by,

Prof. Dr. Gülbin Dural Ünver _____
Dean, Graduate School of **Natural and Applied Sciences**

Prof. Dr. Gönül Turhan Sayan _____
Head of Department, **Electrical and Electronics Engineering**

Prof. Dr. Kemal Leblebicioğlu _____
Supervisor, **Electrical and Electronics Engineering Dept., METU**

Examining Committee Members:

Prof. Dr. Mübeccel Demirekler _____
Electrical and Electronics Engineering Dept., METU

Prof. Dr. Kemal Leblebicioğlu _____
Electrical and Electronics Engineering Dept., METU

Prof. Dr. Ömer Morgül _____
Electrical Engineering Dept., BILKENT University

Prof. Dr. Çağatay Candan _____
Electrical and Electronics Engineering Dept., METU

Prof. Dr. A. Bülent Özgüler _____
Electrical Engineering Dept., BILKENT University

Date: _____

I hereby declare that all information in this document has been obtained and presented in accordance with academic rules and ethical conduct. I also declare that, as required by these rules and conduct, I have fully cited and referenced all material and results that are not original to this work.

Name, Last name: Abdul Ghafoor

Signature:

ABSTRACT

WING IN GROUND EFFECT VEHICLE: MODELLING AND CONTROL

Ghafoor, Abdul
MS, Department of Electrical and Electronics Engineering
Supervisor: Prof. Dr. Kemal Leblebicioğlu
September 2015, 167 pages

The “Ground Effect” is the increase in the force which is acting on a lifting surface like wing, when it come to the close proximity of the ground. Ground effect vehicles (GEV) are the kind of amphibious vehicles that fly in close proximity of ground, making use of the aerodynamic interaction between the wings of the ground effect vehicle and ground (Sea or Earth surface) and it increases their efficiency 3-4 times more. There are many other advantages of the vehicles employing GE; they do not require a take-off/landing place, they can land anywhere in case of malfunctioning, they can be constructed in a variety of sizes for both military and civil purposes.

This study includes a detailed study of Ground Effect (GE), its implementation using Wing in Ground (WIG) effect vehicle or Ground Effect Vehicle (GEV). Next, this thesis report includes its mathematical model explaining GE, motion, translational and rotational dynamics and kinematics, aerodynamics, gravity, atmospheric, mass inertia, forces and moments. Nonlinear 6DOF dynamical model is implemented in Matlab/Simulink and its response is investigated in open loop simulations. Next step is to develop and implement its autopilot. Autopilot consists of a controller and a guidance unit, to get a vehicle to a destination by following a desired trajectory. For

the controller, PID controllers from classical feedback theory are used for controlling pitch, yaw, roll, altitude and speed. Their performances are compared based on simulation studies. Final part is the guidance, which is done for the yaw plane (Heading) using Line Of Sight (LOS) method, through Way Points (WPs). Major challenges during this work are the lack of available technical data and the need for multidisciplinary skills like aerodynamics, mathematical modeling and finding suitable controller design techniques.

Keywords: Autopilot, WIG, GEVs, PID Controller, Guidance

ÖZ

YER ETKİSİNİ KULLANAN ARAÇLAR: MODELLEME VE KONTROL

Ghafoor, Abdul
Yüksek Lisans, Elektrik ve Electronik Mühendisliği
Tez Yöneticisi: Prof. Dr. Kemal Leblebicioğlu
Eylül 2015, 167 sayfa

Yer etkisini kullanan araçlar (WIG's), ne deniz ne de hava araçları olarak sınıflandırılabilir. Onlar aslında hava araçlarına çok benzerler: ancak yer etkisini kullanabilmek için deniz seviyesine çok yakın bir yükseklikte uçmaları gerekir. Temel olarak, yer etkisi, havanın araçla yer (deniz) arasında sıkıştırılması sonucu ortaya çıkan doğrusal olmayan bir etkidir. Yer etkisinin en önemli sonucu, bu etkiyi kullanan araçların faydalı yükleri, kullanmayanlara göre 3-4 kat daha fazla olabilir. Yer etkisini kullanan deniz araçlarının diğer avantajları arasında, bir iniş-kalkış pistine ihtiyaç duymamalarını ve bir makine arızası olduğunda yolcuların maruz kaldığı tehlikenin çok az olduğunu söyleyebiliriz. Ayrıca, WIG'ler çok farklı boyutlarda ve şekillerde inşa edilebilirler ve hem askeri hem de sivil alanlarda kullanılabilirler.

Bu tezin ilk amacı, yer etkisini kullanan uçakların matematiksel modellerini elde etmektir. Sonraki aşamada ise, otopilot adı verilen kontrolcüler tasarlanacaktır. Bu otopilotlar öncelikle PID tipi kontrolcülerden tasarlanacaklardır. Daha sonra, bu otopilotlar kayan kipli kontrolcülerle tasarlanan otopilotlarla karşılaştırılacaklardır. Aracın istenilen bir rota üzerindeki hareketini sağlayacak güdüm yöntemi olarak ara-

nokta güdüm metodu tercih edilmiştir. Tezin son kısmında, WIG'lerin performansını ortaya çıkarmak için, farklı deniz koşullarında ve farklı otopilotlar altında benzetim çalışmaları yapılacaktır. Bu çalışmada karşılaşılan zorluklar arasında, matematiksel modelleme, yer etkisinin doğru bir şekilde ifade edilmesi gibi, farklı disiplinlerin bir araya gelmesi sayesinde aşılabilecek sorunlar vardır.

Anahtar Kelimeler: Otopilot, WIG, GEVs, PID Kontrolcüsü, Güdüm

Dedicated to my parents, family and friends…

ACKNOWLEDGEMENTS

Foremost, I would like to express my sincere gratitude to my supervisor Prof. Dr. Kemal Leblebicioğlu for his guidance, advice, criticism, encouragements and insight throughout the research.

Besides my advisor, I would like to thank the rest of my thesis committee: Prof. Dr. Mübeccel Demirekler, Prof. Dr. Ömer Morgül, Prof. Dr. A. Bülent Özgüler and Prof. Dr. Çağatay Candan for their presence and insightful guidance.

I could not have finished this thesis without the support from my nearest and dearest. I am more than grateful to my family and I would especially like to thank my parents. Finally, I am very grateful to other instructors of the department for their continuous support and encouragement, my friends, Raha Shabani and other lab mates, dorm mates who have been there all the time during my study.

TABLE OF CONTENTS

LIST OF TABLES

TABLES

LIST OF FIGURES

FIGURES

LIST OF SYMBOLS

c	Chord Length	T	Thrust
h	Height	FC	Fuel Consumption
C_L	Coefficient of Lift	I	Inertia
C_D	Coefficient of Drag	J	Advanced Ratio
C_{DI}	Coefficient of Induced Drag	m	Mass
C_m	Pitching Moment Coefficient	n	Revolution per Second
α	Angle of Attack	p	Body Roll Rate
x_{cp}	Center of Pressure	q	Body Pitch Rate
b	Wing Span	r	Body Yaw Rate
S	Projected Wing Area on Ground	u	Body Velocity in X-Direction
AR	Aspect Ratio	v	Body Velocity in Y-Direction
u*	Dimensionless Velocity Vector	w	Body Velocity in Z-direction
p*	Dimensionless Pressure	X	A/C Position in North Direction
T*	Dimensionless Temperature	Y	A/C Position in East Direction

∇	Divergence Operator	H	A/C Altitude
Re	Reynolds Number	I_x	Moment of Inertia along X_B-axis, [kg m2]
U	Reference Velocity	I_y	Moment of Inertia along Y,-Axis, [kg m2]
L	Reference Length	I_z	Moment of Inertia along Z,-Axis, [kg m2]
V	Kinematics Viscosity	I_{xy}	Moment of Inertia along XY-Axis, [kg m2]
Tol	Tolerance	I_{xz}	Moment of Inertia along XZ-Axis, [kg m2]
$x_{a/c}$	Aerodynamic Center	I_{yz}	Moment of Inertia along YZ-Axis, [kg m2]
$m_{C\alpha}$	Slope of Cm vs. α Curve	m	Mass
$L_{C\alpha}$	Slope of C_L vs. α Curve	β	Side Slip Angle
m_{C0}	Intercept of Cm vs. α Curve	ϕ	Roll Angle
V_H	Tail Volume Ratio	θ	Pitch Angle
C_{mwf}	Coefficient of Moment for Wing-Fuselage Combination	ψ	Yaw Angle
C_{mt}	Coefficient of Moment for Propulsion	PID	Proportional-Integral-Derivative
C_{mwft}	Coefficient of Moment for Wing-Fuselage-Prop Combination	GEV	Ground Effect Vehicle
δ	Deflection	SISO	Single Input Single Output

ω	Angular Velocity	MIMO	Multi Input Multi Output
s	Second	WIG	Wing In Ground
m	Meter		

CHAPTER 1

OVERVIEW

This overview is about the introduction to the overall study and its purpose. It consist of a basic introduction to Ground Effect Vehicle (GEV), problem statement, target of the study, what has been done so far, challenges of the projects and literature reviews that how this target was accomplished, step by step and its relation to previous existing literature. At the end, overall scope of the thesis about its organization is given.

1.1 Problem Statement

In this thesis, the problem of modeling and autopilot design for Wing in Ground (WIG) effect vehicles has been considered. Problem consists of four major parts; first is about mechanical design and investigation of different structures, determination of different aerodynamics and geometrics configuration, mass and inertia parameters, second is about 6DOF dynamical model (mathematical) including ground effect, third is about controlling different actions, such as pitch, roll, yaw, speed and altitude motions, and fourth and final part is about guidance, to make it autonomous. These last two steps, controller and guidance, are combined contributing as the autopilot design. For designing an autopilot, which includes controller and guidance, there are some prerequisites, especially for a vehicle like WIG. One of the challenges is to find some suitable airfoils, like for wings, tails, fuselage, and to determine suitable structures for geometry and mechanical design, especially for this special kind of vehicle, in order to get the maximum benefit from the Ground Effect (GE). Another challenge is to find mathematical formulae for the Ground Effect, since not much technical data is available for WIGs.

After discussing different parts and parameters for the vehicle, its implementation in Computer Aided Designing (CAD) software like Solidworks is done. Additionally, using DATCOM, aerodynamics coefficients and stability derivatives are obtained. Mathematical model which includes 6DOF dynamical model of the system considering all types of motions, and all the forces and moments acting on the vehicle is derived using Newton-Euler approach.

Next and final phase is the autopilot design part, which includes pitch, yaw, roll, height and speed controllers and a guidance method to follow a desired trajectory, for reaching destination, autonomously.

1.2 Work Done

All major objectives of the study have been achieved using classical/typical approaches. First, different specifications, structures and parameters were determined on the basis of different studies especially from aerospace related and mechanical systems. Then, those configurations were implemented in Solidworks and different inertial and mass parameters were determined on the basis of this CAD design (since physical/real vehicle has not been implemented yet). Next, stability derivatives and aero-dynamical coefficients were determined using DATCOM. After this, its dynamical nonlinear mathematical model (including all motions, forces, moments, Ground Effect, propulsion, aerodynamics, gravity, etc.) was determined including ground effect formulas. It was implemented in Matlab/Simulink and open loop response and different responses were found and analyzed on the basis of different disturbances and inputs. Some assumptions were made, which are reasonable like body being rigid, and neglecting the curvature and rotation of Earth. After that, autopilot was implemented in Matlab/Simulink. For controller design, simple classical feedback systems approach is used. PID controllers with different inner and outer loop cascaded controllers were designed based on the requirements and dependence of the system states and variables. These Single Input and Single Output (SISO) controllers were implemented successfully. In some cases such as for speed, heading, altitude and control, even MIMO controllers were also developed. Finally, guidance in the yaw plane (heading) was implemented successfully, to follow a desired trajectory.

Guidance is based on Line of Sight (LOS) approach through predefined Way Points (WPs). This study finished with the completion of the guidance.

1.3 Challenges

There were many challenges for this study; some major ones were:

- Lack of available technical data for ground effect; although this topic is not new, still not much of the literature and information is available related to GE. There is a vast potential for research and development in this area of science.
- Need for the multidisciplinary skills like aerodynamics engineering, applied mathematics and control engineering.

1.4 Literature Review

WIG vehicles are special kind of vehicles/crafts, in its nature, function and features. They can fulfill the gap between aircrafts and marine ships. They are unique but very complicated. Proper study of ground effect started at the start of the twentieth century. But yet it is not developed much, there is need to do a lot. It has research potential from different points of view like design, control, stability and guidance.

Different types and classes of GEVs are discussed in [1] and [4]. Since WIG is an amphibious vehicle and contains both properties of aircrafts and marine vehicles, so its classification was initially delayed. These legislation and classification issues were also one of the reasons behind delay in its development. [4] describes division by "International Maritime Organization". GEVs had proved their worth before during WW-II, but with time, there is a growing demand for WIGs, especially for the transportation between coastal cities. WIGs are known for their efficiency, payload capability and fuel consumption [5]. In [12] and [13] their usefulness and how they can serve humanity in different ways have been explained.

Research on WIG has started, basically for the purpose of designing seaplanes and crafts. Wieselsberger 1921 [2] was the first person to study the ground effect properly, mainly focused on Span Dominated Ground Effect (SDGE) and proposed some methods to analyze its effect and also derived a factor (influential coefficient) for GE.

Wieselsberger treated the problem with an extension of the Lanchester-Prandtl theory [3]. After this first derivation, it opened the door for this new field. Russia (former USSR) and the USA are among the first countries to develop experimental aircraft during the early 1960's that make use of GE. Between 60's and 90's extensive research was carried out, lot of experimental and theoretical work and formulations were proposed, different hydrofoil and new strategies [6], [12] and [13] were suggested. Universal Hovercraft (UH) developed a flying hovercraft, a prototype of which first took flight in 1996 [7]. Since 1999, the company has offered planes, parts, kits, and manufactured GEV hovercraft called the Hovering [7]. The studies [8], [9] and [10] are about development of WIGs in Singapore and some main GEVs have been made. Similarly, [11] tells about Koreans advancement in this field. The reference [6] tells about new WIGs with modern technology. Many other countries' projects in this field are also mentioned in [6] and [12].

Modification in mechanical design, for getting benefit from GE, was started after 1960.The idea of this craft (here in this study) is based on current WIG projects taking place in Germany especially with respect to mechanical design. Studies [14] and [15] describe how its fuselage, wings and vertical and horizontal stabilizers can be designed to tackle with both aerodynamics and hydrodynamics. [16], [17] and [21] are about different airfoils from NACA which are used here, keeping in mind special aerodynamics requirements. Although WIGs are getting benefit from GE, but their abnormal pressure distribution can cause instabilities, so [19] and [20] are about the computation and determination of horizontal and vertical stabilizer on the basis of volumetric method, to tackle with this problem.

On ground effect formulations, Savistky carried out an extensive research and experimental program, his goal was to work on prismatic planning of the hull and to find some empirical formulas. K.V. Rozhdestvensky [22] worked on extreme GE and devised different computations and numerical research from different aspects of GE. As is mentioned before, initially, Wieselsberger [1] presented a GE parameter, for SDGE; it was an extension of Prandtl theory [29]. After that Le Sueur [28] made some modification in the Wieselsberger influential coefficient. After a while Tani Itirro [25] and [26] made some new developments; their focus was on general GE exploration in

both SD and CD cases, especially for pitch stability and tail moment. In 1949 Wetmore [27] brought about some experimental work on GE from a test of a glider and verified the existing formulations. Then, between 60's and 90's, extensive research was carried out, lot of experimental and theoretical work and formulations were proposed and suggested different hydrofoil and new strategies [6], [12] and [13]. Zarnick [32] and [33] tried to find some nonlinear Differential-Integral equations (DIE) for aerodynamics in the presence of GE. NTNU, National University of Singapore and Cranfield University are specially focusing in this area for the last few years.

About modeling, a simple idea which is adopted here, is to use general aircraft model and embed GE formulae into it. In this way GE craft can be analyzed. For any aircraft its dynamical, 6DOF model in terms of external forces and moment has been extensively searched and explored, references [34]-[37] provides evidence. They present a comprehensive model and generic versions which can be molded for different aircrafts. Their linearization, coupling, decoupling are also available in these references.

Control theory has been revolutionized, modern techniques have opened new horizons for research. In this study, work on WIG is carried out by using classical techniques due to obvious reasons (simplicity and to avoid complexities, because this model is amongst one of the initial model, a trial to get a unified one), modern techniques will be considered as future work. Control theory started with simple feedback theory and then developed very fast. [46] and [47] present simple and general feedback theory about control systems and focus on proportional, integral and derivative controllers commonly known as PID controllers. [51] and [52] cover in details of PID controllers and some new methods. For PIDs, the major thing is tuning of their gains, determining suitable gains for controller parameters. Different methodologies have been developed for this purpose. Ziegler-Nichols initially devised rules for tuning PID controllers. The reference [53] describes Ziegler-Nichols tuning rule for PID controllers. Then, [54] showed structure and further tuning rules for internal Model Control (IMC)-PID tuning. In time, many other techniques were developed and [53] provides the most comprehensive tool, where tuning is done after analyzing the system dynamics and structure of the control and other available parameters. IMC and Direct Synthesis

proved to be better in performance. [55] used Iterative Feedback Tuning (IFT) method, also known as non-parametric method based on frequency response. In [56] different techniques are evaluated on the basis of performance, robustness and sensitivity. It also provides range of stability of related controller, references, specifications and features. Now, even auto-tuning techniques are available; for example, [57] has become popular and shown their worth.

Guidance is an important stage in designing unmanned vehicles. Unmanned vehicles (UVs) become famous after WW-II. Initially, for defense and now for huge civil applications to serve humans. [64] provides some basic concepts which can be helpful for guidance designing. Massimo Caccia [61] developed some high speed UVs, intelligent and autonomous marines. Well known and authentic book for control and guidance with main focus on marines, is Fossens [60] and [62]. Fossens uses three blocks (Guidance, Control and Navigation (GNC)) for control of motion of vehicles. His method for guidance on the basis of LOS through way points is commonly used and validated for marine vehicles.

Although WIGs or GEVs are not new, still a unified model is not available. Most of the existing work is based on big or middle level vehicles like Ekranoplans, and is in different modular forms. There is a need to explore more in order to use GE in a better way, specifically for small scale GEVs.

To fill this gap, it has been tried here to devise a unified model for small scale GEVs. The simple idea used is to find GE relations for SDGE and CDGE and embed them into an aircraft model. Here it was tried to take all useful information from different sources and tried to unify them specifically for GE. For control and guidance, classical techniques are used instead of modern theories, as the first step. After developing hardware and experimentation on the physical system, they will be modified by applying new robust techniques.

1.5 Thesis Outline (Organization)

This thesis consists of mechanical design, modeling, parameter derivation, controller and guidance design (autopilot) of the WIG effect vehicles or GEVs. In a short summary:

- Chapter 2 is about introduction to GEV, its history, current and previous projects at international level.
- Chapter 3 is about choosing and defining different features of the vehicle, like determination of airfoils, configuration for body structures, geometric and mass inertia parameters.
- Chapter 4 is about ground effect theory, what ground effect is, its types and how it affects the aerodynamics, and cause to increase the lift, decrease drag and results in improved and more beneficial aerodynamics.
- Chapter 5 is about 6DOF nonlinear mathematical modeling of the vehicle, which includes motion, translational and rotational dynamics, kinematics and about all type of external forces and moments acting on the vehicle.
- Chapter 6 is about implementation of a non-linear model in Matlab/Simulink, its open loop responses to different types of inputs and disturbances and its analysis. A linear state space model is also obtained for specific operating conditions using Matlab utilities.
- Chapter 7 is about the first part of autopilot design, i.e., designing basic motion controllers. PID controllers are used, using classical feedback theory, with different inner and outer loops. Pitch, yaw, roll, height and speed controllers are designed.
- Chapter 8 is about the second part of autopilot design, i.e., guidance. An algorithm for guidance has been developed and implemented in the yaw plane for following heading specifications. Guidance is implemented using Line Of Sight (LOS) approach through predefined way points (WPs).
- Chapter 9 is about conclusions and suggestions for future work. This study can be improved by using modern robust and optimal techniques as alternative to already available autopilot controllers. Furthermore, certain actions can be

improved in order to spend minimum energy. Physical construction of a WIG vehicle will be of great help to further extend research on WIG vehicles.

- Appendices include DATCOM files, Solidworks file, coding and Simulink implementations.

CHAPTER 2

INTRODUCTION AND PROJECTS

This chapter consists of basic introduction to Ground Effect Vehicles, their autopilots, history of GEVs, current and previous GEVs projects at international level. Specifically, it is discussed about why we need for GEVs, major advantages that make it prominent than other vehicles.

2.1 Introduction to GEVs

For an aircraft the phenomenon becomes much more appreciable when it is flying close to sea (ground or earth surface). The ground plane alters the flow field around the wing, resulting in a reduction in induced drag and an increase in lift. This phenomenon is represented in the lift-to-drag ratio (CL/CD). This ratio can be high up to 20 or more for flying WIG craft if the ground clearance is less than or equal to one-fifth of the wing chord length. This ground can be any Earth surface such as sea or land. WIG craft exploits this behavior resulting in a unique class of high-speed, low-altitude transport vehicles. These vehicles are much more efficient when it comes to payload, speed and cost as compared with other aircrafts. At the same time they are user friendly and have vast scope civil as well as military applications. There are different kinds of WIG vehicles involving Ekrano planes, tandem WIG, reverse delta WIG [1].

The ground effect was first investigated seriously around 1920 [2]. Wieselsberger (1921) treated the problem with an extension of the Lanchester-Prandtl theory [3] and utilized the basic concept of the induced drag of multiplanes. Tsiolkovsky (1927) described the GE and provided a theoretical investigation for air cushion vehicles.

This study explains studies about ground effect and its advantages in term of improved lift to drag ratio. For the ground effect vehicle to work properly, its hull needs to be stable enough longitudinally to be controllable, yet not too stable so that it cannot be pulled off the water, while the bottom must be formed to avoid excessive pressures on landing and taking off, without loss of lateral stability. Finally it must not create too much spray, which damages the airframe and the engines.

Soviets has best known WIG vehicles known with different names such as Ekranoplans, wing-in-ground-effect (WIG), flare craft, sea skimmer, or wing-in-surface-effect ship (WISE). In last few years large a number of different GEV types have been developed for both civil and military applications. Although WIG effect technology has open new horizons, yet these crafts have not entered into widespread use and need more research and development.

2.2 Types and Classes

GEVs are special and mixture of air and marine vehicles, so they have been classified on a different basis. In fact, GEVs development was also delayed due to classification and legislation problems. The International Maritime Organization has studied the application of rules based on the International Code of Safety for High-Speed Craft (HSC code) which was developed for fast ships such as hydrofoils, hovercraft, catamarans and the like [4]. The Russian rules for classification and construction of small type A Ekranoplans is a document upon which most GEV design is based.

2.2.1 Classes of WIGs

The International Maritime Organization [4] recognizes three classes of ground effect crafts:

Type A: In ground crafts which are for operation only in ground effect, at very low altitude.

Type B: A type crafts which are expected to increase their altitude to a limited height outside the influence of ground effect, temporarily for hurdles, obstacles or other purposes.

Type C: An Out of Ground craft which is for operation outside ground effect and can even go 150 m or more above the ground.

2.2.2-Types of WIG-Craft

WIG-crafts are not just aircrafts or just marine vehicle only. Some Specific design criteria are based on aircrafts while some are not (for example, the takeoff). An aircraft uses an angle of attack about 14 degrees for maximum lift to shorten the takeoff distance. A WIG-craft has to be started without this facility. To flare with high speed so low over a surface they have to be auto stable. Over the years different types of WIG-crafts were developed to optimize these type of crafts. Following are the types of GEVs based on [1].

2.2.2.1 Ekranoplan

Ekranoplans are first GEVs and were invented by Russians. They have wings with a very low aspect ratio of 1 to 4 with endplates and flaps. At the start air blows under the wings to establish an air cushion. At cruising speed the propellers are tilted in a more vertical position for more forward trust for speed.

All Ekranoplans have PAR-WIG crafts (Power Augmented Ram Wing in Ground Effect. Some are huge vehicles, many have been built in different sizes, the largest exceeding 500 tons.

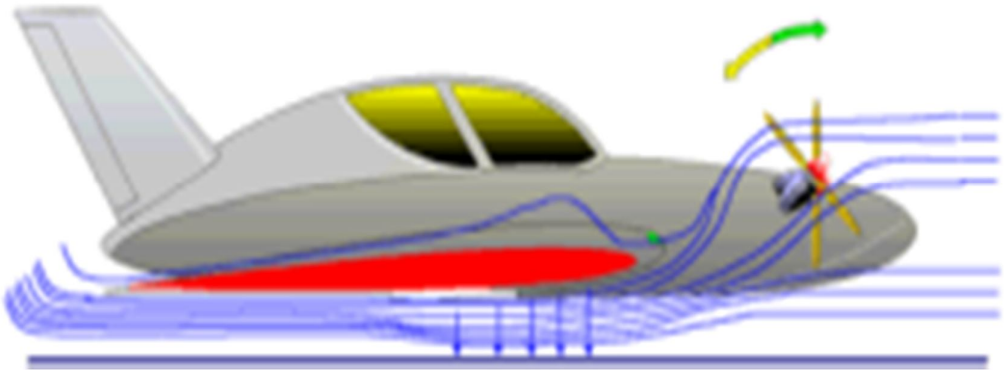

Figure 2.1 Ekranoplans Structure [1]

2.2.2.2 Tandem WIG (Joerg Principe)

These vehicles use two small wings in line. The wings are usually at different angles with respect to (w.r.t) each other. They have excellent stability.

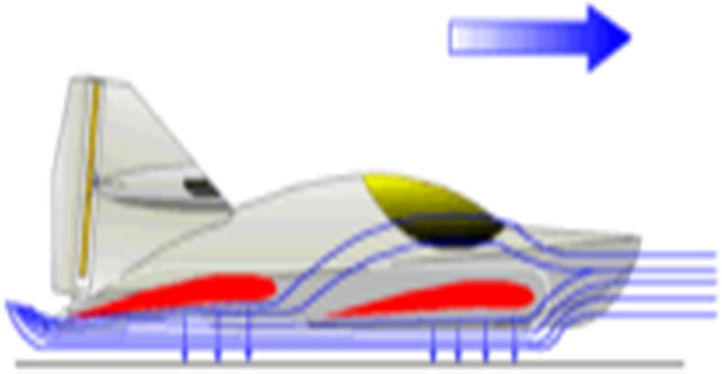

Figure 2.2 Tandem WIGS Configuration [1]

2.2.2.3 Reversed Delta WIG (Lippisch Principe)

Fischer Flugmechanik (Germany) develops these crafts. They can even jump. They use V-hulls. To cover the hump speed of the hull, power is necessary. After flaring condition, power usage can go to even less than half of it before, like in cruising speed phase. Examples of Lippisch vehicles are the airfish series and the flight ship FS 8.

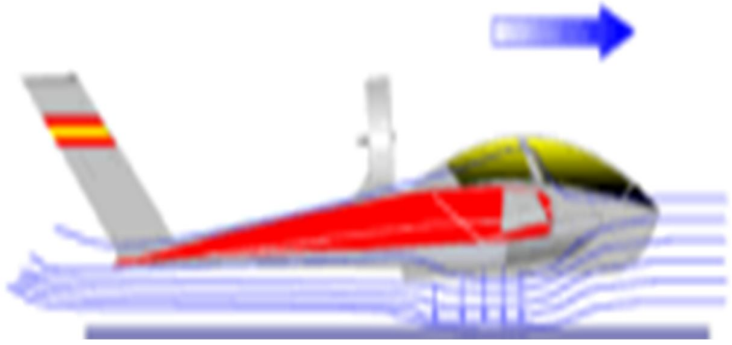

Figure 2.3 Reverse Delta GEVs Configuration [1]

2.2.2.4 Dynamic Hovercraft

These crafts are more or less like hovercrafts but with better efficiency. They need less power to lift of the water surface as a WIG with a V-hull. When it gets in ground effect the forward fan can be switches off for power saving.

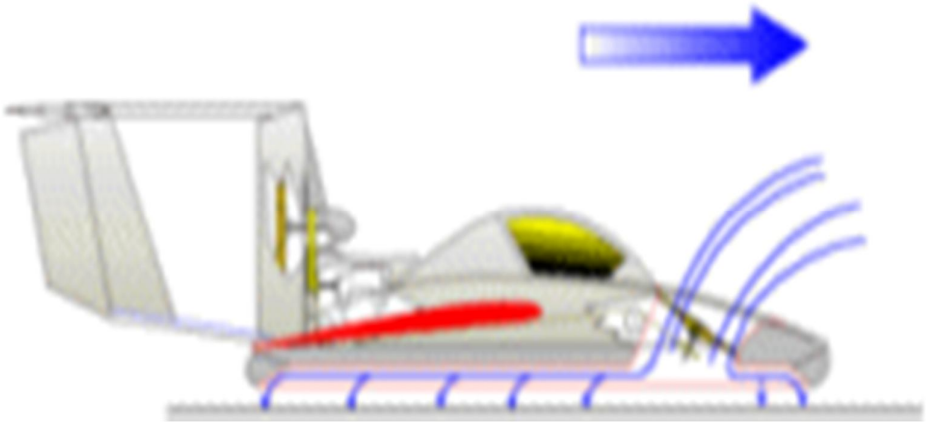

Figure 2.4 Hover GEVs Configuration [1]

2.2.2.5 Other Types

Except these WIG vehicles, other vehicles with enhanced configuration features are being under development. For example in Surface Effect Ships (SES), there is a combination with a WIG craft. Example: the Hovering from Fischer Flugmechanik, or new hovercrafts and ram WIG combinations.

Figure 2.5 Air Fish 8 [1]

2.3 Advantages (Comparison with Other Vehicles)

1. Uniqueness

GEVs are very special vehicles, which have some unique features which other crafts and ships do not have. Some of them are mentioned in following parts.

2. Energy Efficient

WIGs are very energy efficient. Their fuel consumption is 3-4 time less than normal crafts but have more efficiency. A comparison is shown in Figure 2.6.

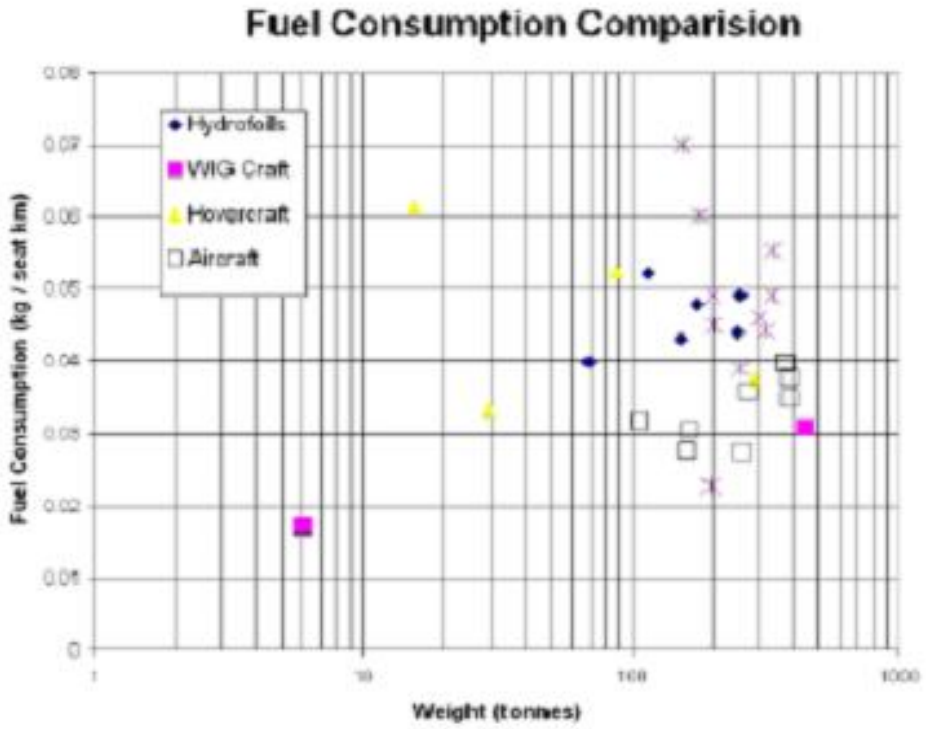

Figure 2.6 a: Fuel Consumption Comparison [5]

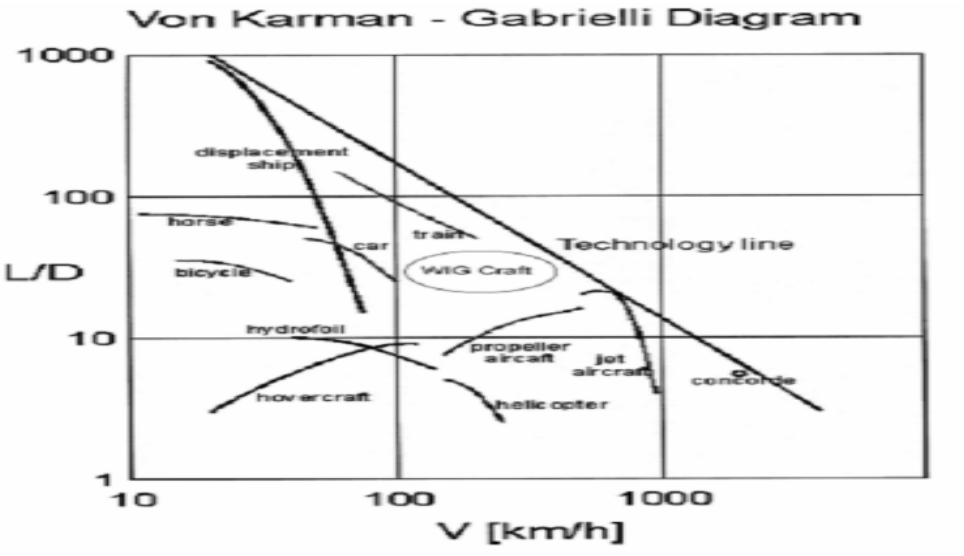

Figure 2.6 b: Von Karman Gabrielli Diagram Comparison [5]

3. Amphibious Performance

WIG crafts can be designed for amphibious operations, so as to be able to load and unload from beaches (as like ships) and operate from airstrips as like aircrafts.

One of the common ideas for amphibious WIG crafts is to provide them with hovercraft ability. The large USSR WIG craft, the Orlyonok as shown in Figure 2.7, courtesy [5], was capable of amphibious operation. The X-l 14 was designed with an undercarriage and could operate from airstrips. Other possibilities for amphibious capabilities are like skis, air cushion skirts and sleds, in addition to GEVs configurations.

Figure 2.7 USSR Orlyonok [5]

4. Stealth Property

Since WIG vehicle flight at low altitude and their speed is very fast, so they can also be used for stealth purposes in military.

5. Environment Friendly

WIG vehicles are environment friendly. They make much less noise and their exhaust is also less in quantity and also less hazardous comparatively.

Some other unique features are:

- Does not require fixed runways, operating from water etc. WIG craft have the potential for more efficient operations than aircrafts, due to the increased lift to drag ratio, they have the benefit of having no restriction on takeoff and landing field lengths.
- Door to door speed is comparable to air travel.
- Infrastructure requirements are identical to a boat, but much more efficient. So, it is a boat and an air craft, at the same time.
- Less noisy.
- WIG crafts have the potential to carry heavy payload weights while operating at high speed. They can be much faster at the same time carrying heavy payloads. They are advantageous as compared to ships which can carry heavy loads but not fast and air crafts that are faster but cannot carry heavy loads.
- If the water is relatively calm, a WIG craft could land at any time. For recreational purposes, some small craft could be operated by civilians with a boat license, rather than a pilot's license.
- With regard to safety, should a WIG craft experience an engine failure and crash, damage is likely to be minimal as the craft will not have far to fall, particularly if the craft falls on to water.

6. Theoretical Benefits of the Ground Effect

Efficiency of a vehicle is related to its ability to carry a payload over a given distance, which is directly related to the craft's lift to drag ratio. Since WIG crafts have higher and improved lift to drag ratio, this results in an increase in their efficiency.

Crafts are governed by the Breguet range equation, for which the representation for propeller driven craft is shown in Equation 2.1:

$$Range = \frac{\eta_P}{C_p} . \frac{L}{D} . ln \frac{W_i}{W_i - W_f} \qquad (2.1)$$

where

η_p $propeller\ efficiency$

C_p $specific\ fuel\ consumption$

L/D $lift\ to\ drag\ ratio$

W_i $initial\ weight$

W_f $final\ weight$

It is very clear from the equation that an increase in the lift to drag ratio will result in increasing the available range with a given payload.

7. Sea State

Sea state or atmospheric state affects the operation of a vehicle in negative and usually causes problems. The data below is taken from [5], which shows WIGs advantages even in atmospherics or sea disturbances. Figure 2.8, (a) shows general sea effects on different crafts, while (b) and (c) show WIG cases which are clearly advantageous.

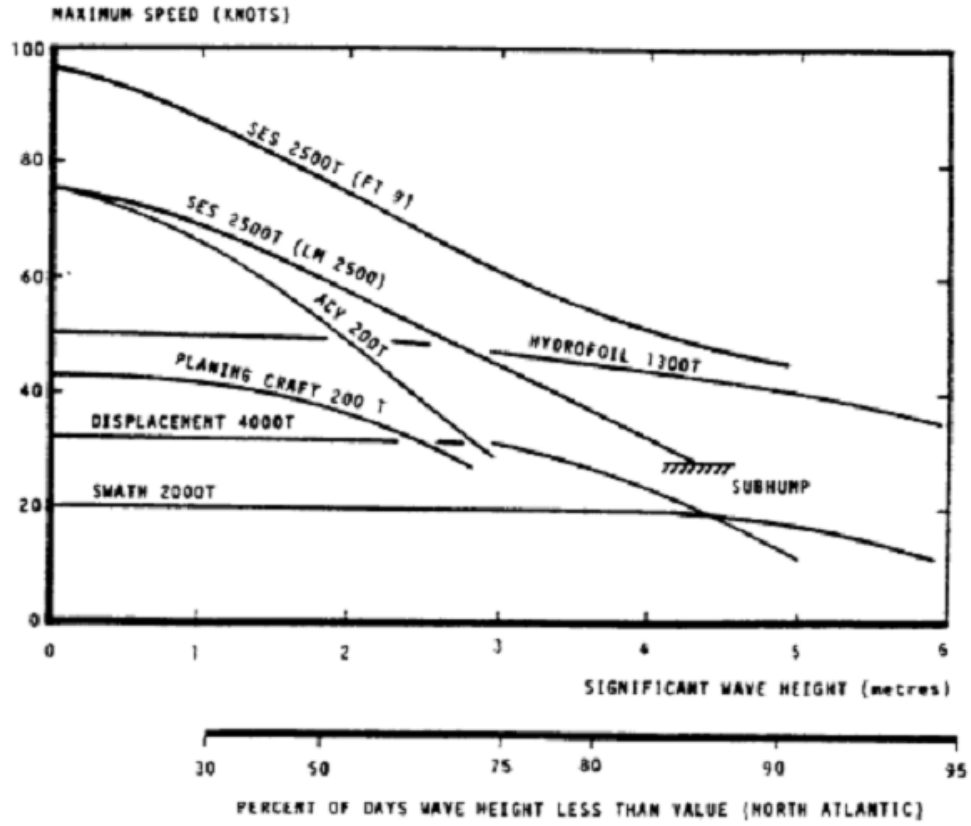

Figure 2.8 a: Sea Effect on Different Crafts

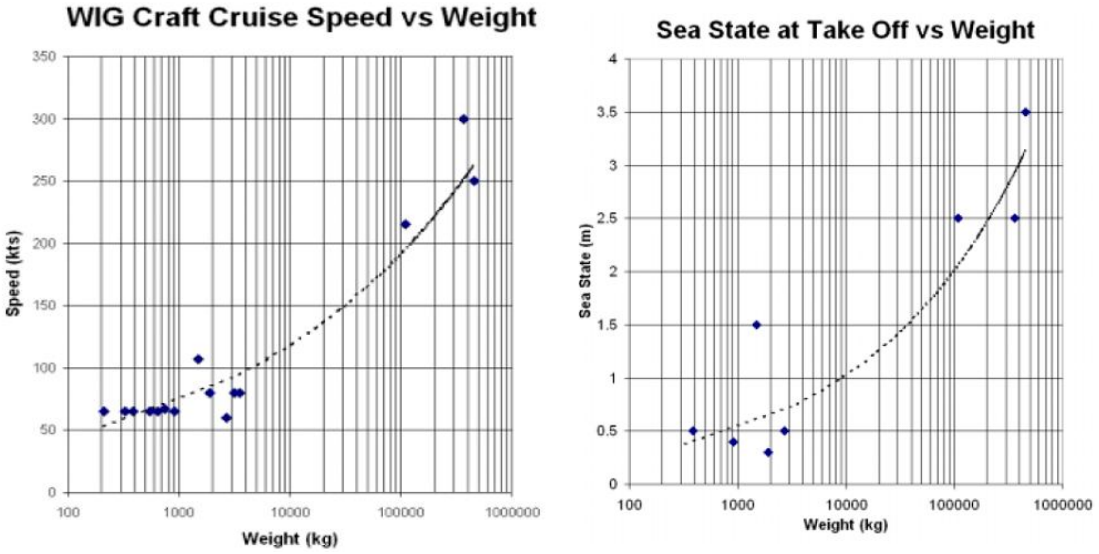

Figure 2.8 b: Sea State Impact Comparison [5]

8. Efficiency Benefits Compared to Aircraft

WIG has different advantages over aircrafts:

- WIG crafts have the potential for more efficient operation than aircraft, due to the increased lift to drag ratio.
- WIG craft generally have the benefit of having no restriction on takeoff and landing field lengths like long runways.
- WIGs payload (weight) carrying efficiency during landing and take-off is much more than aircrafts, which is very serious issue in operations for normal aircrafts operations.

There are however, a number of obstacles in designing to be overcome prior to WIG craft fulfilling their full efficiencies.

9. Comparison to Water Borne Craft

WIG has different advantages over ships:

- A comparison of WIG craft to water borne craft shows an obvious potential speed advantage.
- Large displacement craft have high fuel efficiencies with large payload volumes and weights.
- WIG craft have the potential to carry heavy payload weights while operating at high speed.
- Unlike conventional waterborne craft, WIG craft are not speed limited in high sea states.
- Whilst their range or payload ability may be reduced in heavy seas, there is no substantial reduction in cruise speed.

2.4 Vast Scope of Applications

It is the distinction of WIG vehicles that they have a lot of applications in military as well as in civil fields [12], [13].

2.4.1 Civil Applications Areas

Some of the common probable applications are below:

1. Cargos and Shipments: The Wingship aircraft like the Aerocon could potentially be used in many different applications, such as commercial transport of large numbers of people, major search, shipments, cargos and rescue operations.

2. Water Faring: GEVs are also a suitable option as water-faring airplanes.

3. Surveying for Geophysicist: WIG craft can potentially be used as surveying aircraft for geophysicists, because they can cover a large area of land or sea at low altitudes.

4. Fishing Vessel: They could be used as fishing vessels.

5. Coastal Guard: They can be used in coastal guard operations.

6. Courier Services: In courier/delivery applications over seas and oceans.

7. Commuter Crafts: Small WIG aircrafts can be used similarly to light aircrafts as commuter crafts and light transports.

8. Customs Patrol: The WIG craft's high speed is utilized to patrol and apprehend vessels. Sprint and drift applications - coupled with ASW and patrol duties.

9. Tourism/Passenger Carriers: Developing commercial ekranoplans to carry passenger's cargo, to be used for tourism.

10. Leisure Purposes: It can also be used for leisure as well as for special purposes.

11. Search and Rescue Operations: The vehicle can land and conduct rescue operations even in small level stormy environment.

12. Global Sea Rescue System: An international level concerning of developing an effective rescue measures on the high seas, again reminds the need for WIGs.

A global level sea rescue system has been proposed, comprising of 50 heavy weight ekranoplans, basing in 12 selected focal base-ports throughout the world [5]. Each ekranoplan of the system is designed to have high takeoff/touchdown seaworthiness, corresponding to sea state 5 and enabling its operation on the open sea during 95% of the time year around.

2.4.2 Military Applications Areas

GEVs have also shown their importance in military applications. There are a number of military and naval applications of WIG craft that have much potential of its usage now and in the future [12].

1. Attacking Aircraft: WIG aircraft are quite effective, for an attack aircraft in naval operations. Stealth property makes it un-visible on radars.

2. Missile Launchers: One of the possible applications of WIG crafts can be its use for nuclear launches or as missile launch craft.

3. Antisurface Warfare: WIGs are also one of the favorable options for antisurface warfare. It can reduce the horizon-limited detection ranges of defending aircraft early warning systems, also reducing warning time.

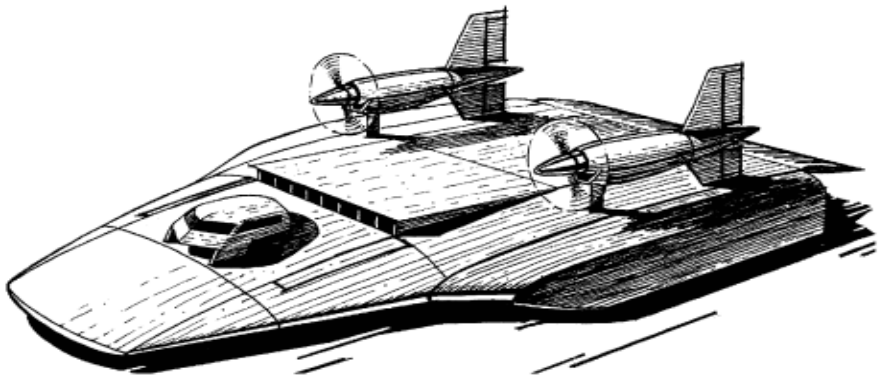

Figure 2.9 Missile WIG Developed by Gruman [6]

4. Anti-Submarine warfare: The ekranoplan would also be a favorite choice for platform for antisubmarine warfare, since it has the capacity to determine the position and to destroy submarines even at long ranges from station.

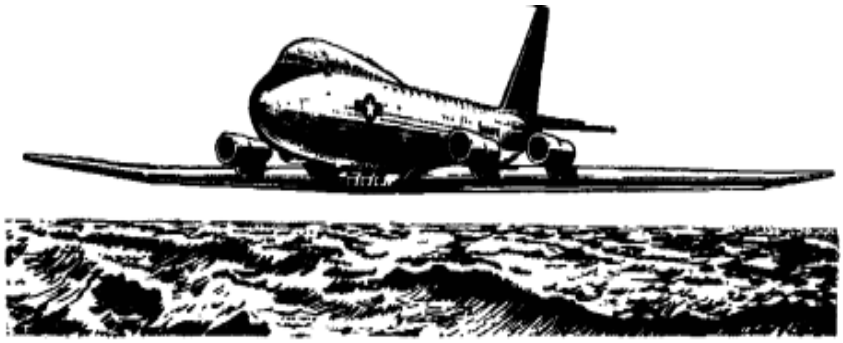

Figure 2.10 Low Boy: An Anti-Submarine [6]

5. Amphibious Warfare: Being amphibious, WIGs are very useful in warfare; ‘‘Orlyonok’’ has been shown before, for its usefulness in such situations.

6. Sea Lift Providers: Ekranoplans are effective in providing a sealift and other similar functions.

7. Nuclear Warfare: It is also a suitable option for a launch platform for tactical and strategic cruise missiles. Since it is efficient in sea skimming cruise capabilities, it has sea loitering feature.

8. Reconnaissance and Patrol: One of the mission applications for large WIGs may be in reconnaissance or patrol.

9. ‘‘Wingship’’ Naval Missions (Weapon and Troops Carrier): Since it has the capacity to carry large payloads, like the Aerocons, it enables the rapid deployment of military units to any location, and it can be even any part of world.

There are many other possible applications for WIG aircrafts in both civilian and military fields. There are many potential projects which are under development. But

WIG crafts are yet to become more in use, even though more research and development into the efficiency and effectiveness of such aircrafts is required.

2.5 History and Major Projects

All kind of aircrafts observe the ground effect, but it was a problem before, especially during take-off and landing, because it causes instability. Fortunately, studies started in early 20th century enable us to make use of it advantageously.

Research started on WIG for designing seaplanes or crafts. Wieselsberger was (1921) the first person to study the ground effect properly, mainly focusing on Span Dominated Ground Effect (SDGE) and he proposed some methods to analyze its effect and also derived a parameter used in the calculation of GE [2]. Between 60's and 90's extensive research was carried out, lots of experimental and theoretical work and formulations were proposed and suggested for different hydrofoil structures. USSR and USA are the first countries to develop experimental aircrafts during early 1960's, utilizing GE. Germany started developing GEVs in 1960's. Germany, Russia, and the United States have provided most of the momentum, while there are some developments coming from Australia, China, Japan, Korea, Taiwan and Iran [12]. In these countries, small crafts up to ten seats have been designed and built. Other larger designs as ferries and heavy transports have been proposed, but have not been carried to actual operation.

Besides the development of appropriate design and structural configurations, special automatic control systems and navigation systems are also being developed. These include special altimeters with high accuracy for small altitude measurements and also to provide lesser dependence on weather conditions [6].

UH is developed as a flying hovercraft, a prototype which first took flight in 1996 [7]. Since 1999, the company has offered plans, parts, kits, and manufactured GEV hovercraft called the hovering [7].

In Singapore, "Wiget Works" has continued development and obtained certification from Lloyd's Register for entry into a class of WIG crafts [8].

On 31 March 2011, Airfish 8-001 became one of the first WIGs to be flagged with the Singapore Registry of ships, one of the largest ship registries [9]. “Wiget Works” has also partnered with National University of Singapore's Engineering Department to develop higher capacity WIG craft [10]. In Korea, Wing Ship Technology Corporation has developed and tested a 50 seat passenger version of a WIG craft named the WSH-500 [11].

It is Russia that brings about largest research in this field, through military funded developments. Most of today’s knowledge regarding WIG craft goes back to them. Rostislav Evgenievich Alexeyev was a designer of high speed ship building. He invented and designed the world's first Ekranoplans. His work has been compared to that of A.N Tupolev in aviation and S.P Korolev in space flight. He is now generally considered as the father of ground effect vehicle design. Several documentaries have shown details of his work (including the KM) [12].

In his career working for the military, he created a ten engine ekranoplan referred to at the time by American intelligence as "The Caspian Sea Monster". The KM or "Korabl-Maket", the largest ekranoplan ever built, was one of the first very successful vehicles designed by Alexeev and built by his Central Hydrofoil design Bureau. The KM was intended as a test platform to examine the possibilities of the "Wing in Ground Effect” [13].

The KM, powered by eight Dobrynin VD-7 turbojets in front of the fuselage, and two on the tail for extra thrust during take-off, first took to the air in October 1966. During its extensive test career, it was continually modified. The wingspan was altered to be between 32m and 40m, and the length varied from 92m to 106m.

Alexeev began to work on a medium-sized ekranoplan suitable for military transportation duties. Dubbed A-90 "Orlyonok" ("Eaglet"), the 140 ton, 58 meter long aircraft had its maiden flight in 1972. In fact, Russia has proved himself to be best in this field till now.

CHAPTER 3

MAJOR FEATURES/STRUCTURES OF THE VEHICLE

This chapter describes the design of a small scale WIG effect vehicle or GEV and the factors that are considered during the design, such as how different configuration/structures should be chosen for different parts, and what its different features are about. Geometric, mass and inertial properties of the vehicle are described and wings, fuselage, horizontal and vertical stabilizer configurations and their drawings and CAD implementation have been discussed. This chapter also explains about airfoils and the reasons behind their selection. Additionally, some other factors are described which can affect aerodynamics and other forces.

3.1 Platform: Introduction to Vehicle

The platform used in this study is a small scale GEV which is designed in Solidworks and then mathematically modeled and simulated in a virtual (Matlab/Simulink) environment. This craft will be manufactured if resources like financial, time and manufacturing facilities allow at Middle East Technical University (METU). It has a fuselage, long and low-wing configuration for wings and T-tail configuration with twin beams (double T-Tail). Basic structure is given in Figure 3.1 and drawings, geometric and technical characteristics are given in Figure 3.7. Table 3.1 also shows some of the characteristics. Estimated weight is around 25lb and it will be sufficient to take payload roughly around 20 lb. It is also assumed that it has onboard instrumentation like IR, day light cameras etc., which will be needed for guided operations and flights. It has control surfaces such as elevators and ailerons and two propellers (thrusters). These control surfaces will be actuated by servo motors with capable of producing sufficient torque. Motors and a small diesel engine are both

feasible options; currently only motors are considered, and their place is also considered at comparatively rear part.

Following characteristics are expected:

- Autonomous flight,
- Take-off and landing with no or relatively smaller runway,
- It has all the required instrumentation on it, such as GPS, gyros, cameras.

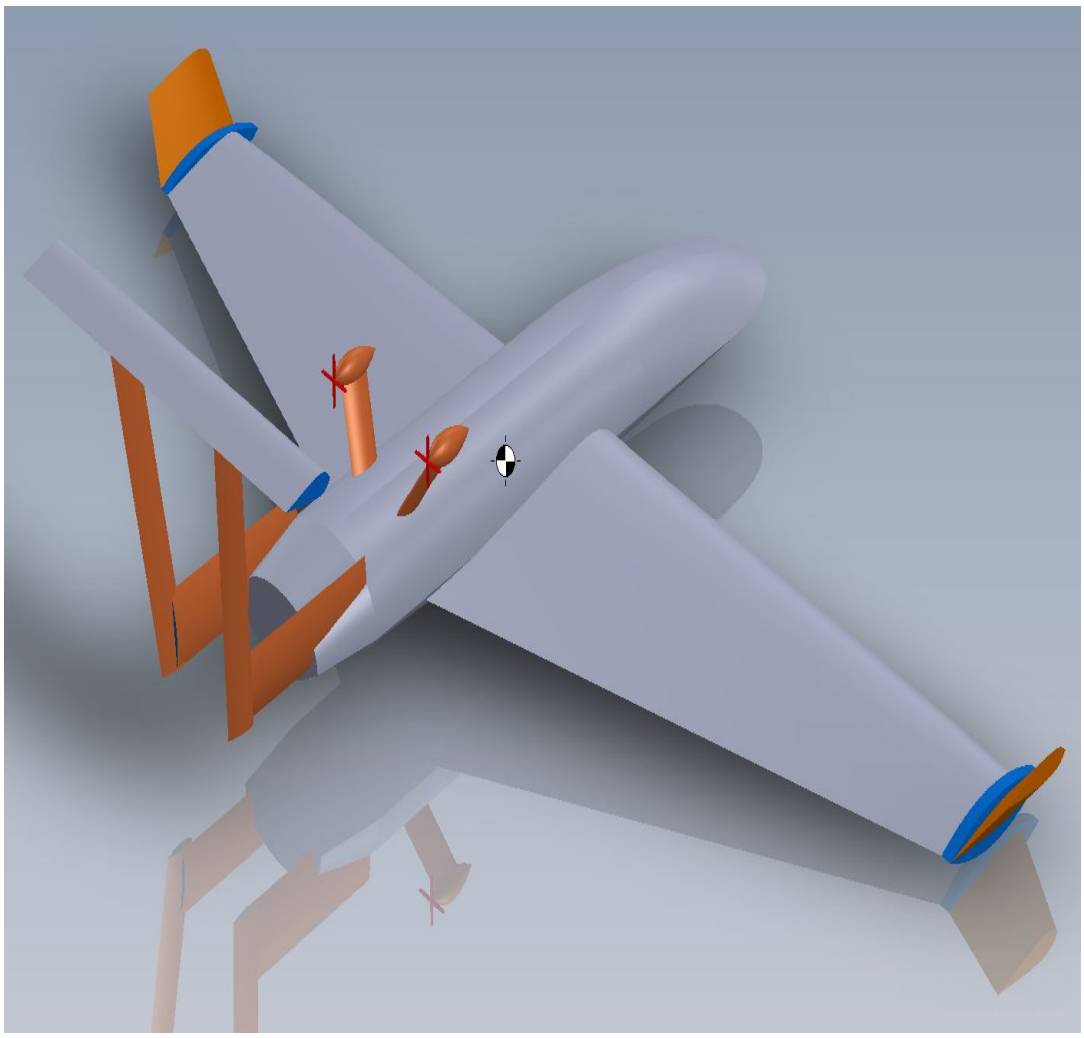

Figure 3.1 3D View of the WIG Vehicle

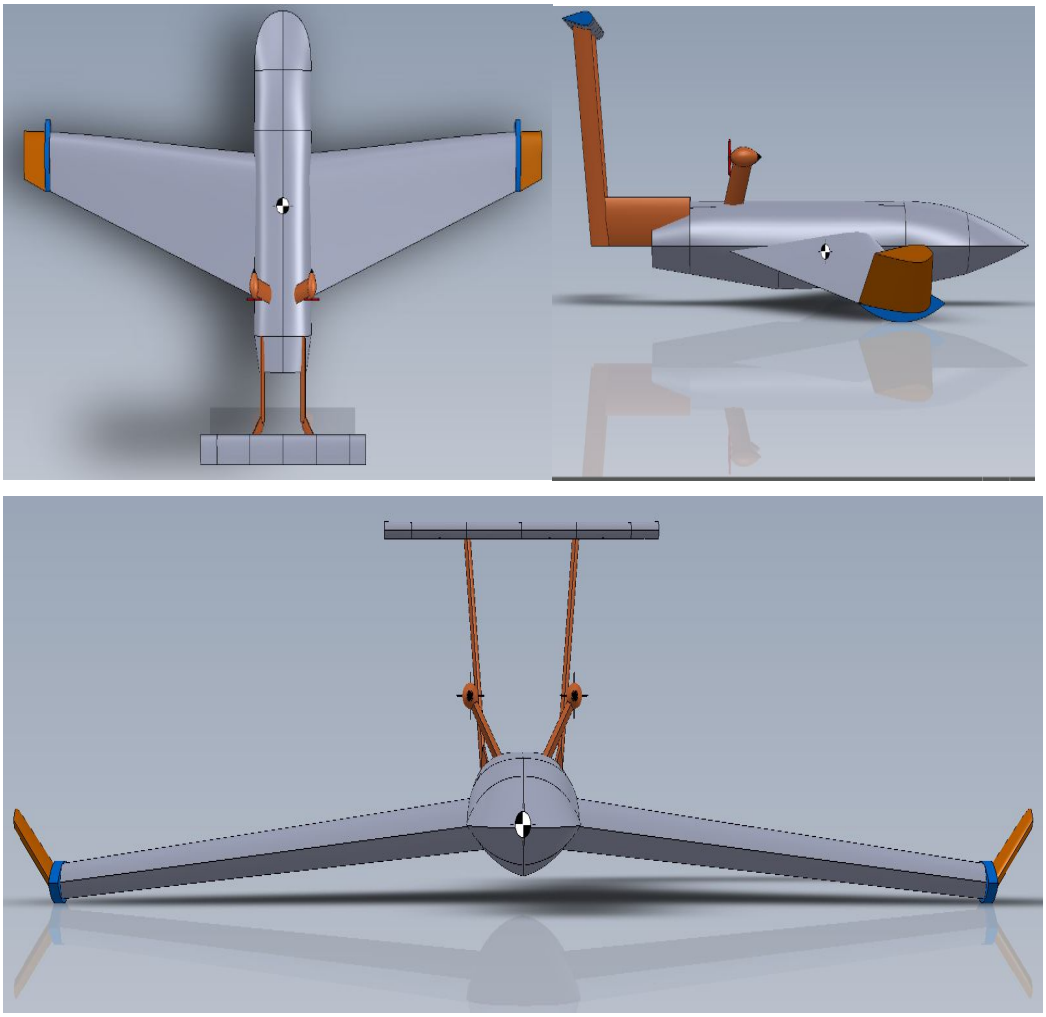

Figure 3.2 Different Views of the Vehicle

Table 3.1 Technical Specifications of the WIG Vehicle

Wing Span	4.5 m
Length	3.3 m
Width of Fuselage	0.5m
Wing Sweep	10 deg
Aerodynamic Chord at Root	5 feet
Wing Dihedral	5
Wing Profile	NACA 4412

X_{cg}	5.25 feet
Y_{cg}	0
Z_{cg}	0
M	25lb
I_{xx}	8.93
I_{yy}	11.24
I_{zz}	18.90
I_{xz}	-3.3

A look at different parts has been given separately in the following sections:

3.2 Fuselage Design

Current design is based on aircrafts, operating as aircrafts in ground effect, but it is considered and planned that in the future, it will be upgraded so that it can go down to water surface or can even sail (like a boat) if needed; therefore “Catamaran Empennage Configuration” is considered for hovering (fuselage) with a double T-tail because it is easier and secure when operating near or with water. A “Catamaran Empennage Configuration” creates a static air cushion through diverting propeller slip-stream, which creates about 80% of the lift to carry crafts weight.

This type of design has the capability to tackle both aerodynamics as well as hydrodynamics acting as aircraft or a ship. See the references [14] and [15] for details.

3.3 Wing Design

Conventional wing configuration with "Reverse Delta" structure has been used. Most special reason for this design is its role in longitudinal stability, especially in case of WIG, which is generally more unstable in longitude because of its pressure center, can be different from CG. Other advantages of "Reverse Delta” are that it get high stall angle when angle of attack is increasing, because of vortex generated are attached to the upper leading edge. In addition, it has more space and volume which can be used

for fuel, carriage or equipment. It is also simple and much stronger than swept design. It is also easier to build and is economical.

Major disadvantage of this design is small loss of lift (energy), usually it occurs when it is tailless, but in our case, we have double T-tail design which overcomes this major disadvantage.

A low wing configuration provides very effective use of ground effect and has feasible maneuvering capabilities during take-off and landing. Also it results in better cruise performance. 5° dihedral angle is set for (hovering) wing. It increases the spiraling capability and Dutch roll stability. It will also decrease ground clearance to get more benefit from ground effect. Root chord is around 5 feet while tip chord is around 1.5 feet. [14] and [15] can be seen for details of wing design.

3.4 Airfoil

The Airfoil NACA4412 is chosen for wing. It has comparatively flat bottom side which provide suction as wing comes in ground proximity.

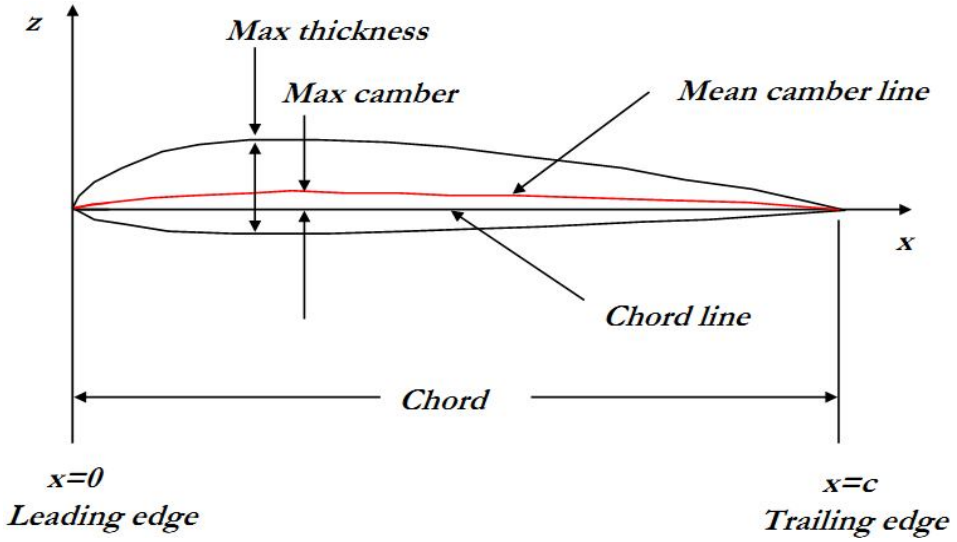

Figure 3.3 Wing Parts [15]

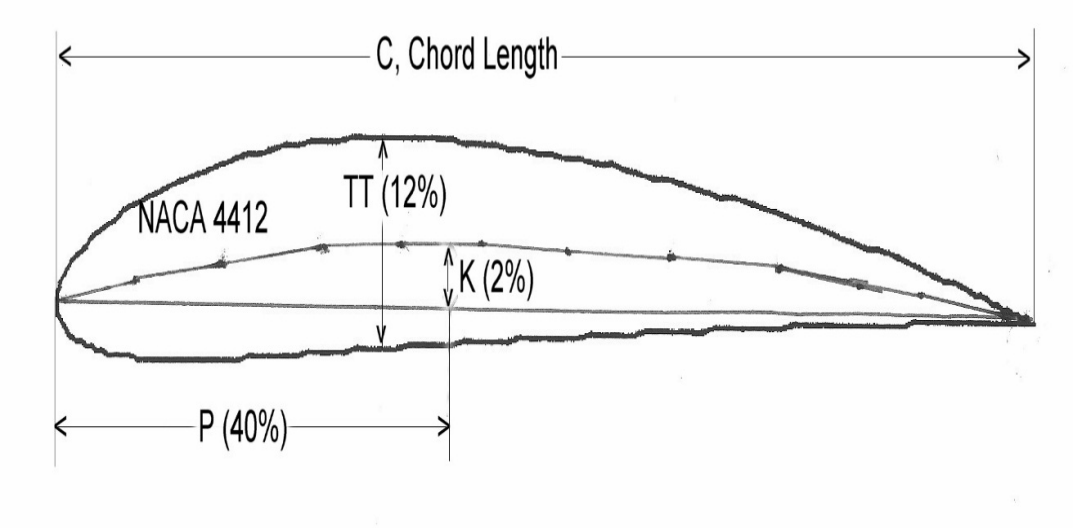

Figure 3.4 NACA 4412 [17]

General concept of symmetric airfoil is ignored here because detailed studies proved that symmetric airfoil gives less cross sectional area and also cause drop in static pressure. Swept angle is kept very low, i.e., around 10 degrees because Mach number (speed of vehicle/Speed of sound) will remain in a small range (see [16] and [17]).

3.5 Control Surfaces

Following surfaces are used for control and stability:

- Elevators to control pitch angle and symmetric (longitudinal) movements.
- Aileron to control roll angle and unsymmetrical (lateral) movements.
- Propellers (for forward speed and heading controllers).
- Winglets or wing tips (used for stability and improved lift and also will be useful for handling buoyancy forces, especially when the system will be upgraded for amphibious features like marine boats).

Wing tip tanks are used as winglets, which are helpful for storing fuel at the center of gravity, and evenly distribution of weight. Wingtip also produces vortices from the wing underside, while they are rotating, hit the cambered surface, which causes forces upward and forward like lift and sailing. So, these winglets convert somewhat wasted energy to apparent thrust. These winglets are also very useful when the vehicle acts as a boat [14].

3.6 Rear Part

Double T-tail design has been chosen for the rear part. It has both advantages and disadvantages, but overall advantages overweight disadvantages, both are elaborated in the following paragraphs. It even becomes more advantageous for a special case of GE. Disadvantages include apparently more exposition to downwash, the fins must be stronger to tackle with tail forces, take more weight.

On the other hand, double T-tail design makes more use of aerodynamics. Mounted T-tail (Double T-tail) keeps tail plane out of air flow. Smooth air flow gives a better pitch control, since it is not behind the wing. It is also out of way from rear fuselage so engine or some other weight can be put there, to take advantage of this configuration. Another merit is the distance between tail plan and wing. It improves aerodynamics and is more beneficial; but it does not add much weight. These advantages outweigh disadvantages and therefore suited for our design (see [14] and [15]).

3.7 Horizontal Stabilizer

The horizontal stabilizer provides longitudinal stability and trim for the vehicle. It can be mounted behind the wing in the conventional way, same as used here, or in some cases in front, which is not preferred here. Volume method is used to find different specifications of horizontal stabilizer.

Horizontal stabilizer must be mounted uninfluenced of the ground effect, since height stability is also required in parallel with longitudinal stability (see [19] and [20]).

The total pitching moment of rear part is the sum of the combined pitching moment due to wing-fuselage and the tail around CG. It is given by Equation 3.1:

$$Cm_{wf} + Cm_{wt} = Cm_{wft} \qquad (3.1)$$

where Cm_{wf} is the pitching moment due to fuselage and wings, Cm_{wt} is the pitching moment due to wing and tail and Cm_{wft} is their sum. The other relations are

$$Cm_{\alpha t} = -V_H C_{L\alpha t} \qquad (3.2)$$

$$Cm_{0t} = -V_H C_{L\alpha t}(\varepsilon_0 + i_w - i_t) \qquad (3.3)$$

where Cm_{0t} is the tail pitching moment at zero angle of attack (AoA), $Cm_{\alpha t}$ and $C_{L\alpha t}$ are pitching moment and lift coefficients at angle of attack α, respectively, V_H is the tail volume, i_w and i_t are wing and tail incident angels, respectively and ε_0 is downwash at zero AoA.

It can be calculated that the required tail size should have a span of 0.4 meters with a chord of 0.2 meters mounted at an incident angle of 0.65 degrees.

Using this data, the root chord of the horizontal stabilizer is determined to be 1.65 meters and is same for the whole length. The taper ratio was calculated to be 0.57 (it is a ratio so unitless) for the horizontal stabilizer. It also has zero degrees of leading edge sweep. The NACA 4412 airfoil is chosen for the horizontal stabilizer as well. The maximum lift coefficient is 1.65 for this airfoil.

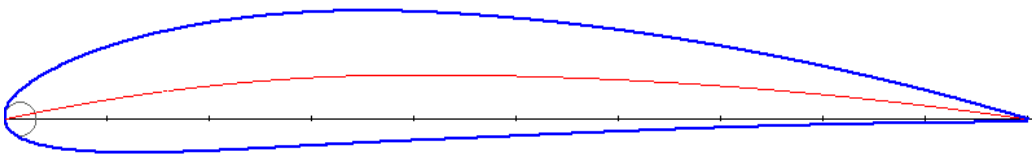

Figure 3.5 Horizontal Wing Airfoil [17]

It is of prime importance to note that the maximum lift of the wing is strongly related to horizontal stabilizer's root chord and it is the reason for the horizontal stability even at low speeds. It is also observed that even in dust and roughness, its characteristics does not change much.

3.8 Vertical Stabilizer

Vehicle has two vertical stabilizers. The volumetric method is used for the calculation of their different specifications. It is preferred to be smaller to avoid height weathercock stability, ([19] and [20]). The following equation is used to find the volume:

$$V_v = \frac{X_v S_v}{Sb} \qquad (3.4)$$

where V_v is the vertical stabilizer volume, X_v the position of the vertical stabilizer, S_v is the vertical size of empennage, S is the vertical wing surface area and b is the vertical wing span.

The vertical stabilizer will have 45 degrees leading edge sweep. It will have no dihedral angle and will be located 90 degrees from the horizontal tail. NACA 63012 airfoil will be used for the vertical stabilizer [21].

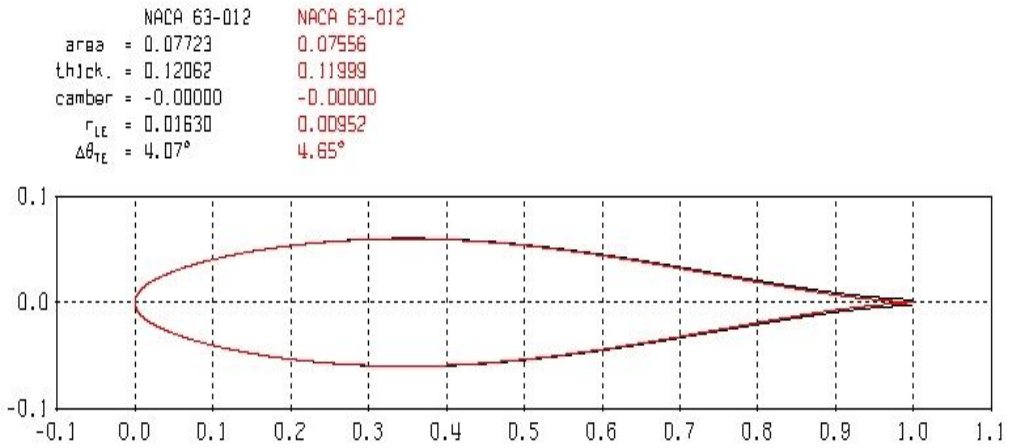

Figure 3.6 Vertical Wing Airfoil [21]

These are for some major features only. Further details are clear from drawings shown in Figure 3.7. Some of the remaining features like propulsion and aerodynamics will be discussed in the mathematical modeling part, in Chapter 5.

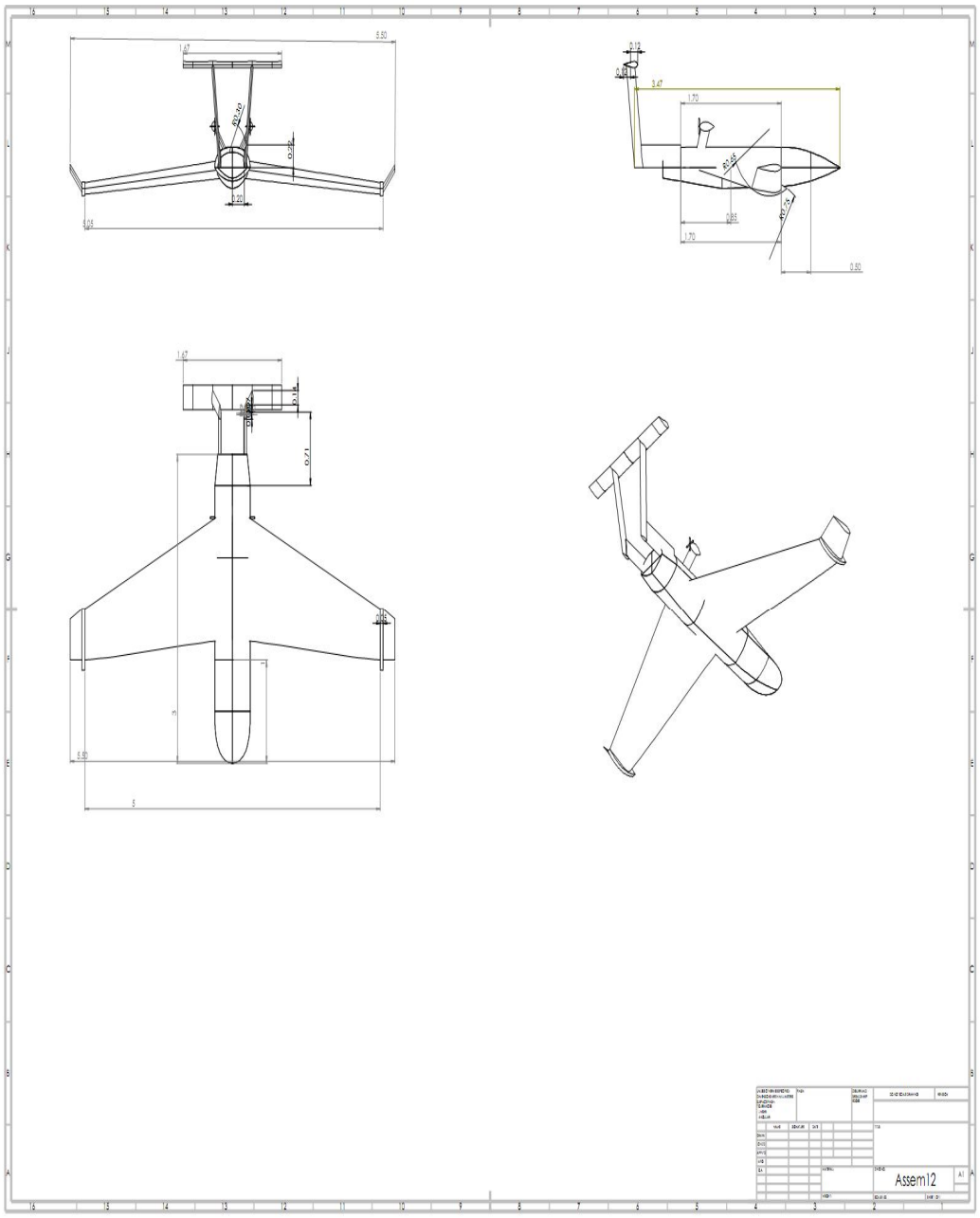

Figure 3.7 Drawing of the Vehicle with Dimensions

CHAPTER 4

THEORY OF GROUND EFFECT

In this chapter general theory of ground effect and its types have been discussed. Its mathematical formulation will also be discussed and conditions will be analyzed about how the aerodynamics of the system can be improved.

4.1 Brief Introduction to Lift and Drag Forces

As a wing moves through air a resultant force is generated according to

$$F = \oint -(P.n)\, dA \qquad (4.1)$$

where *P* is the pressure on the wing and n is the unit normal toward the wing and A is the total area of the wing. This resultant force can be decomposed into lift (perpendicular to the free stream velocity) and induced drag (parallel to the free stream velocity). Other forms of drag are also present which are the result of friction as the aircraft moves through the air and are referred to collectively as parasitic drag. The total drag is the combination of both parasitic drag and the induced drag.

$$F_y = L = \int -P(cos(\alpha + \emptyset))\, dA \qquad (4.2)$$

$$F_x = D = \int -P(cos(\alpha + \emptyset))\, dA \qquad (4.3)$$

Here α and $\emptyset$ are AoA and roll angle, respectively. To handle different wind conditions, non-dimensional (unitless!) representations are used based on the pressure coefficient:

$$F_{Px} = 2.\frac{P_x - P_\infty}{\rho_\infty} = \frac{P_x - P_\infty}{U_\infty} \qquad (4.4)$$

P_x is the local static pressure and P_∞ the free-stream (at ∞) static pressure, nondimensionalized by the free-stream dynamic pressure and U_∞ is the forward free stream velocity. To use forces, lift (L) and drag (D), and moment (M) as dimensionless terms, new coefficients are defined in the following equations:

$$C_L = \frac{L}{QS} \qquad (4.5)$$

$$C_D = \frac{D}{QS} \qquad (4.6)$$

$$C_m = \frac{M}{QSc} \qquad (4.7)$$

where $Q = \frac{1}{2}.\rho.V^2$ is the dynamic pressure, and L and D are the lift, drag forces, M is the pitching moment and ρ is the density of air, S is the projected area on ground plane and c is the chord length [23].

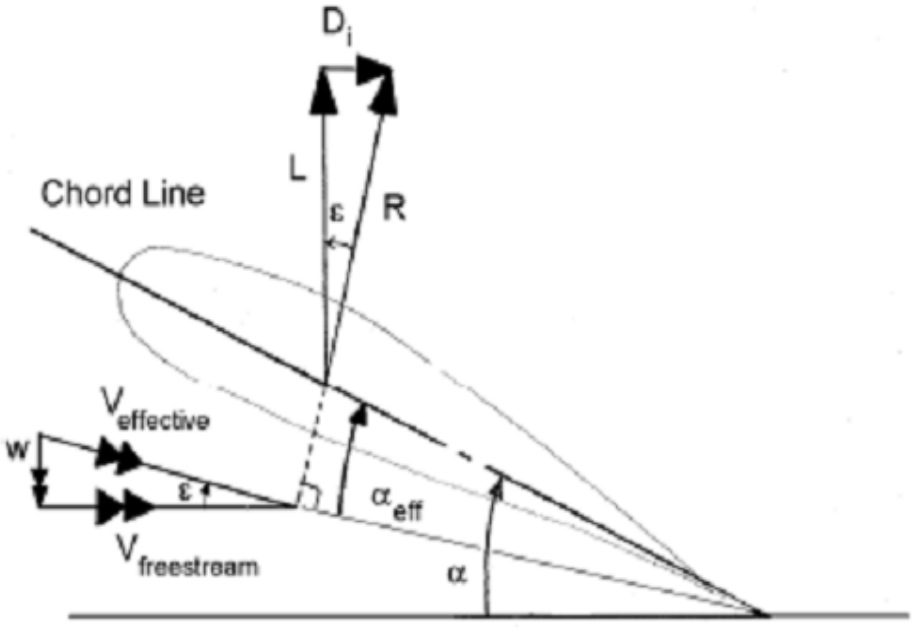

Figure 4.1 Lift & Drag [23]

In Figure 4.1, $\propto_{eff}$ is the effective AoA and ε is the downwash angle.

4.2 Ground Effect

When a wing or lifting surface approaches the ground, an increase in lift as well as a reduction in drag is observed which results in an overall improved lift-to-drag ratio. The cause of the increase in lift is normally referred to as Chord Dominated Ground Effect (CDGE) or the ram effect. Meanwhile, the Span Dominated Ground Effect (SDGE) is responsible for the reduction in drag. The combination of both CDGE and SDGE will lead to an increase in the L/D ratio, and hence causing overall improvement in the efficiency.

Figure 4.2 WIG Effect Phenomenon [1]

4.2.1 Span Dominated Ground Effect (SDGE)

Height-to-span (h/b) is related to SDGE. The total drag is the sum of the profile drag and induced drag. Skin friction and flow separation contribute to profile drag while the induced drag occurs in finite wings when there is a “leakage” at the wing tip which creates the vortices that decrease the efficiency of the wing. In SDGE, strength of the

vortices decreases due to boundary limits. As a result, the wing now seems to have a higher aspect ratio (effective aspect ratio AR') as compared to its geometric aspect ratio AR, resulting in a reduction in induced drag ratio.

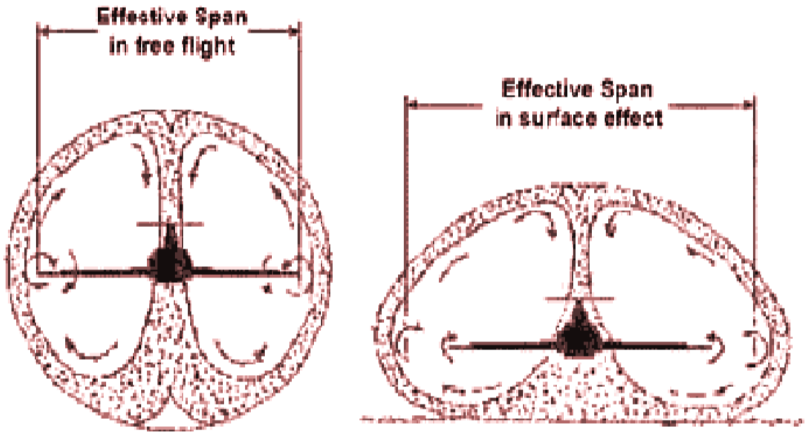

Figure 4.3 Vortex of an Aircraft in Flight a) Out of Ground Effect b) In Ground Effect [24]

SDGE was first studied by Wieselsberger [24]. For the development of the theory, the methods of [24], [25] and [26] all employ the assumption that the effects of the ground on a wing are the same as the effect which would be induced by the flow about an identical image wing symmetrically disposed with respect to the real wing on the opposite side of the ground plane. Weisselsberger's model predicts the increase of lift by assuming that the induced drag is reduced because of the proximity to the ground measured by a parameter,

$$\sigma_{ge} = \frac{1-0.66(2\mathrm{H}/b)}{1.05+3.7(2\mathrm{H}/b)} \qquad (4.8)$$

In reference [27], Equation 4.8 is simplified as

$$\sigma_{ge} = e^{-.48(2\mathrm{H}/b)^{0.768}} \qquad (4.9)$$

where σ_{ge} is the ground effect influence parameter, H is the height above the ground surface and b is the wing span. In order to use the actual elevation (H), it can be multiplied by a factor of two.

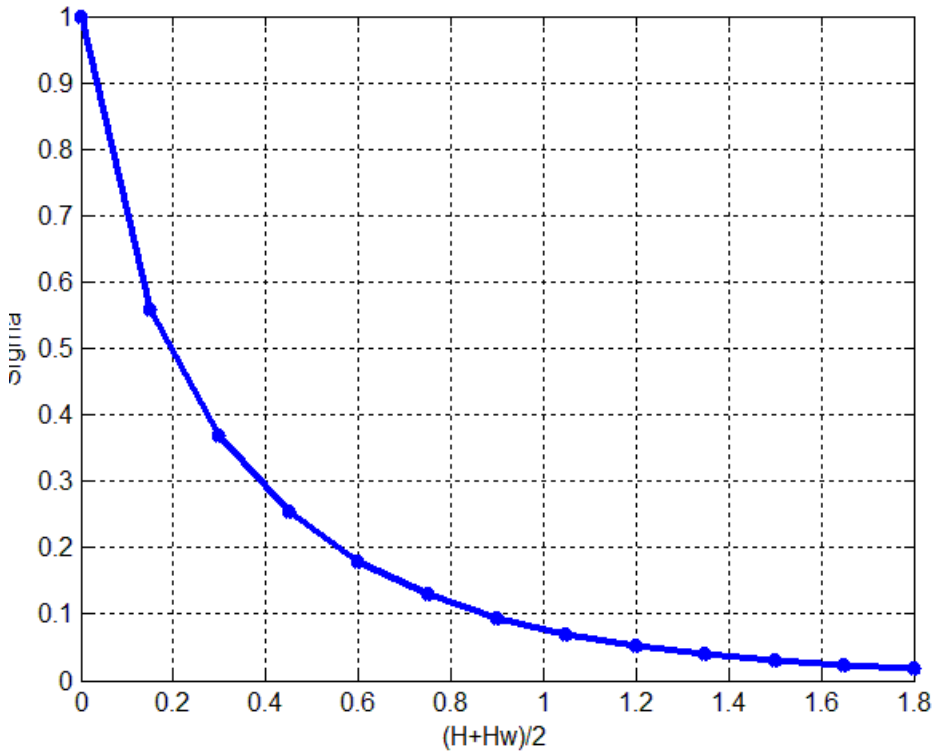

Figure 4.4 Sigma vs Height

It is directly quoted from his discussion: “we may employ the following approximation formula of Prandtl, which holds well from H/b = 1/15 to H/b = 1/2.” Since Wieselsberger attributes the formula to Prandtl, it is called as Prandtl’s formula here. Le Sueur [28] states, “H being than twice the height of the wing above the ground”. Figure 4.5 is copied from [24] for further clarification.

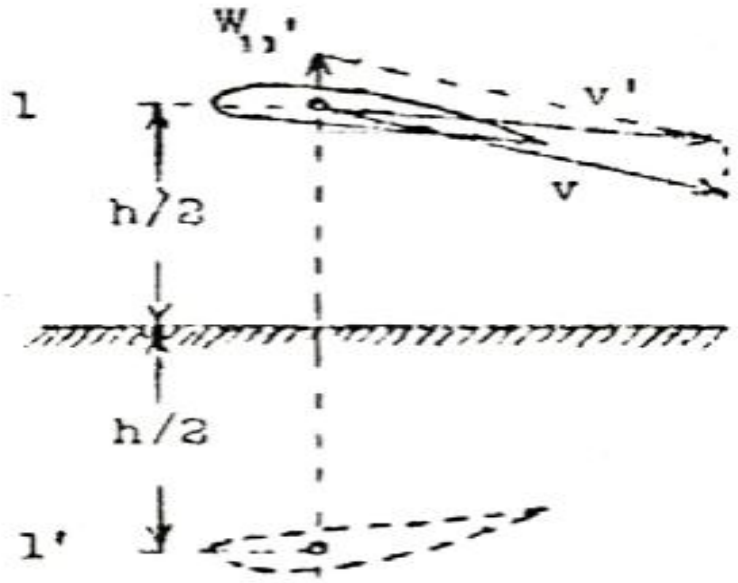

Figure 4.5 Wing Clearance from Ground [24]

From Prandtl lifting line theory [29], the induced drag can be calculated by

$$C_{D_i} = \frac{C_L^2}{\pi e \mathrm{AR}} \qquad (4.10)$$

where e is known as the span efficiency and AR is the aspect ratio of the wing. Since the aspect ratio is

$$AR = \frac{b^s}{S} \qquad (4.11)$$

In ground effect, the effective (increased) aspect ratio is defined by

$$AR' = AR/(1 - \sigma_{ge}) \qquad (4.12)$$

Maurice Le Sueur' also showed the similar results in his studies [28]. Maurice Le Sueur clarified the use of the equation above. At a given lift coefficient, the drag due to lift coefficient is

$$C_{D_L} = (1 - \sigma)\frac{C_L^2 S}{\pi b^2} \qquad (4.13)$$

$$C_{D_L} = (1-\sigma)\frac{C_L^2}{\pi\, AR'} \qquad (4.14)$$

In the presence of ground effect, Rozhdestvensky [22] has also shown similar expressions that drag will be reduced at small height. It is directly proportional to height and span efficiency is inversely proportional to height. Rozhdestvensky shows that:

$$C_{D_i} \propto h \qquad (4.15)$$

$$e \propto {}^{1}/_{h} \qquad (4.16)$$

The lift curve formula in Von Mises ([30], page 243) is

$$C_L = \frac{L}{(\rho/2)V^2 S} = \frac{\pi B \Gamma}{2VS} \qquad (4.17)$$

Further manipulation [30] results in

$$C_L = \frac{2.\pi}{(1+2/AR)}\alpha \qquad (4.18)$$

Along with the camber and flaps needed to add a minimum lift term [31]

$$C_L = \frac{2.\pi}{(1+2/AR)}\alpha + C_{L0} \qquad (4.19)$$

The C_{L0} is the lift coefficient at zero angle of attack. So, here we can also see the effect of AR on lift.

By Wieselsberger, the resulting changes in angle of attack (AoA) and drag coefficient at a constant lift coefficient are expressed by the equations

$$\Delta\alpha = -57.3\,\frac{C_L}{\pi A}\sigma \text{ (Deg)} \qquad (4.20)$$

$$\Delta C_D = -\frac{C_L^2}{\pi.AR}\sigma \qquad (4.21)$$

Except the effect of the trailing vortices (Wieselsberger considered only the effect of the trailing vortices of the image wing) the method of references [25] and [26] takes also wing thickness, the effects of the bound vortices circulation and the longitudinal velocity. With these factors, relations are

$$\Delta\alpha = -57.3\,\frac{C_L}{\pi A}\sigma + rTC_L^2\text{-rB+}K_e \qquad (4.22)$$

$$\Delta C_D = -\frac{C_L^2}{\pi A}\sigma + r - \left(C_{Da} - \frac{C_L^2}{\pi A}\sigma\right)\frac{m}{57.3}TC_L \qquad (4.23)$$

where T takes account of the reduction in longitudinal velocity, $\Delta\alpha$ in Equation 4.22 shows the change in angle of attack due to the change in circulation, r is the appropriate factor for reducing B and K_e is the effect of wing thickness, e being the ratio of maximum thickness to chord. C_{DL} is the wing drag coefficient induced by the given lift coefficient under free-air conditions. It is the derivative of the lift cofficient to the angle of attack $\frac{dC_L}{d\alpha}$.

$$T = \frac{57.3}{8\pi m} * \frac{\frac{h}{c}}{(\frac{h}{c})^2+\frac{1}{64}} \qquad (4.24)$$

Here h and c is the height of the quarter-chord point and c is the chord of the wing, respectively. For computing B, reference [25] can be used. The factor r is given by the relation

$$r = \sqrt{1 + (\frac{2h}{b})^2} - \frac{2h}{b} \qquad (4.25)$$

The quantity K is expressed by

$$K = 57.3(0.00300)\left(\frac{h}{c}\right) * \frac{1}{\left(\left(\frac{h}{c}\right)^2+\frac{1}{64}\right)^2} + \frac{3}{\left(\left(\frac{h}{c}\right)^2+\frac{9}{64}\right)^2} \qquad (4.26)$$

4.2.2 Chord Dominated Ground Effect (CDGE)

The CDGE is related to the suction side of the airfoil. A fact found by designers dictates the suction side of an airfoil should be flat to improve the chord dominated ground effect (this point was specially noticed in designing the vehicle, as was mentioned in Chapter 2, while choosing the airfoil). However, this effect (sometimes

termed as extreme ground effect) is very complicated to model, as it is a strong function of the geometry of the entire vehicle. All in all, one can use the GE parameter in calculating the lift force.

In the study of CDGE, one of the main parameters is the height-to-chord (*H/c*) ratio. The term *H* height here is distance from the ground surface to the vehicle body. The increase in lift is due to the increase in static pressure which causes an air cushion at low height. This ramming effect leads to the increase in lift. Figure 4.6 below shows the difference between an airfoil without ground effect (a) and with ground effect (b) [31]. Theoretically, as the height becomes zero, resulting in stagnant air, the highest possible static pressure with a unity value of coefficient of pressure is created.

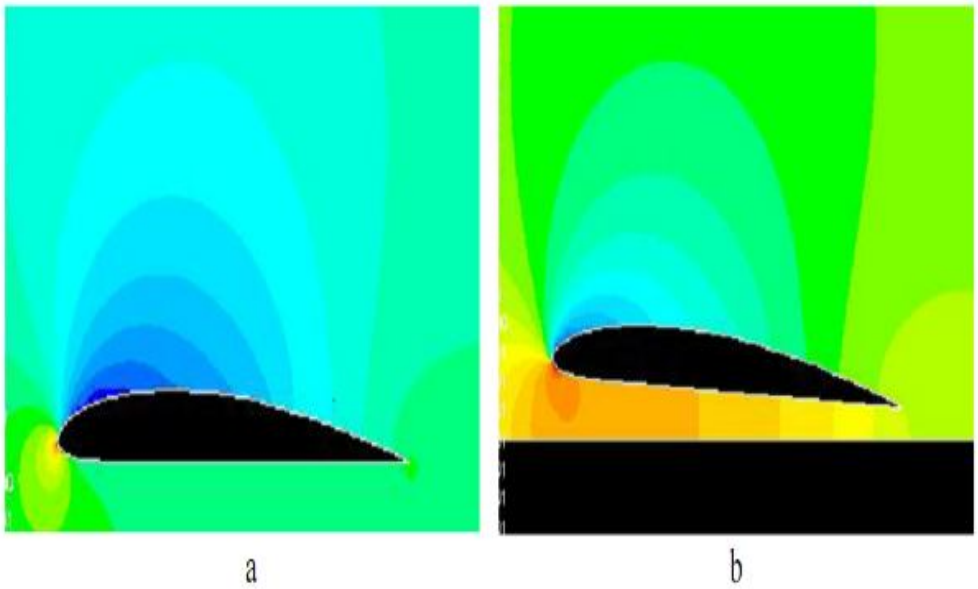

Figure 4.6 Contour Plot of Static Pressure on An Air Foil a) Out of Ground Effect b) In Ground Effect [31]

Rozhdestvensky predicted for the case of flat plate (similar airfoil is used here) with infinite span in the presence of extreme ground effect ($^{H}/_{c} \leq 0.1$), a closed form

solution for C_L and C_M can be obtained by a modification of the thin airfoil theory [22] and the associated formulas are given as

$$C_L = \frac{\alpha}{H} \qquad (4.27)$$

$$C_L m = -\frac{\alpha}{3H} \qquad (4.28)$$

In Equation 4.28, the coefficient of moment is taken with respect to the leading edge.

It must also be kept in mind that, Equations 4.27 and 4.28 also bring a problem about pressure center. They imply pressure center to be around one third of the chord; generally it is one forth. When it is out of ground, this thing must be considered during an aerodynamic analysis.

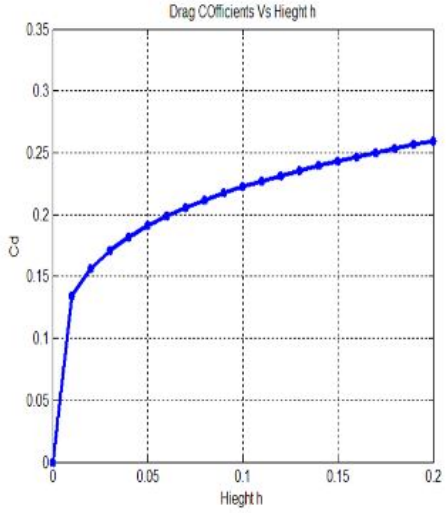

Figure 4.7 a: C_D vs H

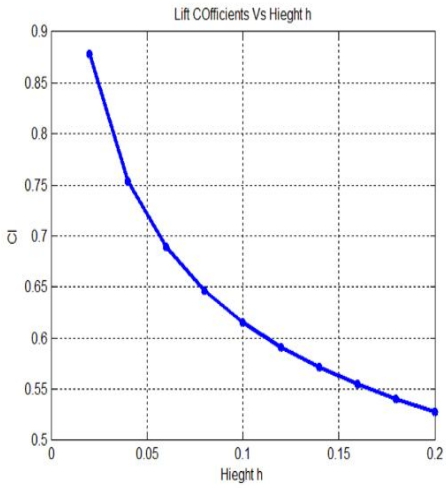

Figure 4.7 b: C_L vs H

Figure 4.7 H vs Aerodynamics

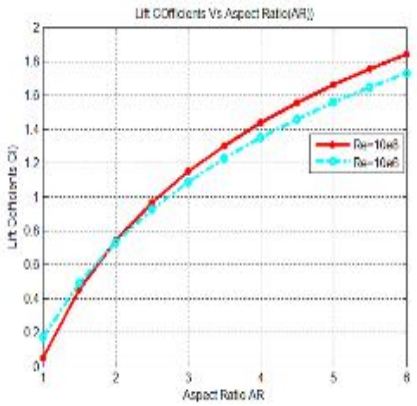

Figure 4.8 a: C_L vs H

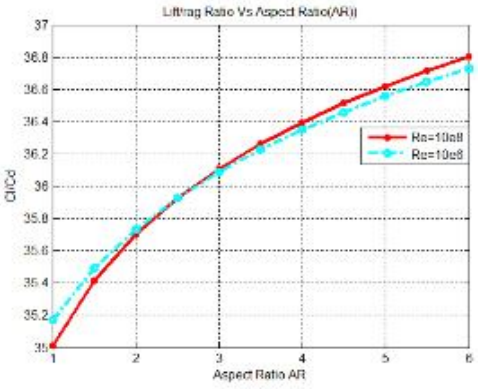

Figure 4.8 b: C_L/C_D vs H

Figure 4.8 AR Effect on L & D

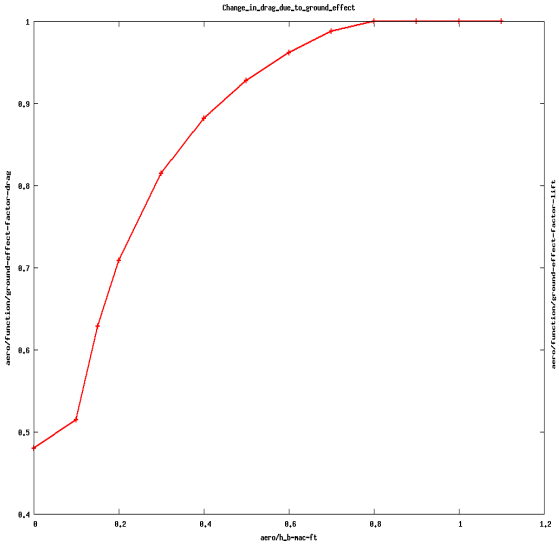

Figure 4.9 a: Change in Lift Due to GE

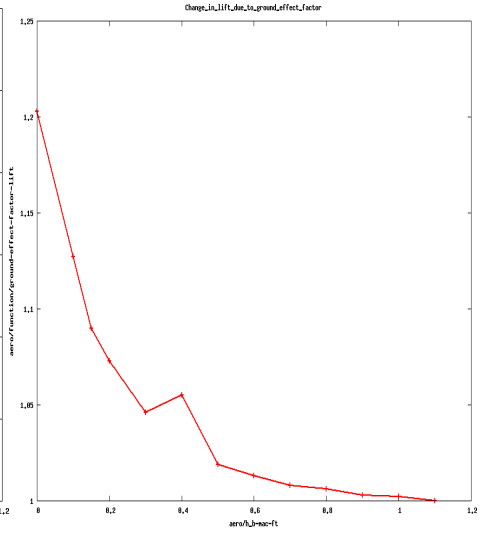

Figure 4.9 b: Change in Drag Due to GE

Figure 4.9 Effect of GE on L & D

CHAPTER 5

MATHEMATICAL MODELLING (DYNAMICS) OF WIG VEHICLE

This chapter is about the mathematical modeling of the vehicle in detail. It consists of development of a 6DOF nonlinear dynamical model, all forces and moments including ground effect, aerodynamics, propulsion, gravity, atmospheric elements and mass-inertia having been included.

The nonlinear equations of motion of the craft are developed by applying Newton's second law and law of conservation of linear momentum. The equations are written in a body fixed axis system, which moves with the airplane and which has its origin at the craft's center of mass. The vehicle is assumed to be a rigid body with six degrees of freedom. Three translational degrees describe the motion of the center of mass and three attitude degrees describe the orientation of the vehicle. Plane XZ is a plane of symmetry of the airplane and YZ plane is also considered as plane of symmetry, although it has a smaller value of I_{yz} which is negligible. For details about aircraft modeling and dynamics of flight, please refer to [34], [35] and [36]. Before going into the derivation of the mathematical model, it is important to consider frames and coordinate systems first.

5.1 Frames of Reference / Coordinate Systems

Frames and coordinate systems are of primary importance for modeling and system representation and its analyses, to simulate its movement and dynamics. Following frames are used:

1. Inertial Frame: A non-rotating non-accelerating frame is required to develop and visualize the equations of motions, so that Newton's laws are applicable in it**.** This frame is called Inertial Reference Frame [34]. However no such frames exist in realty; to resolve this issue, it has been assumed that Earth is fixed, non-rotating and its surface is flat. In fact, for WIG it is a very genuine assumption, since WIG always keeps itself at low flight. So, Earth surface can be considered as flat, non-rotating and also non-accelerating and its surface can be used as a reference. Therefore, Earth fixed reference frame has been introduced, which is fixed on Earth surface (control room) and considered as the inertial frame which is taken as a reference for all other frames. Position of the vehicle is always calculated wrt. this inertial frame. Its origin is on Earth surface with Oz is directed towards downward, X axis is towards North and Y axis is towards East.

2. Vehicle Carried Normal Frame: Another frame known as vehicle carried frame or Navigation frame or North East Down frame is defined such that its origin is attached with the Centre of Gravity (CG) of the vehicle and Z axis is downwards in the direction of Gravity, while X is again towards North and Y to the East.

3. Wind Frame: It is another important frame used, especially for representing wind and atmospheric elements. Its X axis is towards the velocity of air (parallel to free velocity of stream), Y axis is towards acceleration of air and Z axis can be found by the right hand rule.

4. Body Frame: Another major and important frame is the Body Frame or Orthogonal-Body coordinate frame [36]. Here, the vehicle is considered as a rigid body. Although it is not an inertial frame, it is very important for dynamics; in fact, all motions, forces and moments are described (transformed) in this frame. Again its center is the CG of the vehicle body and X axis is from CG towards the nose of the craft. Z axis is again downwards towards the center of Earth and Y axis towards right side, if looked from rear, as a right handed coordinate system.

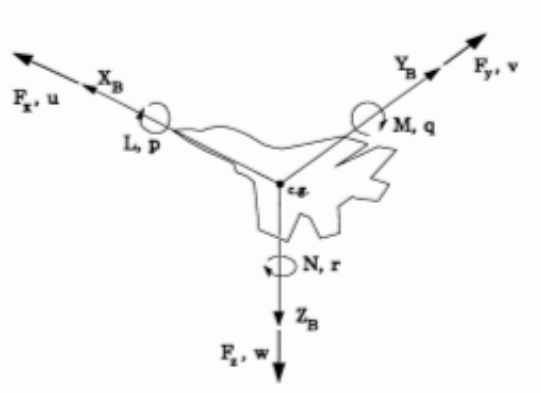

Figure 5.1 Body Frame and Motions about It

5.1 Relationship between Frames: Any vector can be transformed from one frame to another by transformation matrices. As mentioned before, vehicle's dynamic velocities, forces and moments are considered in the body frame. Here, two major transformations are important, besides some others, as well,

- One is from Earth fixed frame (EFF) to Body frame (BF) for gravitational forces.
- Other is from Wind to Body frame for aerodynamics.

Vectors from EFF to BF can be obtained simply by multiplying them by the transformation matrix,

$$X_B = T_{B \to E} X_E \qquad (5.1)$$

This transformation is called Direction Cosines matrix. It is orthonormal and gives the orientation of BF wrt. EFF and is the result of the following three rotation sequence:

- Rotation about the z-axis (yaw Ψ).
- Rotation about the new y-axis (pitch θ).
- Rotation about the new x-axis (roll φ).

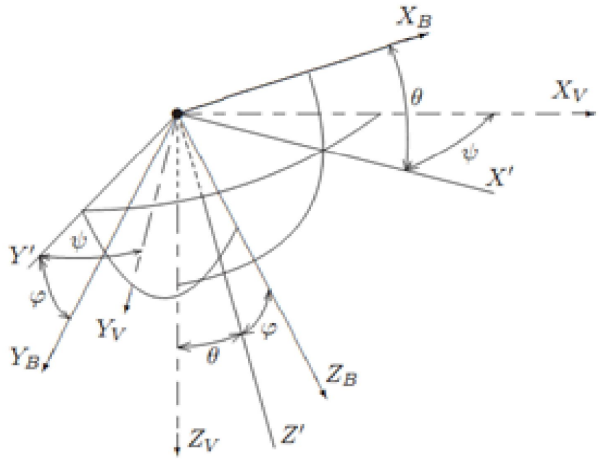

Figure 5.2 Rotations between Different Frames

These yaw, pitch and roll angles are called Euler Angles.

$$C_1 = \begin{bmatrix} cos(\psi) & -sin(\psi) & 0 \\ sin(\psi) & cos(\psi) & 0 \\ 0 & 0 & 1 \end{bmatrix} \quad (5.2)$$

$$C_2 = \begin{bmatrix} cos(\theta) & 0 &) \\ 0 & 1 & 0 \\ -sin(\theta) & 0 & cos(\theta) \end{bmatrix} \quad (5.3)$$

$$C_3 = \begin{bmatrix} 1 & 0 & 0 \\ 0 & cos(\phi) & -sin(\phi) \\ 0 & sin(\phi) & cos(\phi) \end{bmatrix} \quad (5.4)$$

Resultant transformation matrix is:

$$T_{bn} = \begin{bmatrix} cos\psi cos\theta & sin\psi cos\theta & -sin\theta \\ cos\psi sin\theta sin\phi - sin\psi cos\phi & sin\psi sin\theta sin\phi + cos\psi cos\phi & cos\theta sin\phi \\ cos\psi\ sin\theta cos\phi - sin\psi sin\phi & sin\psi sin\theta cos\phi - cos\psi sin\phi & cos\theta cos\phi \end{bmatrix}$$

(5.5)

The other one, transformation from the Wind Frame (WF) or Wind axis to BF consists of two simple transformations or rotations, one is by angle alpha α around y axis. This angle is also known as the angle of attack (AoA). The other rotation is by the angle beta β, around z axis of WF. This angle is also known as the side slip angle. These

angles are also of primary importance for aerodynamics and for the movement of the whole body.

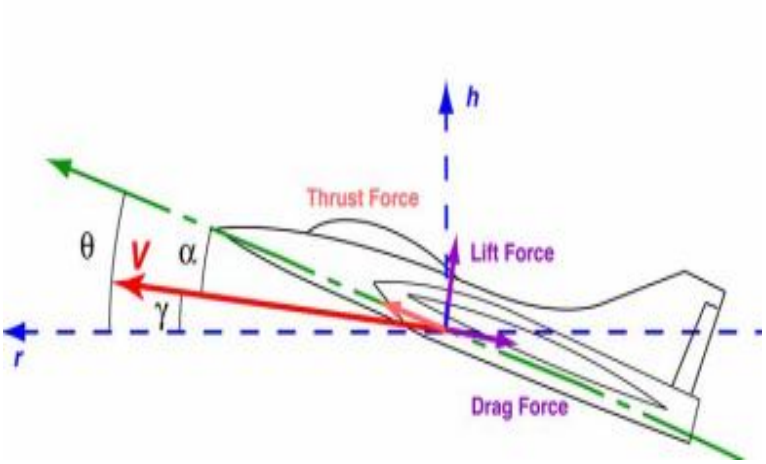

Figure 5.3 a: Different Flight Angles

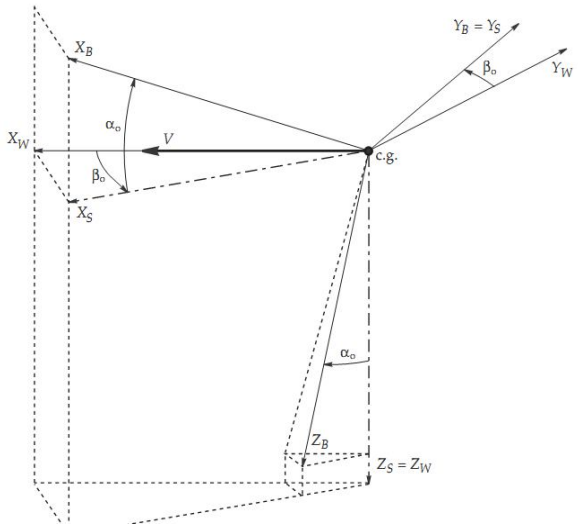

Figure 5.3 b: Frames Rotations

Figure 5.3 Transformation Frames

The transformation matrix is:

$$T_{bw} = \begin{bmatrix} cos\alpha\ cos\beta & -cos\alpha\ sin\beta & -sin\alpha \\ sin\beta & cos\beta & 0 \\ sin\alpha\ cos\beta & sin\alpha\ sin\beta & cos\alpha \end{bmatrix} \qquad (5.6)$$

5.2 Dynamic Equations of Motion (6DOF)

Before going into details, here are some important assumptions:

- Vehicle body is considered to be rigid, during motion.
- Mass of the vehicle is also considered to be constant (no change in mass due to fuel consumption). In other words, center of gravity does not change during the time of simulation.
- Earth is assumed to be fixed (no rotation).
- The curvature of the Earth is neglected.
- Steady atmospheric state (non-steady atmospheric state adds some disturbances which are neglected).

The equations of motion for the vehicle can be developed by writing Newton's second law for each differential element of mass in the vehicle,

$$d\vec{F} = \vec{a}dm \qquad (5.3)$$

To find the total force, it is integrated over the entire vehicle. The components of velocity and force along the axes Ox, Oy and Oz are denoted by (u, v, w) and (X, Y, Z), respectively. The first task is to define the inertial acceleration components resulting from the application of disturbance force components on the aircraft. Consider the motion referred to an orthogonal axis set (Oxyz) with the origin O coincident with the CG of the body. The body, and hence the axes, are assumed to be

in motion with respect to an external reference frame such as Earth (or inertial frame). The components of angular velocity and moment about the same axes are denoted by (p, q, r) and (L, M, N), respectively. The point p is an arbitrarily chosen point within the body with coordinates (x, y, z). The local components of velocity and acceleration at p relative to the body axes are denoted by (u, v, w) and (ax, ay, az), respectively. The velocity components at any point p (x, y, z) relative to O are given in Figure 5.4. During working out the acceleration of each mass element, the contributions of its velocities from both linear velocities (u, v, w) in each of the coordinate directions and rotational velocities (p, q, r) about the axes, are taken into account.

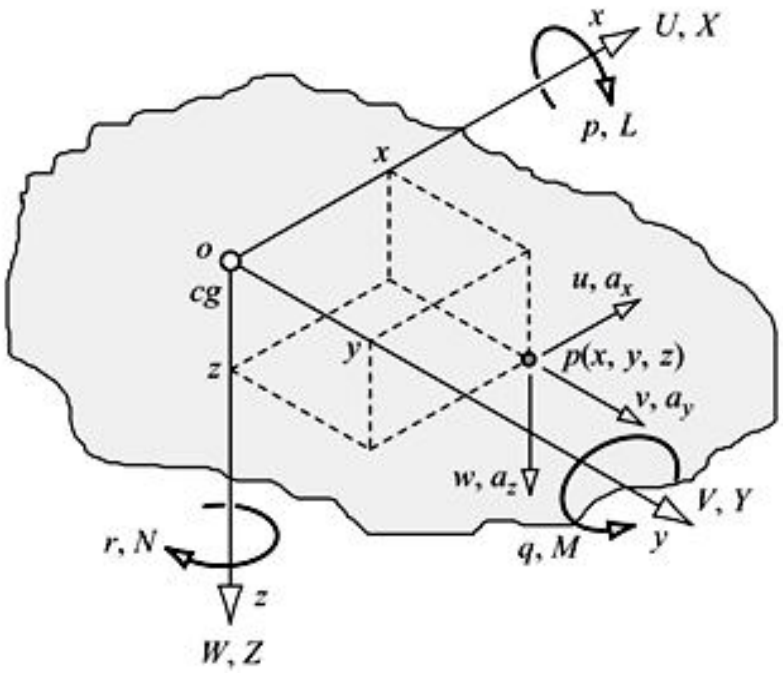

Figure 5.4 Different Motions of Rigid Body [35]

Motion can be divided into two parts, first is known as the translational motion which is due to change of position in space and the other is rotational motion due to change of orientation in space. Both changes contribute to total 6DOF.

5.2.1 Translational Dynamics

Translational motion is the change in the position. It can be explained by the motion of the CG or center of mass (CM). From Newton's second law:

$$d\vec{F} = \mathrm{m}.d\vec{a} = \mathrm{m}.\overrightarrow{d\left(\frac{d}{dt}(\vec{V})\right)} \qquad (5.4)$$

where F is total force on the body and V is total velocity of the body. Derivative of velocity (wrt. EFF) can be determined by the sum of cross product of angular velocity and linear velocity and total velocity of body (BF) as given in Equation 5.5.

$$\frac{d}{dt}\left(\vec{V}_T\right)_E = \left(\frac{d}{dt}\vec{V}_T\right)_B + \vec{\omega} \times \vec{V}_T \qquad (5.5)$$

The second term in Equation 5.5, which is also known as the Coriolis Effect is the motion resulting from the relative angular velocity of the moving frame with respect to the reference frame. In body frame, these vectors can be expressed as:

$$\vec{V}_T = \vec{\imath}u + \vec{\jmath}v + \vec{k}w \qquad (5.6)$$

$$\vec{\omega} = \vec{\imath}p + \vec{\jmath}q + \vec{k}r \qquad (5.7)$$

where i, j and k are the unit representative vectors along x, y, z axes of BF, respectively. The local components of velocity and acceleration at p (x, y, z) relative to the body axes are given by

$$\begin{cases} u = \dot{x} - ry + qz \\ v = \dot{y} - pz + rx \\ w = \dot{z} - qx + py \end{cases} \qquad (5.8)$$

Now, since the body in Figure 5.3, is assumed to be rigid, so locally $\dot{x} = \dot{y} = \dot{z} = 0$ holds. Then, Equation 5.8 is converted to

$$\begin{cases} u = -ry + qz \\ v = -pz + rx \\ w = -qx + py \end{cases} \qquad (5.9)$$

The resultant components of the total force acting on the rigid body are given by

$$
\begin{aligned}
m(\dot{U} - rV + qW) &= X \\
m(\dot{V} - pW + rU) &= Y \\
m(\dot{W} - qU + pV) &= Z
\end{aligned}
\qquad (5.10)
$$

where m is the total mass of the body, (X, Y, Z) are the total force components acting on the body and (u, v, w) are the velocity components. Individual components along BF axes are,

$$
\begin{aligned}
\dot{u_e} &= \frac{X}{m} + rV - qw \\
\dot{v_e} &= \frac{Y}{m} - ru + pw \\
\dot{w_e} &= \frac{Z}{m} - pv + qu
\end{aligned}
\qquad (5.11)
$$

Sometimes V, α and β are used instead of u, v and w. so, their equivalent are given in Equation 5.12. For the derivation, reference [37] is useful. Steady atmospheric environment is assumed, so wind disturbance part is considered zero:

$$
\begin{aligned}
\dot{V} &= \frac{1}{m}(X cos\alpha cos\beta + Y sin\beta + Z sin\alpha sin\beta) \\
&\quad + (Non\ steady\ atmospheric\ disturbances\ cosidered\ zero\ here) \\
\dot{\alpha} &= \frac{1}{V cos\beta}\left\{\frac{1}{m}(-X sin\alpha + Z cos\alpha)\right. \\
&\quad \left. + (Non\ steady\ atmospheric\ disturbances\ cosidered\ zero\ here)\right\} \\
&\quad + q - (p cos\alpha + r sin\alpha) tan\beta \\
\dot{\beta} &= \frac{1}{V}\left\{\frac{1}{m}(-X cos\alpha sin\beta + Y cos\beta - Z sin\alpha sin\beta)\right. \\
&\quad \left. + \begin{pmatrix} Non\ steady\ atmospheric\ disturbances\ cosidered \\ zero\ here \end{pmatrix}\right\} \\
&\quad + q - (p sin\alpha + r cos\alpha)
\end{aligned}
\qquad (5.12)
$$

5.2.2 Rotational Dynamics

Rotational motion is regarded with change in orientation; it is around the frame axis. Again from Newton second law of motion, torque can be written as:

$$\vec{M} = \frac{d}{dt}(\vec{H}) \qquad (5.13)$$

where H is the angular momentum and M is the torque on the body. Angular momentum can be given as:

$$\vec{H} = I\vec{\omega} \qquad (5.14)$$

ω is the angular velocity and I is the inertia matrix. The inertia matrix is given in Equation 5.15:

$$I = \begin{bmatrix} I_{xx} & -I_{xy} & -I_{xz} \\ -I_{xy} & -I_{yy} & -I_{yx} \\ -I_{xz} & -I_{yz} & -I_{zz} \end{bmatrix} \qquad (5.15)$$

$$\begin{aligned} I_x &= \int_m (y^2 + z^2)\, dm \\ I_y &= \int_m (z^2 + x^2)\, dm \\ I_z &= \int_m (x^2 + y^2)\, dm \end{aligned} \qquad (5.16)$$

$$Ixy = \sum xy\ \delta m \qquad (5.17)$$

$$I_{xz} = \sum xz\ \delta m \qquad (5.18)$$

$$I_{yz} = \sum yz\ \delta m \qquad (5.19)$$

These different I_s are the moments of inertia and can be considered as the resistance of the body to rotational motion. They act the same as the mass in translational motion. They depend on the axis system and its location. I_{xy}, I_{xz} and I_{yz} are the product of inertia terms, and taken to be the zero since WIG vehicle is symmetric in yz and xz planes. That is the reason of why the cross product of the last term is zero.

Similarly, the other relations can be given as:

$$\frac{d}{dt}(\vec{H})_E = \frac{d}{dt}(\vec{H})_B + \vec{\omega} \times \vec{H} \qquad (5.20)$$

The moment equation in the BF is

$$\vec{M} = \left(\dot{p}I_{xx} + qr\left(I_{zz} - I_{yy}\right)\right)\bar{\imath} + \left(\dot{q}I_{yy} + pr(I_{xx} - I_{zz})\right)\bar{\jmath} + \left(\dot{r}I_{zz} + pq(I_{yy} - I_{xx})\right)\bar{k} \qquad (5.21)$$

From Equation 5.21, three components of moment along axes can be written as:

$$\begin{aligned} I_x\dot{p} - \left(I_y - I_z\right)qr - I_{xz}(pq + \dot{r}) &= L \\ I_y\dot{q} - (I_x - I_z)pr + I_{xz}(p^2 - r^2) &= M \\ I_z\dot{r} - \left(I_x - I_y\right)pq + I_{xz}(qr + \dot{p}) &= N \end{aligned} \qquad (5.22)$$

Finally $\dot{p}$, $\dot{q}$ and $\dot{r}$ can be written as:

$$\dot{p} = qr(I_{yy} - I_{zz})/I_{xx} + M_x/I_{xx} \qquad (5.23)$$

$$\dot{q} = pr(I_{zz} - I_{xx})/I_{yy} + M_y/I_{yy} \qquad (5.24)$$

$$\dot{r} = pq(I_{xx} - I_{yy})/I_{zz} + M_z/I_{zz} \qquad (5.25)$$

Equation 5.25 can be transformed to Equation 5.26 by using the definition in Table 5.1:

$$\begin{aligned} \dot{p} &= P_{pp}p^2 + P_{pq}pq + P_{qq}q^2 + P_{qr}qr + P_{rr}r^2 + P_lL + P_mM + P_nN \\ \dot{q} &= Q_{pp}p^2 + Q_{pq}pq + Q_{qq}q^2 + Q_{qr}qr + Q_{rr}r^2 + Q_lL + Q_mM + Q_nN \\ \dot{r} &= R_{pp}p^2 + R_{pq}pq + R_{qq}q^2 + R_{qr}qr + R_{rr}r^2 + R_lL + R_mM + R_nN \end{aligned} \qquad (5.26)$$

Some definitions which are used previously and in Equation 5.26, are given below in Table 5.1:

Table 5.1 Mass and Inertial Parameter Definitions [43]

symbol	definition
$\|I\|$	$I_{xx}I_{yy}I_{zz} - 2J_{xy}J_{xz}J_{yz} - I_{xx}{J_{yz}}^2 - I_{yy}{J_{xz}}^2 - I_{zz}{J_{xy}}^2$
I_1	$I_{yy}I_{zz} - {J_{yz}}^2$
I_2	$J_{xy}I_{zz} + J_{yz}J_{xz}$
I_3	$J_{xy}J_{yz} + I_{yy}J_{xz}$
I_4	$I_{xx}I_{zz} - {J_{xz}}^2$
I_5	$I_{xx}J_{yz} + J_{xy}J_{xz}$
I_6	$I_{xx}I_{yy} - {J_{xy}}^2$
P_l	$I_1 \ / \ \|I\|$
P_m	$I_2 \ / \ \|I\|$
P_n	$I_3 \ / \ \|I\|$
P_{pp}	$-(J_{xz}I_2 - J_{xy}I_3) \ / \ \|I\|$
P_{pq}	$(J_{xz}I_1 - J_{yz}I_2 - (I_{yy} - I_{xx})I_3) \ / \ \|I\|$
P_{pr}	$-(J_{xy}I_1 + (I_{xx} - I_{zz})I_2 - J_{yz}I_3) \ / \ \|I\|$
P_{qq}	$(J_{yz}I_1 - J_{xy}I_3) \ / \ \|I\|$
P_{qr}	$-((I_{zz} - I_{yy})I_1 - J_{xy}I_2 + J_{xz}I_3) \ / \ \|I\|$
P_{rr}	$-(J_{yz}I_1 - J_{xz}I_2) \ / \ \|I\|$
Q_l	$I_2 \ / \ \|I\|$
Q_m	$I_4 \ / \ \|I\|$
Q_n	$I_5 \ / \ \|I\|$
Q_{pp}	$-(J_{xz}I_4 - J_{xy}I_5) \ / \ \|I\|$
Q_{pq}	$(J_{xz}I_2 - J_{yz}I_4 - (I_{yy} - I_{xx})I_5) \ / \ \|I\|$
Q_{pr}	$-(J_{xy}I_2 + (I_{xx} - I_{zz})I_4 - J_{yz}I_5) \ / \ \|I\|$
Q_{qq}	$(J_{yz}I_2 - J_{xy}I_5) \ / \ \|I\|$
Q_{qr}	$-((I_{zz} - I_{yy})I_2 - J_{xy}I_4 + J_{xz}I_5) \ / \ \|I\|$
Q_{rr}	$-(J_{yz}I_2 - J_{xz}I_4) \ / \ \|I\|$
R_l	$I_3 \ / \ \|I\|$
R_m	$I_5 \ / \ \|I\|$
R_n	$I_6 \ / \ \|I\|$
R_{pp}	$-(J_{xz}I_5 - J_{xy}I_6) \ / \ \|I\|$
R_{pq}	$(J_{xz}I_3 - J_{yz}I_5 - (I_{yy} - I_{xx})I_6) \ / \ \|I\|$
R_{pr}	$-(J_{xy}I_3 + (I_{xx} - I_{zz})I_5 - J_{yz}I_6) \ / \ \|I\|$
R_{qq}	$(J_{yz}I_3 - J_{xy}I_6) \ / \ \|I\|$
R_{qr}	$-((I_{zz} - I_{yy})I_3 - J_{xy}I_5 + J_{xz}I_6) \ / \ \|I\|$
R_{rr}	$-(J_{yz}I_3 - J_{xz}I_5) \ / \ \|I\|$

5.2.3 Kinematic Dynamics

Kinematic differential equations (of motion) are used to describe the geometric and orienteering relations of flight between BF and EFF. In fact, it is important and necessary to specify the orientation of BF wrt. EFF.

5.2.4 Translational Kinematics

Relationship of velocity component between EFF and BF can be given as:

$$\begin{bmatrix} \dot{x} \\ \dot{y} \\ \dot{z} \end{bmatrix} = T_{B\to E} \begin{bmatrix} u_e \\ v_e \\ w_e \end{bmatrix} \qquad (5.27)$$

where (u, v, w) are the velocities in BF and (x, y, z) are the coordinates in the EFF. The navigation equations relate aircraft translational velocity components in BF to Earth-axis components, neglecting wind effects. These differential equations describe the time evolution of the position of the aircraft's CG relative to Earth axes as follows:

$$\dot{x}_E = u\cos\psi\cos\theta + v(\cos\psi\sin\theta\sin\phi - \sin\psi\cos\phi) + w(\cos\psi\sin\theta\cos\phi + \sin\psi\sin\phi) \qquad (5.28)$$

$$\dot{y}_E = u\sin\psi\cos\theta + v(\sin\psi\sin\theta\sin\phi) \ldots \qquad (5.29)$$

$$+w(\sin\psi\sin\theta\cos\phi - \cos\psi\sin\phi)$$

$$\dot{z}_E = -u\sin\theta + v\cos\theta\sin\phi + w\cos\theta\cos\phi \qquad (5.30)$$

where x_E, y_E and z_E are the x, y, z are in EFF, [34], [35]. Also, as a common practice, altitude (H) of aircraft is used instead of the coordinate Z, through the relationship

$$\dot{H} = -\dot{Z} \qquad (5.31)$$

Negative sign is used since Z axis in EFF is negative upward, opposite to altitude H.

5.2.5 Rotational Kinematics

Differential equations of the Euler angles are called rotational kinematic equations (RKE). Common practice to get RKE, is by direction cosines which are orthonormal. Orientation position change occurs because of rotational rates or angular velocities.

For RKEs, basic transformation from EFF frame to BF are defined in the following equations.

$$\vec{V}_B = C_E^B \vec{V}_E \qquad (5.32)$$

$$\frac{d}{dt_E}\vec{V}_B = C_E^B \dot{\vec{V}}_E \qquad (5.33)$$

$$\frac{d}{dt_B}\dot{\vec{V}}_B = \dot{\vec{V}}_B = C_E^B \dot{\vec{V}}_E + \left(\dot{C}_E^B\right)V_E \qquad (5.34)$$

$$\frac{d}{dt_E}\dot{\vec{V}}_B = \dot{\vec{V}}_B - \dot{C}_E^B \vec{V}_E \qquad (5.35)$$

The Coriolis Effect can be written as shown below:

$$\vec{\omega}_B \times \vec{V}_B = \Omega_B C_E^B \vec{V}_E \qquad (5.36)$$

The rotational kinematic equations, which relate Euler angular rates to body-axis angular rates, are given by

$$\omega_B = [p \quad q \quad r]^T \qquad (5.37)$$

$$\begin{aligned} \dot{C}_E^B &= -\Omega_B C_E^B \\ \Omega_B &= \dot{C}_E^B C_E^B \end{aligned} \qquad (5.38)$$

The rotational kinematic equations, which relate Euler angular rates to body-axis angular rates, are given by

$$\begin{aligned} \dot{\theta} &= q\cos(\phi) - r\sin(\phi) \\ \dot{\phi} &= p + q\sin(\phi)\tan(\theta) + r\cos(\phi)\tan(\theta) \\ \dot{\psi} &= (q\sin(\phi) + r\cos(\phi))\sec(\theta) \end{aligned} \qquad (5.39)$$

where θ, ϕ, ψ are the pitch, row and yaw attitude angels, respectively. The 12 ordinary differential equations from Equations 5.39, 5.30, 5.26, 5.11 and 5.12 define basic dynamics of rigid body and will constitute the main structure for simulation.

5.3 Force and Moment Equations

Together, above motion equations comprise the generalized six degrees of freedom equations of motion of a rigid body with a symmetric airframe having a uniform mass distribution. Further development of the equations of motion requires that the terms on the right hand side of the equations adequately describe the disturbance forces and moments. The traditional approach, after Bryan (1911), is to assume that the disturbance forces and moments are due to aerodynamic effects, gravitational effects and movement of aerodynamic controls. Therefore, we can write:

$$\begin{aligned} X = X_a + X_g + X_c,\ Y = Y_a + Y_g + Y_c,\ Z = Z_a + Z_g + Z_c \\ L = L_a + L_g + L_c,\ M = M_a + M_g + M_c,\ N = N_a + N_g + N_c \end{aligned} \quad (5.40)$$

5.3.1 Gravity Model

The gravitational force components are first transformed from EFF to BF and can be described by Equation 5.14 [34]:

$$\begin{aligned} X_g &= -mg \sin\theta_e - mg \cos\theta_e \\ Y_g &= mg\psi \sin\theta_e + mg\phi \cos\theta_e \\ Z_g &= mg \cos\theta_e - mg\theta \sin\theta_e \end{aligned} \quad (5.41)$$

5.3.2 Aerodynamics

Aerodynamic forces and moments can be determined in two ways: by experimental methods (flight tests or wind tunnel tests), by computational and/or empirical methods. Second method is used here, based on DATCOM, [38]. The main emphasis is on the so-called build-up method for modeling aerodynamic and thrust forces and moments. In this method, the craft is assumed to be built up from a number of components. The total forces and moments, which act on the airplane, are then assumed to follow from summing the forces and moments, which act on these components, [35], [36]. In these components, aerodynamic forces can be expressed as follows:

$$F_{AA/C} = F_{Awb} + F_{Atail} + F_{Av} \quad (5.42)$$

DATCOM or digital DATCOM or Stability and Control DATCOM is a computer software that is used to determine the control and dynamic derivative characteristics and static stability, of aircrafts with fixed wings or fixed structures, by using computational methods to determine stability and control derivatives. This program is produced and licensed by United State Air Force (USAF). DATCOM requires an input file containing a geometric description of an aircraft, and outputs its corresponding dimensionless stability derivatives according to the specified flight conditions. The values obtained can be used to calculate meaningful aspects of flight dynamics.

DATCOM provides good initial idea/guess about aerodynamics. Basically these values can be used as an initial guess and further improvements can be brought by system identification methods or other methods like Computational Fluid Dynamics (CFD) etc.

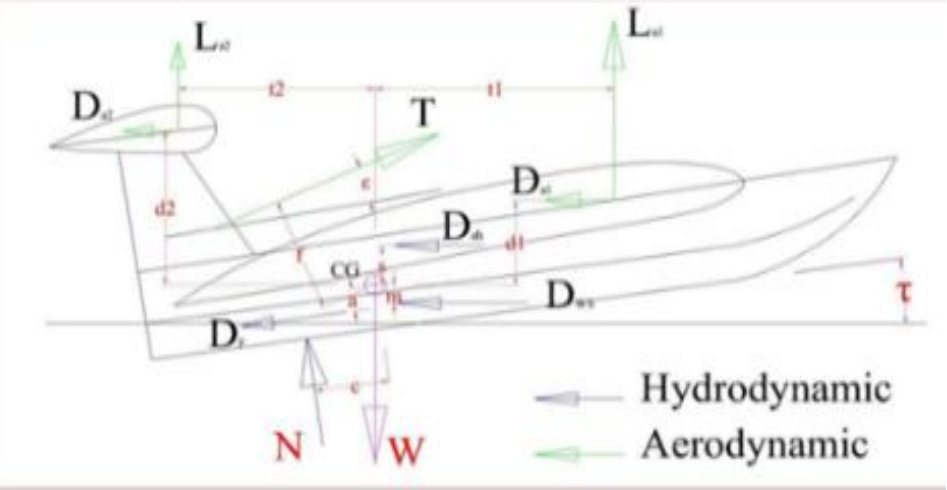

Figure 5.5 Longitudinal and Lateral Forces

Figure 5.5 illustrates the longitudinal aerodynamic forces and moments that act on the WIG craft in a steady state flight condition. In the stability axis system, longitudinal forces and moments are written as:

$$F_{Axs} = X = -D \quad \text{Along x axis} \quad (5.43)$$

$$F_{Azs} = \mathrm{Z} = -L \text{ Along z axis} \qquad (5.44)$$

$$M_{As} = M_{As} \text{ Airplane pitching moment} \qquad (5.45)$$

In stability axis system, aerodynamical lateral moments are

$$L_{As} = L_A \text{ Rolling Moment} \qquad (5.46)$$

$$F_{Ays} = \mathrm{Y} = Y_A \text{ Side Force} \qquad (5.47)$$

$$N_{As} = N_A \text{ Yawing Moment} \qquad (5.48)$$

The steady state models for airplane drag force, lift force and aerodynamic moment can be given as:

$$D = C_D qS \qquad (5.49)$$

$$L = C_L qS \qquad (5.50)$$

$$M_A = C_m qS\mathrm{c} \qquad (5.51$$

where C_D, C_L and C_M are drag, lift and moment coefficients, respectively, which are defined as:

$$C_L = C_{L0} + C_{L_a}\alpha + C_{L\delta_e} + C_{L\delta_f} \qquad (5.52)$$

$$C_D = C_{D0} + C_{D_a}\alpha + C_{D\delta_e} + C_{D\delta_f} \qquad (5.53)$$

$$C_m = C_{m\alpha}\alpha + C_{m_a}\dot{\alpha} + C_{m\delta_e}\delta_e + C_{mq}q + C_{m\delta_f}\delta_f \qquad (5.54)$$

$C_{D_a} = \frac{dCd}{d\alpha}$: The change of airplane drag due to change in airplane angle of attack.

$C_{D\delta_e} = \frac{dCd}{d\delta_e}$: The change of airplane drag due to change in δ_e.

$C_{D\delta_e} = \frac{dCd}{d\delta_f}$: The change of airplane drag due to change in δ_f.

$C_{L_a} = \frac{dCl}{d\alpha}$: The change of airplane lift due to change in airplane angle of attack.

$C_{L\delta_e} = \frac{dCl}{d\delta_e}$: The change of airplane lift due to change in δ_e.

$C_{L\delta_e} = \frac{dCl}{d\delta_f}$: The change of airplane lift due to change in δ_f.

Altogether, they can be written as:

$$F_{Axs} = -\mathrm{D} = -C_D \bar{q} Sb = \left(C_{D0} + C_{D_a}\alpha + C_{D\delta_e} + C_{D\delta_f}\right) qSb \qquad (5.55)$$

$$F_{Fxs} = -\mathrm{L} = -C_L \bar{q} S = \left(C_{L0} + C_{L_a}\alpha + C_{L\delta_e} + C_{L\delta_f}\right) qS \qquad (5.56)$$

$$L_{As} = L_A = C_l \bar{q} Sb = (C_{n0} + C_{n\beta}\beta + C_{np}p + C_{nr}r + C_{n\delta_a}\delta_a + C_{y\delta_r}\delta_r) qSb \qquad (5.57)$$

$$L_{As} = L_A = C_l \bar{q} Sb = (C_{yo} + C_{l\beta}\beta + C_{lp}p + C_{lr}r + C_{l\delta_a}\delta_a + C_{l\delta_r}\delta) qSb \qquad (5.58)$$

$$F_{As} = Y_A = C_y \bar{q} S = (C_{yo} + C_{y\beta}\beta + C_{yp}p + C_{yr}r + C_{y\delta_a}\delta_a + C_{y\delta_r}\delta_r) qS \qquad (5.59)$$

$$L_{As} = L_A = C_l \bar{q} Sb = (C_{n0} + C_{n\beta}\beta + C_{np}p + C_{nr}r + C_{n\delta_a}\delta_a + C_{y\delta_r}\delta_r) qSb \qquad (5.60)$$

As mentioned before, these coefficients are determined by using DATCOM. Now, in the steady trimmed flight condition, all of the perturbation variables and their derivatives are, by definition, zero. Thus, in the steady state we can have:

$$X_{ae} = mg\sin\theta_e\,,\ Y_{ae} = 0,\ Z_{ae} = -mg\cos\theta_e \qquad L_{ae} = M_{ae} = N_{ae} = 0 \qquad (5.61)$$

It should be noted that the lift force (L) should be modified with $L' = L/(1-\sigma_{ge})$ because of GE.

Following are some of aerodynamic files, presenting the relations between different parameters of aerodynamics of the vehicle, which are determined by using DATCOM+.

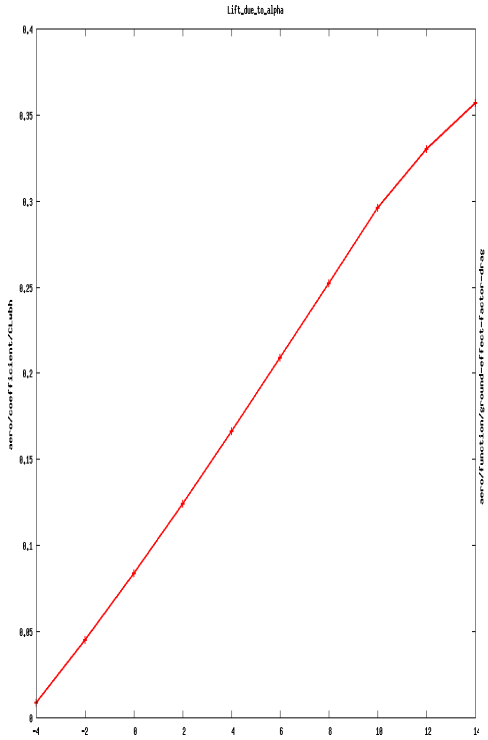

Figure 5.6 a: Change Lift due to AoA

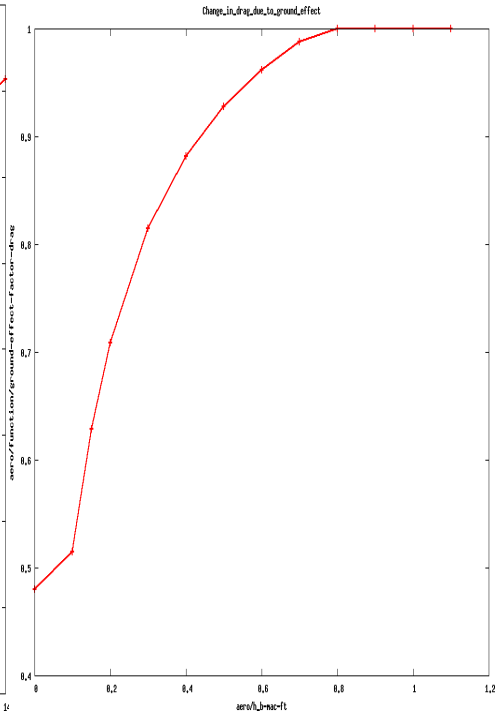

Figure 5.6 b: Change in D due to GE

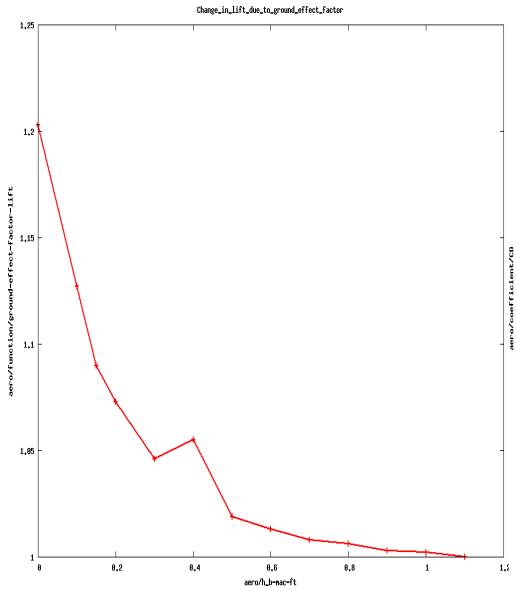

Figure 5.6 c: Change in L due to GE

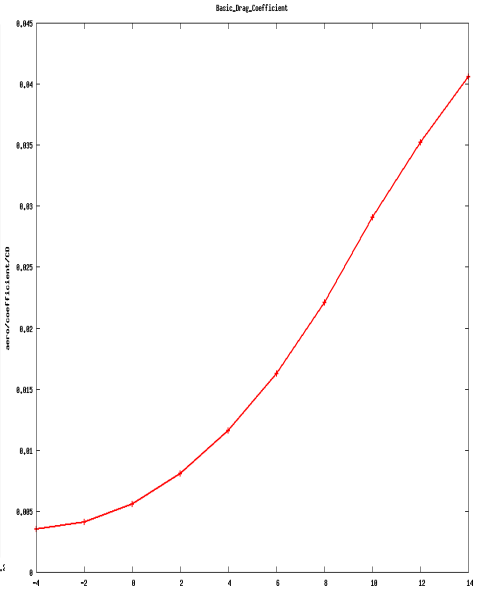

Figure 5.6 d: Basic C_D vs AoA

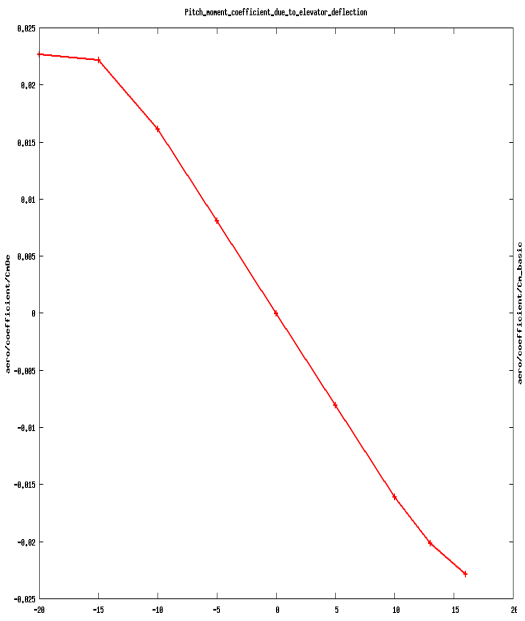

Figure 5.6 e: Cm vs Aileron Deflection

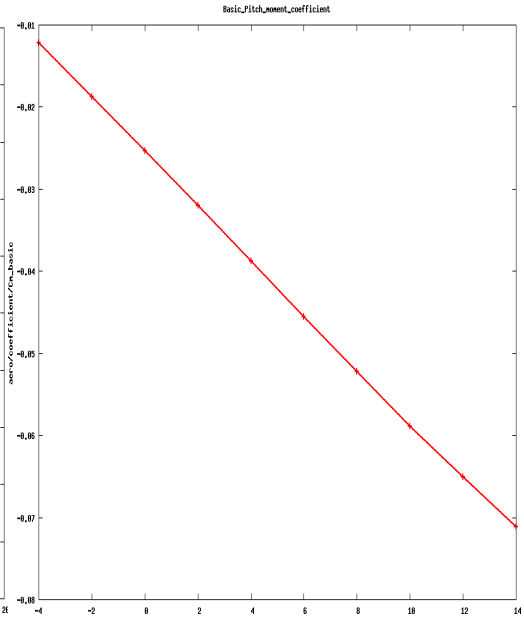

Figure 5.6 f: Basic Cm vs AOA

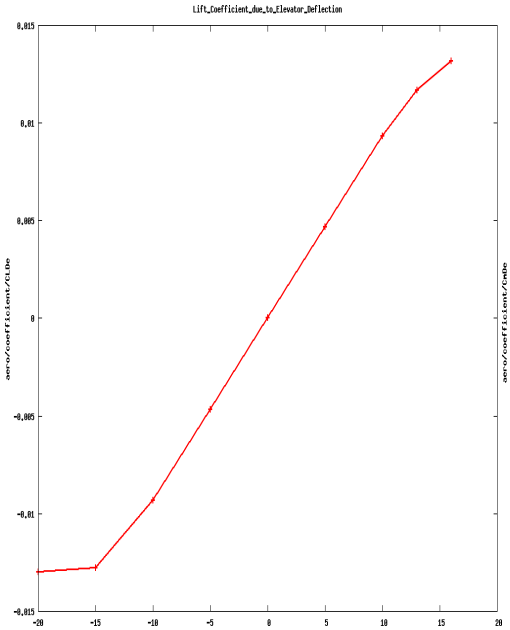

Figure 5.6 g: C_L vs Elevator Deflection

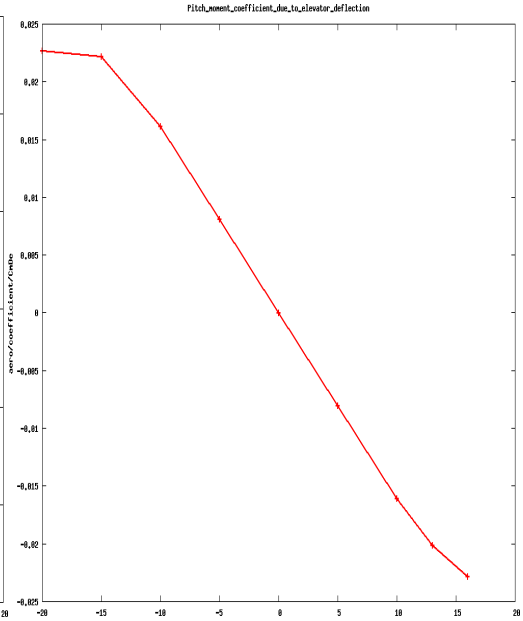

Figure 5.6 h: Cm vs Elevator Deflection

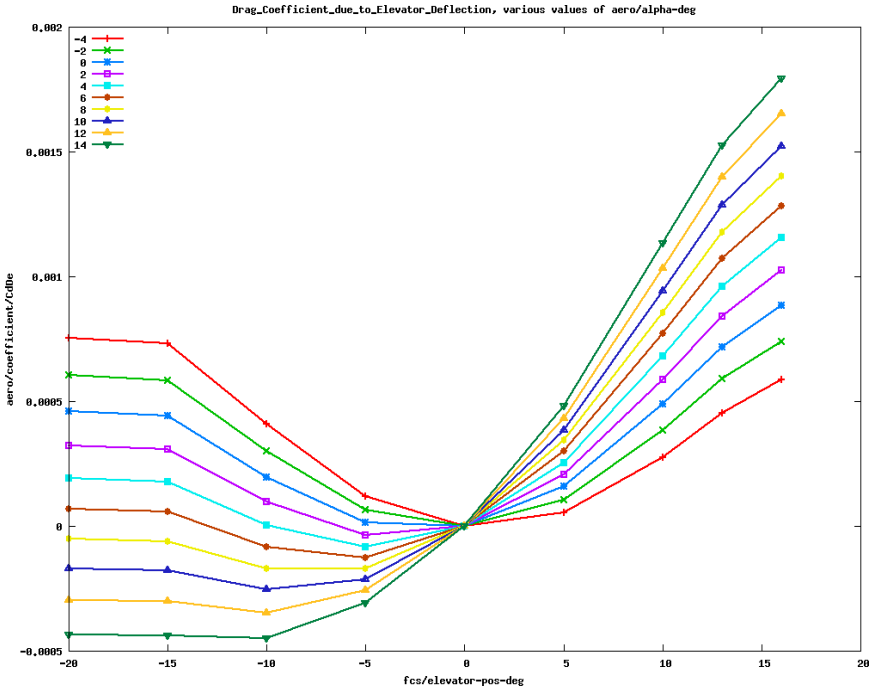

Figure 5.6 i: C_D vs Elevator Deflection

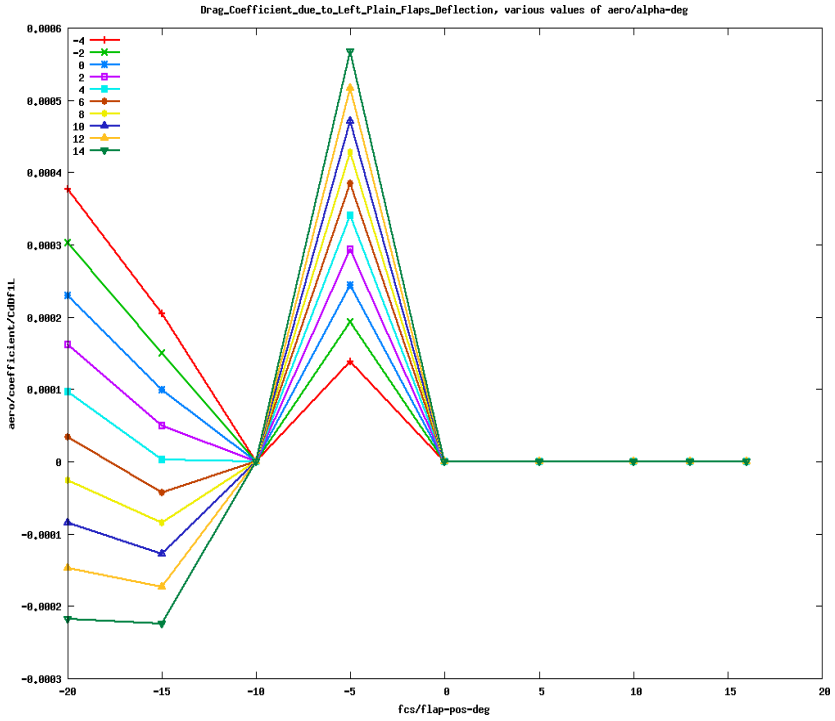

Figure 5.6 j: C_D vs Aileron Deflection

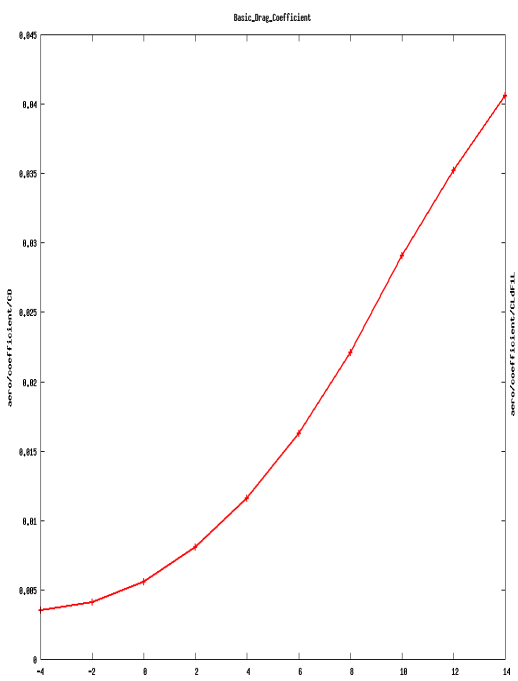

Figure 5.6 k: C_L vs Elevator Deflection

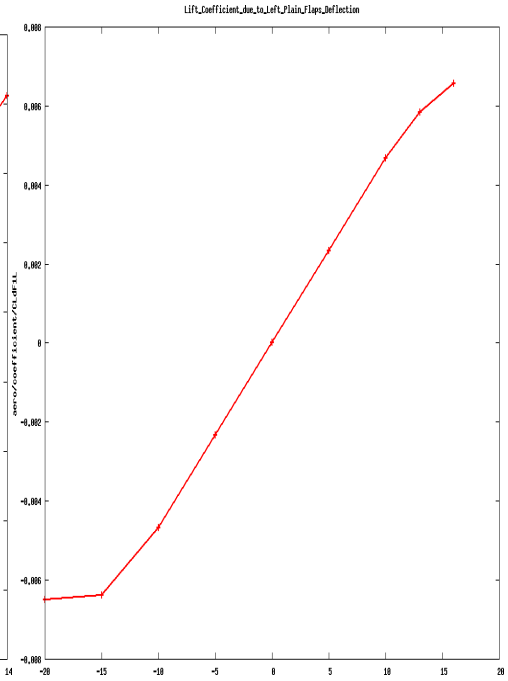

Figure 5.6 l: C_L vs Aileron Deflection

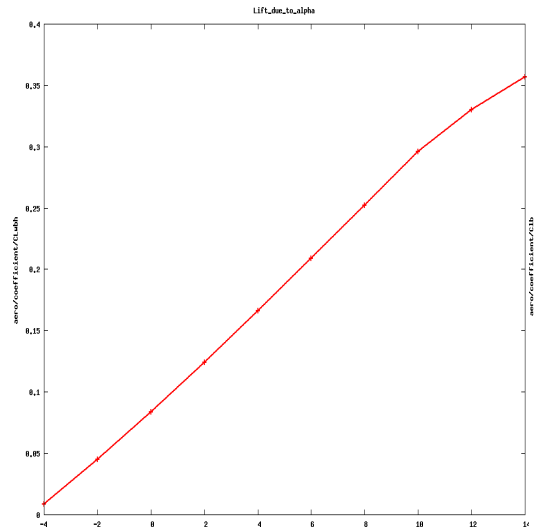

Figure 5.6 m: Cn vs Elevator Deflection

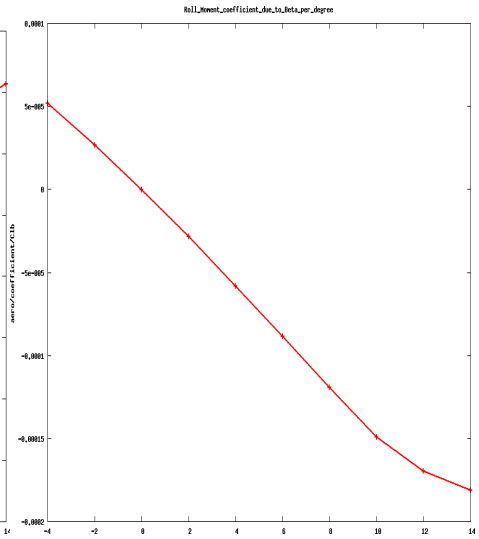

Figure 5.6 n: Lm vs AoA

Figure 5.6 Aerodynamics Variations

5.3.3 Propulsion

The required thrust for propelling the vehicle to the forward direction depends on drag. So, the selection of propulsion source depends on the cruising speed. Here, instead of giving a sophisticated model, a simple model is presented. Basic purpose is to find the expression for propulsion efforts, its point of application and orientation. A simple model generally used to define the modulus of thrust is

$$T = k_m \rho V_a^{\lambda} \delta x \qquad (5.62)$$

The symbol λ depends on the type of engine, ρ is the air density. The modulus of the aerodynamic velocity is represented by V_a, with k_m being a constant and δx representing the position of the throttle, between 0 and 1, inclusive.

The following values characterize approximately the type of engine

$\lambda = -1$ For propeller propulsion and high bypass ratio turbofan.

$\lambda = 0$ For turbojet engine with no fan.

$\lambda = 1$ For turbojet engine with after burner.

$\lambda = 2$ For the ram-jet.

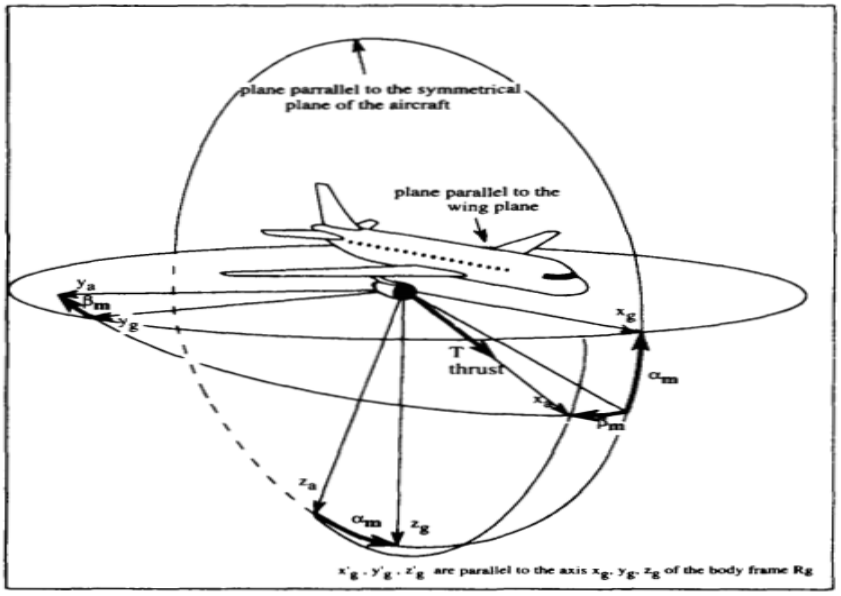

Figure 5.7 Position of Thrusters [34]

Engine is considered to deliver thrust T whose point of application M has coordinates $(x_b,\ y_b, z_b)$ in the body frame F_b. It is assumed that the engine is positioned at angles of pitch setting at α_m, and yaw setting β_m wrt. the aircraft. For further simplification, it is also assumed that the engines are symmetric (at equal distance from y axis), β is very small, i.e., $\beta \cong 0$, and the setting α_m, is low, $\lambda = -1$ and identical for both of the engines. The resultant relations are given below.

$$T = \sum_i^n F_i \begin{bmatrix} 1 \\ 0 \\ \alpha_m \end{bmatrix} \qquad (5.63)$$

$$M_b = \sum_i^n M_{Fi} \left(z_b - x_b \alpha_m\right) \begin{bmatrix} 0 \\ 1 \\ 0 \end{bmatrix} \qquad (5.64)$$

Since we are using two propellers, n = 2. Reference [34], page 230-250 can be seen for further details.

5.4 Mass Inertia model

The mass inertia model contains some mass and geometric parameters of the craft. The mass is lumped and concentrated at the center of gravity and the inertia tensors are calculated with respect to the CG. These mass and inertial parameters for the vehicles are determined with the help of Solidworks, and are given in Chapter3 in detail. For our vehicle, mass = 25 lb., $I_{xx} = 8.93$, $I_{yy} = 11.24$, $I_{zz} = 18.90$, $I_{xz} = -3.3$ are used. The change of the gross weight and CG location of the WIG is neglected during operation for simulation purposes. For WIG, change in the CG location is very little, even in real life, and its position moves towards the nose of the airplane during the flight, increasing longitudinal stability of the aircraft. Moments of inertia are considered to be constant for all the time during operation.

5.5 Actuator Models

The actuators are assumed to be first order servos with a transfer function

$$C_t = \frac{T}{s+\mathrm{T}} \qquad (5.65)$$

Dynamics of control surfaces (elevators, ailerons) are assumed to be faster than dynamics of the WIG vehicle, the bandwidth T has been chosen equal to ± 150 deg/sec. The inputs to the actuators are subjected to strict limits on the range of variations that can be achieved. These limitations include physical limitations on the actuators themselves and also ensure the system of being damaged. Elevator deflection is constrained within $\pm 30^{\circ}$ (degree), while rudder and ailerons deflections are also limited to $\pm 30^{\circ}$.

5.6 Atmospheric Model

An atmosphere model is used for developing more accurate aerodynamic model of the vehicle, [39], [36]. The main parameter that has an influence on the aerodynamics,

like thrust forces and moments, is air density, pressure and temperature, all depending on altitude.

Here are some major formulae for atmospheric elements:

$$T = T_0 + \lambda H \qquad (5.66)$$

where

$T = air\ temperature, [K]$

$H = altitude\ above\ sea\ level, [m],$

$T_0 = air\ temperature\ at\ sea\ level, [K],$

$\lambda = temperature\ gradient\ in\ troposphere = -0.0065\ Km^{-1}$

Air pressure depends on altitude:

$$dp_s = -\rho g dH \qquad (5.67)$$

Ideal gas law:

$$\frac{p_s}{\rho} = \frac{R_a}{M_a} T \qquad (5.68)$$

Gravitational acceleration (gravity) relation:

$$g = g_0 \left(\frac{R_{Earth}}{R_{Earth}+h}\right)^2 \qquad (5.69)$$

$R_{Earth} = radius\ of\ the\ Earth = 6371020\ m$

Air density Relation:

$$\rho = \frac{p_s M_a}{R_a T} = \frac{p_s}{RT} \qquad (5.70)$$

Mach number M is needed for air compressibility:

$$M = \frac{V}{V_s} \qquad (5.71)$$

where V_s is speed of sound and V is the vehicle velocity.

Reynold Number:

$$R_e = \frac{\rho V}{\mu} \qquad (5.72)$$

μ is the coefficient of dynamic viscosity, which can be given as:

$$\mu = \frac{1.458 \cdot 10^{-6} T^{\frac{3}{2}}}{T+110.4} \qquad (5.73)$$

Some atmospheric effects are taken from COESA. The COESA is a Simulink block which implements the mathematical representation of the standard atmosphere [39], due to 1976 committee.

So, overall 6DOF nonlinear model can be given by the following 12 ODEs. They define dynamics of the vehicle body and will constitute the main structure for simulation.

$$\dot{u_e} = \frac{X}{m} + rV - qw$$
$$\dot{v_e} = \frac{Y}{m} - ru + pw$$
$$\dot{w_e} = \frac{Z}{m} - pv + qu$$

$$\dot{p} = qr(I_{yy} - I_{zz})/I_{xx} + M_x/I_{xx}$$

$$\dot{q} = pr(I_{zz} - I_{xx})/I_{yy} + M_y/I_{yy}$$

$$\dot{r} = pq(I_{xx} - I_{yy})/I_{zz} + M_z/I_{zz}$$

$$\dot{x}_E = u\cos\psi\cos\theta + v(\cos\psi\sin\theta\sin\phi - \sin\psi\cos\phi) + w(\cos\psi\sin\theta\cos\phi + \sin\psi\sin\phi)$$

$$\dot{y}_E = u\sin\psi\cos\theta + v(\sin\psi\sin\theta\sin\phi) + w(\sin\psi\sin\theta\cos\phi - \cos\psi\sin\phi)$$

$$\dot{z}_E = -u\sin\theta + v\cos\theta\sin\phi + w\cos\theta\cos\phi$$

$$\dot{\theta} = q\cos(\phi) - r\sin(\phi)$$

$$\dot{\phi} = p + q\sin(\phi)\tan(\theta) + r\cos(\phi)\tan(\theta)$$

$$\dot{\psi} = (q\sin(\phi) + r\cos(\phi))\sec(\theta)$$

Except these motion equations, all forces including aerodynamics, gravitational, propulsion and GE, are given in corresponding sections.

CHAPTER 6

IMPLEMENTATION, LINEARIZATION AND OPEN LOOP RESPONSES

This chapter is about the implementation of 6DOF nonlinear model of our WIG, in Matlab/Simulink, which is already described in Chapter 5. Next, its open loop responses and their analyses are discussed. Using Matlab utilities, system was trimmed to find different equilibrium points, linearized at those trim points and state space matrices belonging to, lateral and longitudinal parts are determined and investigated from different aspects.

6.1 Nonlinear Simulation

First of all, the nonlinear model, which is described in Chapter 5, was implemented in Matlab/Simulink. Block diagram in Figure 6.1 explains the idea about the overall implementation. It is clear that control surfaces (elevators and ailerons) and propulsion (engine power) are used as inputs while all 12 states along with angle of attack α, side slip angle β and speed V are the outputs. First, all external forces including aerodynamics, gravitational forces, propulsion, and their moment are calculated. Next, these forces and moments are summed up in a sum/add block. After that, the heart of system simulation -12 ODEs-, are expressed in terms of these forces and moments. In this way derivatives of states/outputs are calculated. This integration produces the states themself, which are coupled back to the system again. So it continues to run cyclically.

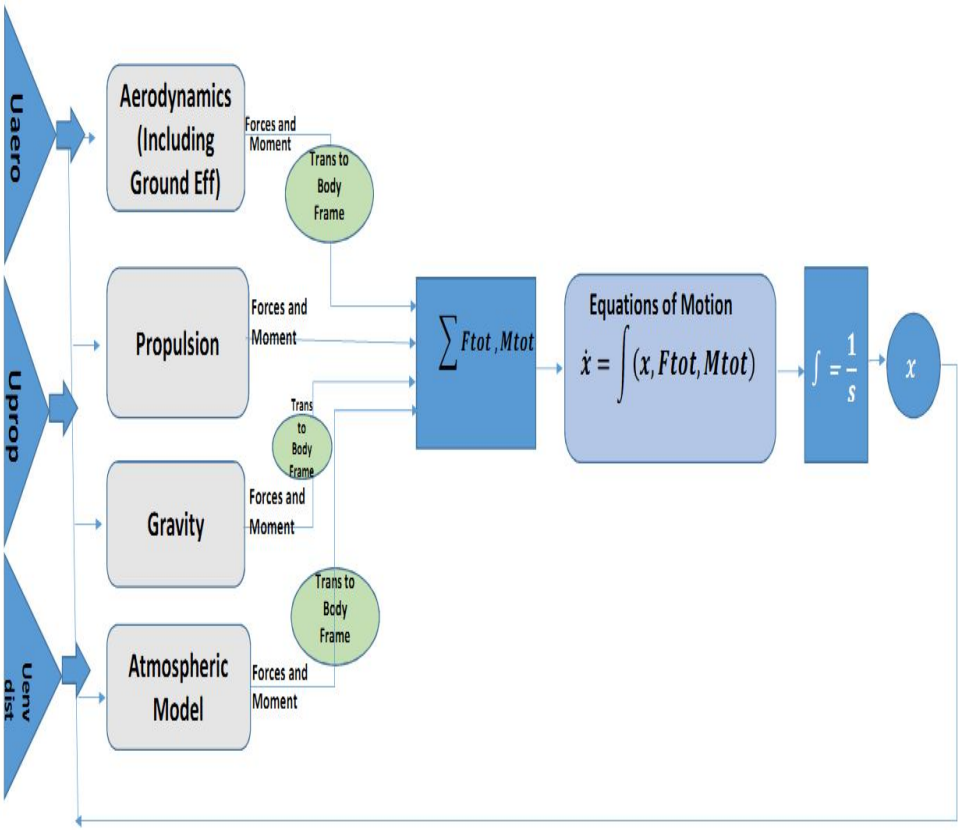

Figure 6.1 Implementation in Simulink

Explanations of different blocks for the implementation of the model are described below:

- One block is about the propulsion system, which implements and calculates thrust/forward forces/moments.
- One block is designed for the calculation of the weight (gravitational force) and its impact on other parameters.
- One block is for the determination of aerodynamics forces and moments. It also includes different atmospheric elements like air density, pressure and temperature.

- One block is dedicated to calculate different extra terms like sines, cosines of different angles, etc., which are used at different places in the Simulink internally.
- One block is used to add all these forces and moments to get their sum in their three different axes, like all forces along x axis (F_x or X) etc.
- Heart of the simulation is the block, which includes all the equation of motion of all states. It includes 12ODEs and calculates the derivatives and states itself along with angle of attack, side slip angle and speed V.

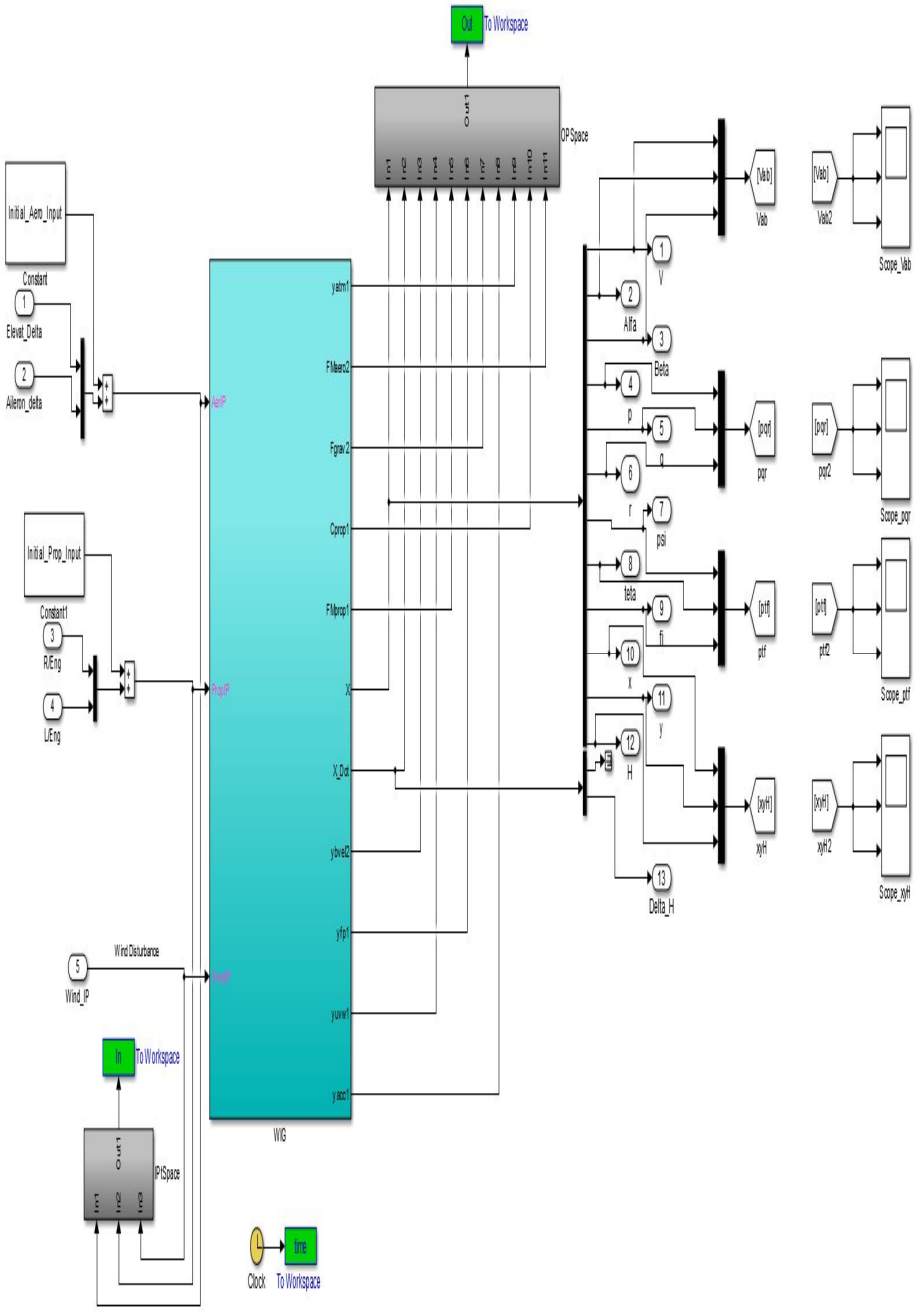

Figure 6.2 Outer Structure of System Implementation in Simulink

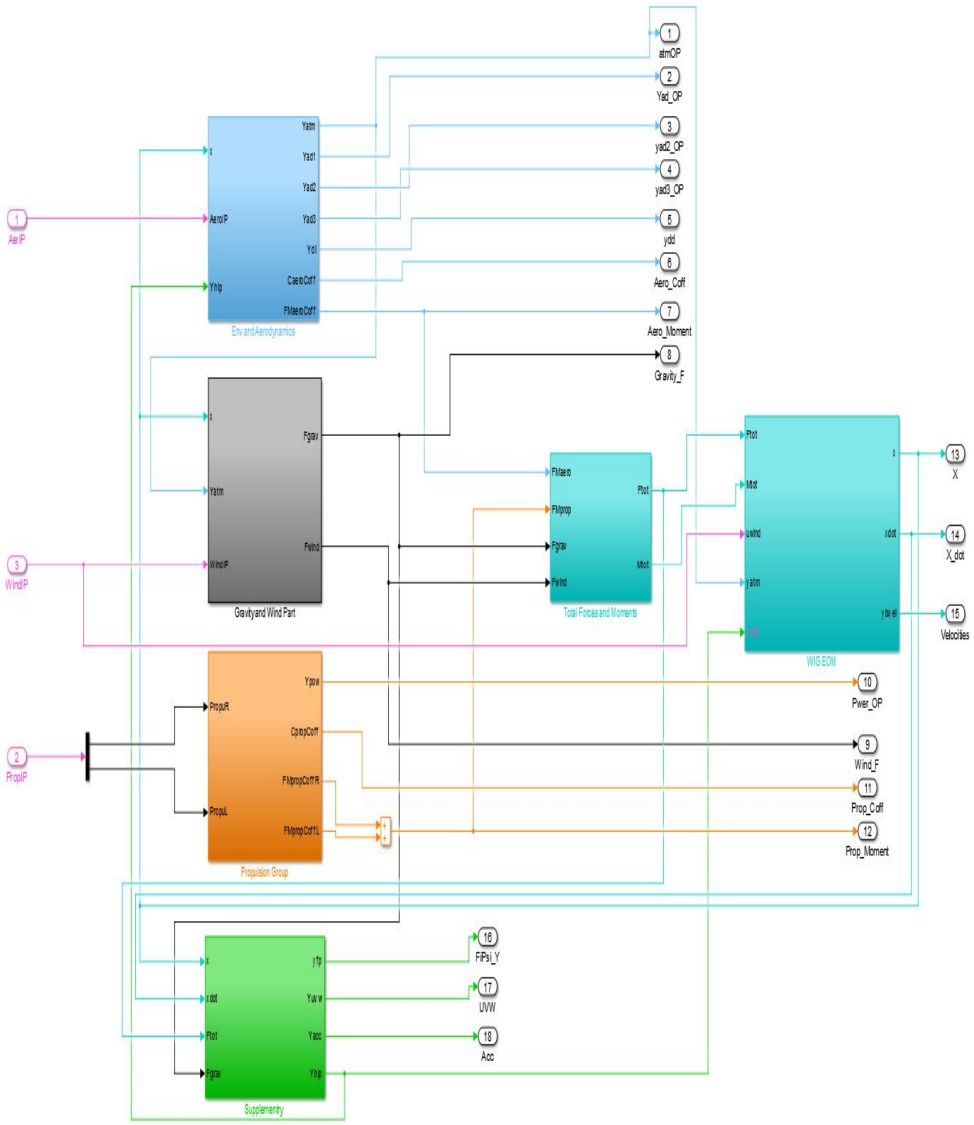

Figure 6.3 Inner Structure of System Implementation in Simulink

6.2 Open Loop Simulation

Open-loop simulations actually give the response of the system to the deflection or disturbances in the control surfaces and other inputs. As was mentioned before, both active controls (through thruster) and passive controls (through control surfaces) are used. Elevator is used for longitudinal controls, while ailerons are used for lateral

control and thrusters for speed and heading. Open-loop response simulations are performed on the nonlinear models of the WIG.

Giving the elevator a deflection of a few degrees (as shown in the graphs below) for a finite time interval, allows us to observe system's open-loop response. Figure 6.4 and Figure 6.5 clearly show that it takes too much time to go back to a stable state once it is disturbed; therefore we need a good controller for this purpose.

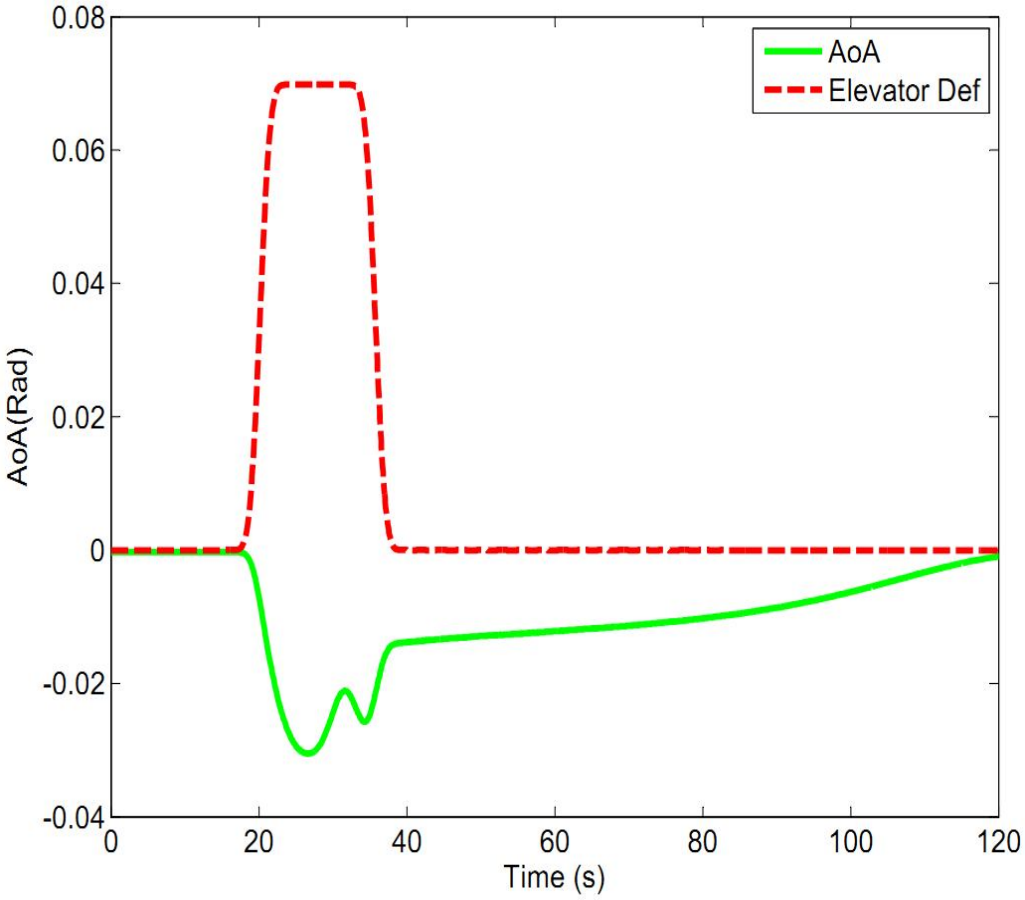

Figure 6.4 a: AoA vs δe

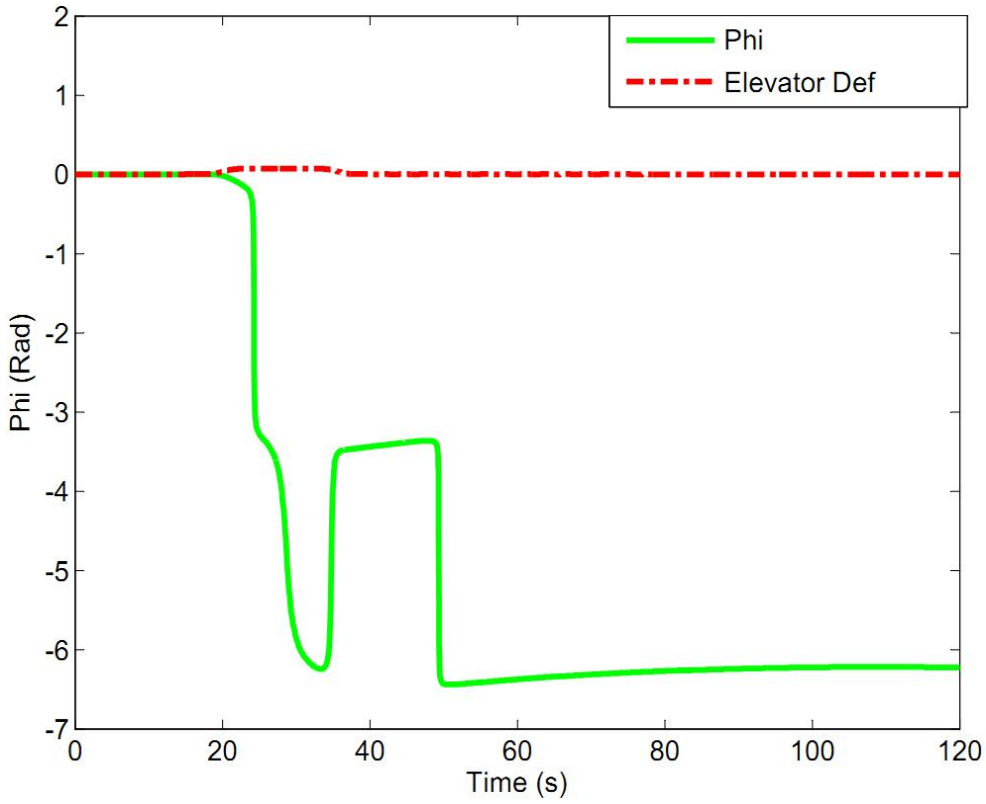

Figure 6.4 b: Phi vs δe

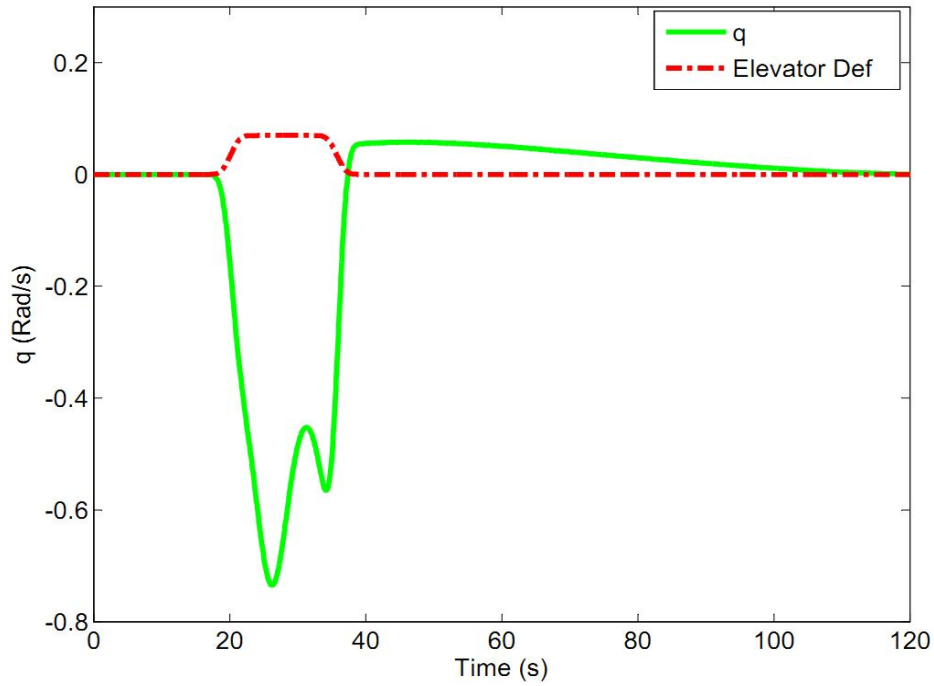

Figure 6.4 c: q vs δe

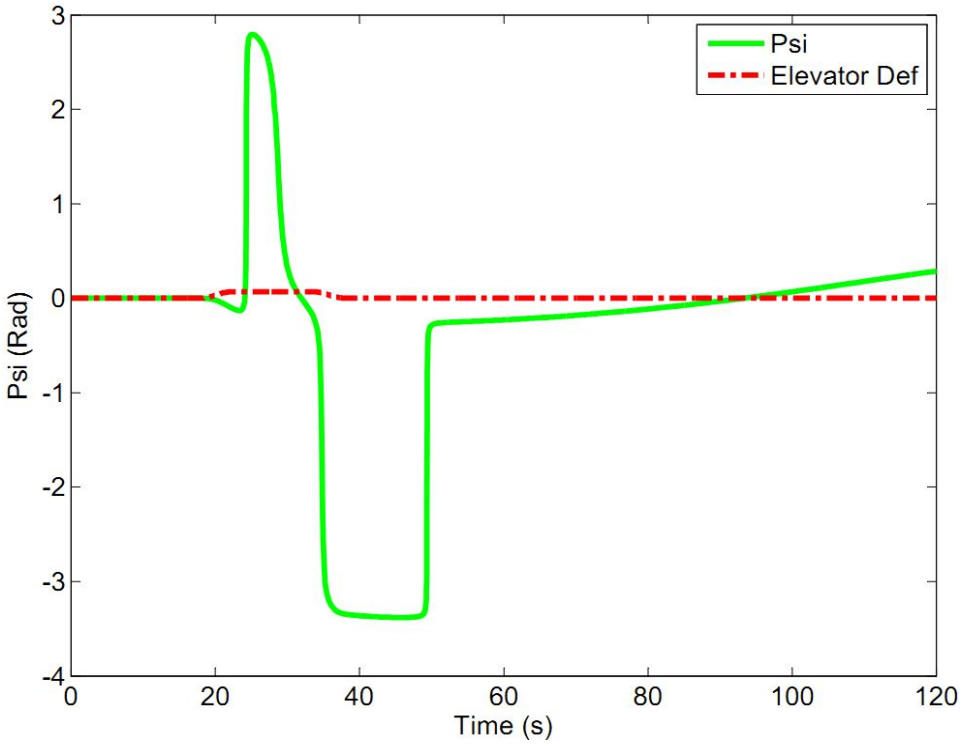

Figure 6.4 d: Psi vs δe

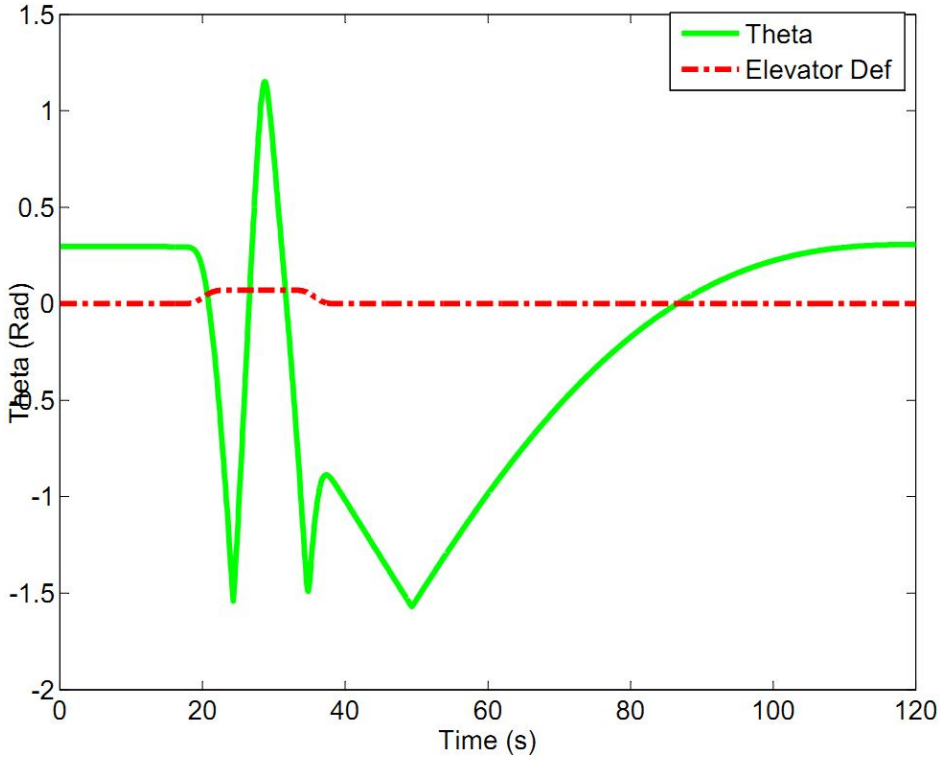

Figure 6.4 e: Theta vs δe

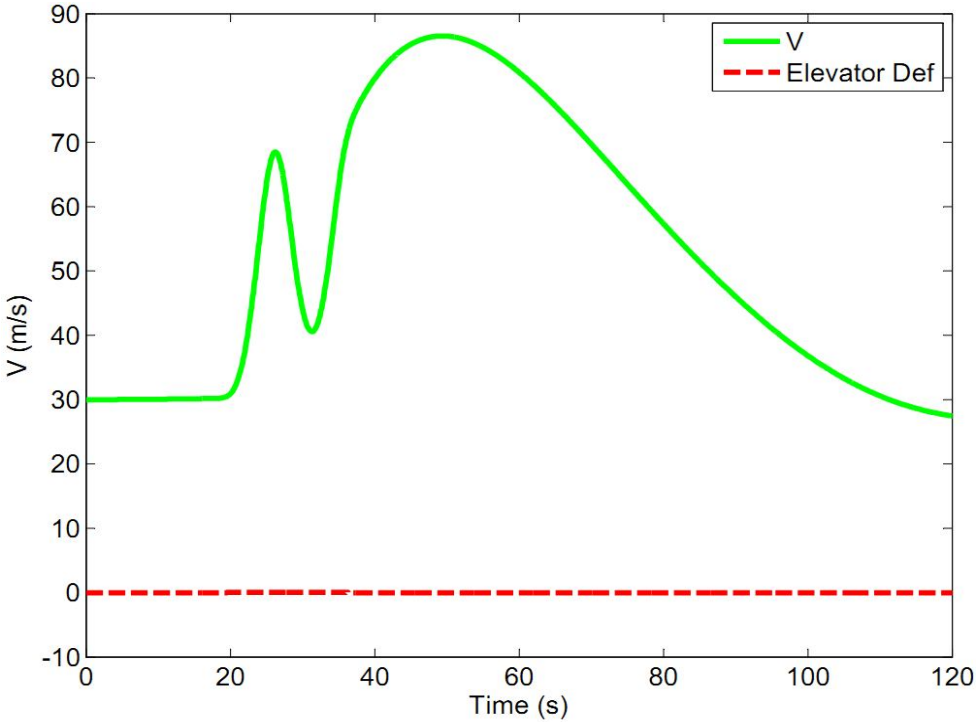

Figure 6.4 f: V vs δe

Figure 6.4 Open Loop Responses to Elevator Deflections

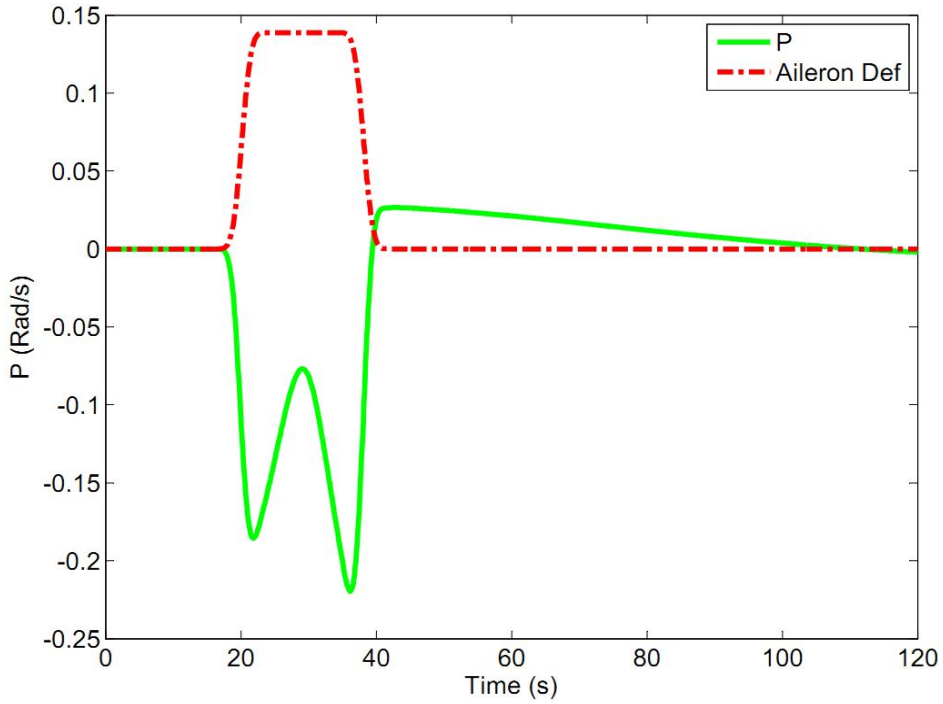

Figure 6.5 a: p vs δa

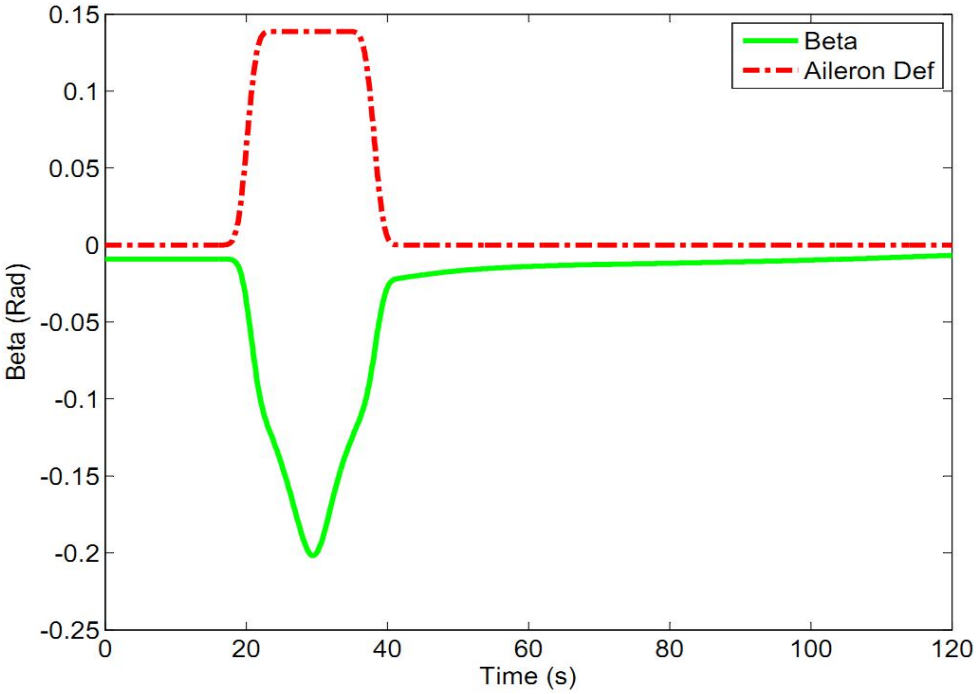

Figure 6.5 b: Beta vs δa

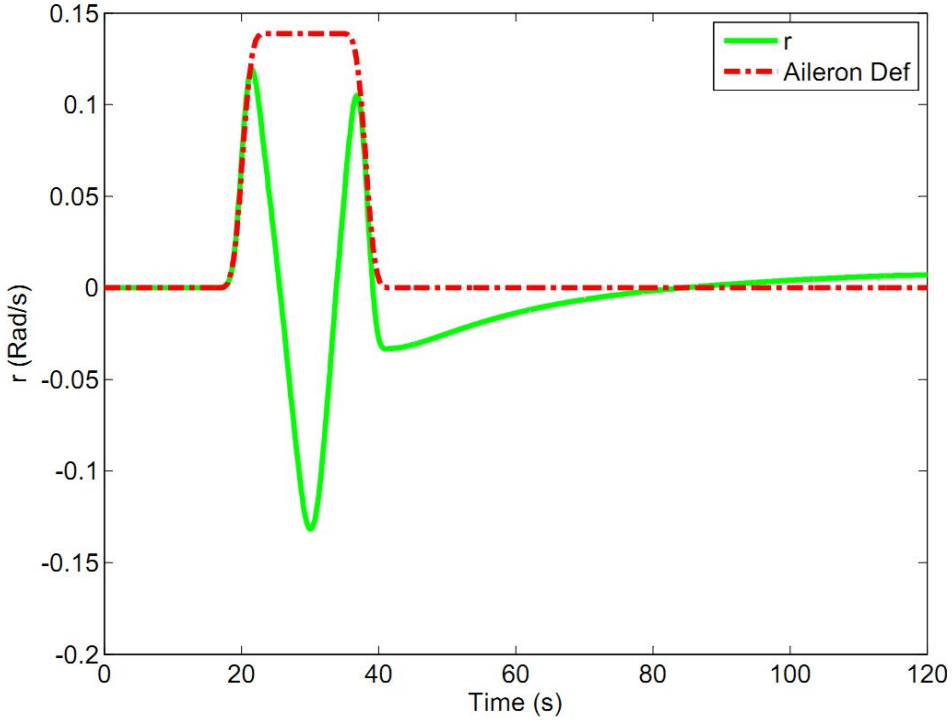

Figure 6.5 c: r vs δa

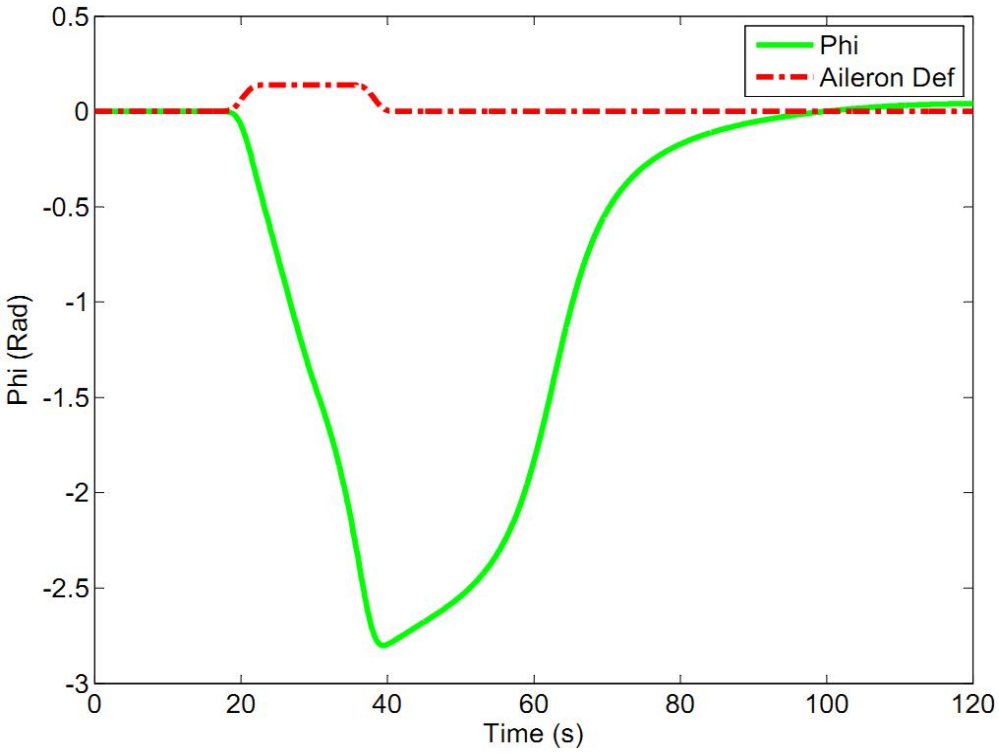

Figure 6.5 d: Phi vs δa

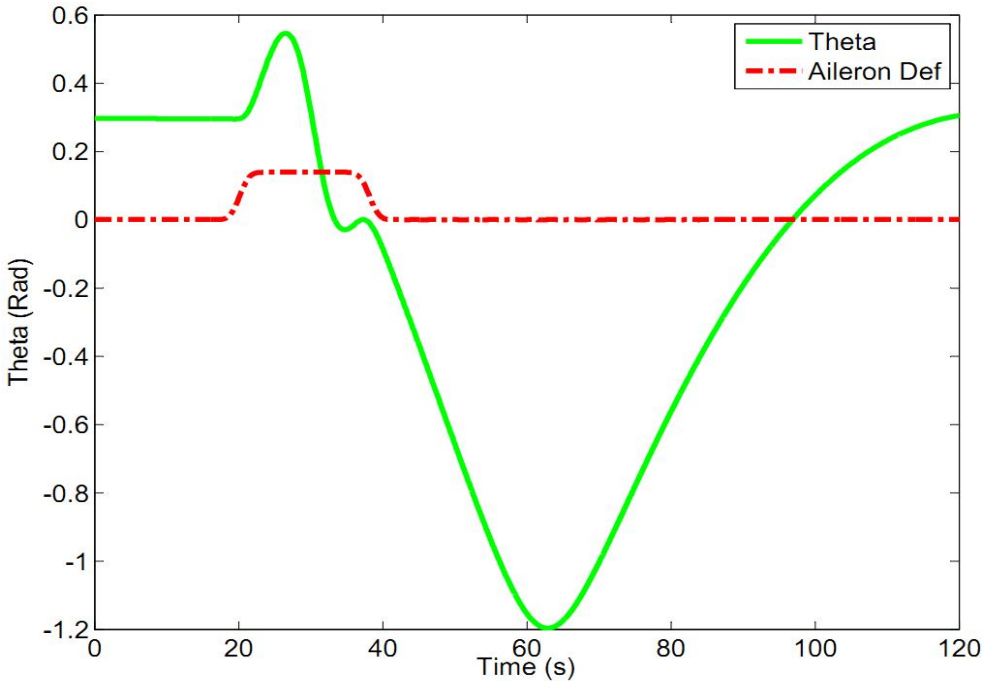

Figure 6.5 e: Theta vs δa

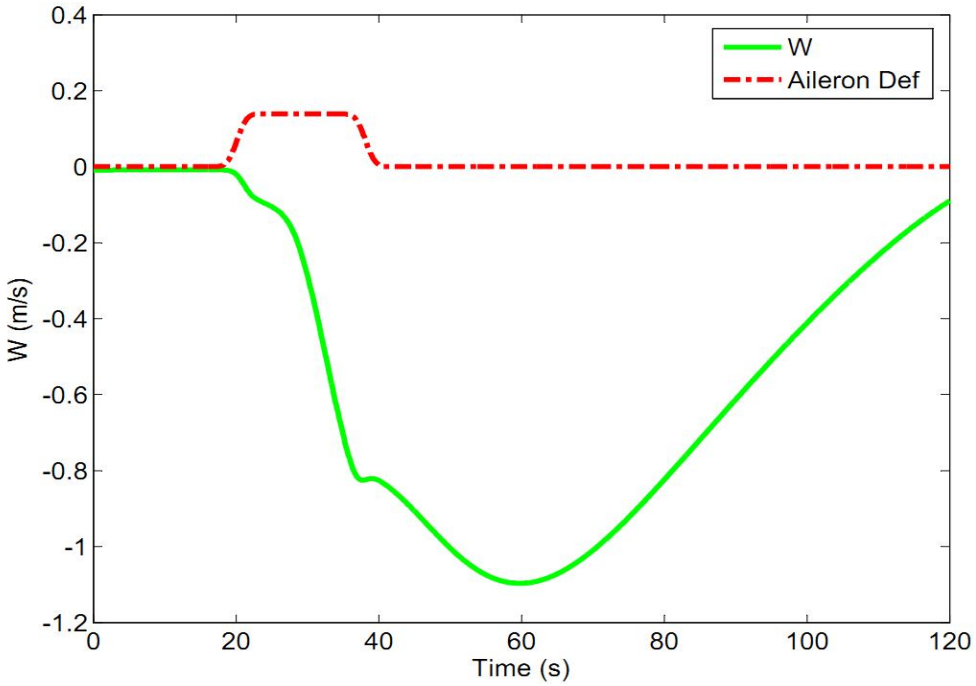

Figure 6.5 f: W vs δa

Figure 6.5 Open Loop Responses to Aileron Deflections

6.3 Linearization

Linearization is an important and useful tool to study the system behavior, and also it is helpful in designing controllers. Here, controller is designed on the basis of linearized system; first, the system is linearized and controller is designed for the linear system, next, it is used for the nonlinear system with some modifications in controller gains. Small disturbance theory is used for linearizing system equations. WIG plane is linearized for small disturbances around some equilibrium points. These equilibrium points are also called as trim points, in which all forces and moments are considered zero on the body of craft. For linearization, certain assumptions and considerations are made: motion equations can be uncoupled and even lateral and longitudinal responses can be studies separately. For example, generally for lateral response analysis, flat Earth is assumed, neglecting rotor gyroscopic effects and existence of plane of symmetry are considered, aerodynamics cross coupling is also neglected [36]. More or less, similar assumptions are made to study longitudinal response.

Linearization of the non-linear WIG model has been done using different Matlab utilities such as “System Linear Analysis”. Trim points are found using “trim function” utility. These are pioneering trim points. System is linearized at different speed and altitude points, since they contribute to the states space in the flight of WIG.

For our WIG vehicle, these trim points are found for the pairs (V = 30 m/s, h = 1 m) and (V = 45 m/s, h = 10m).

In order to check the trim point‘s authenticity, trim point values are used for states variables/inputs and applied to the system. If trim point selection was right, then it is expected that rotation rates like p, q r should stay at zero, or close to zero. It was checked by system simulation and results are shown in Figure 6.6:

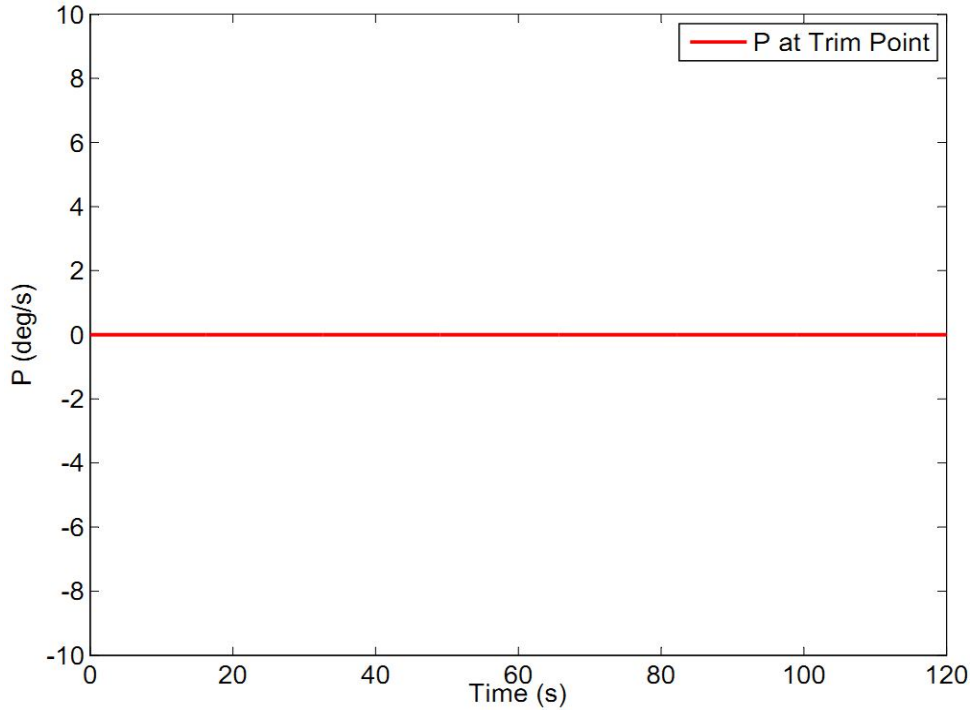

Figure 6.6 a: p (Rotation Rate around X-Axis) at Trim Points

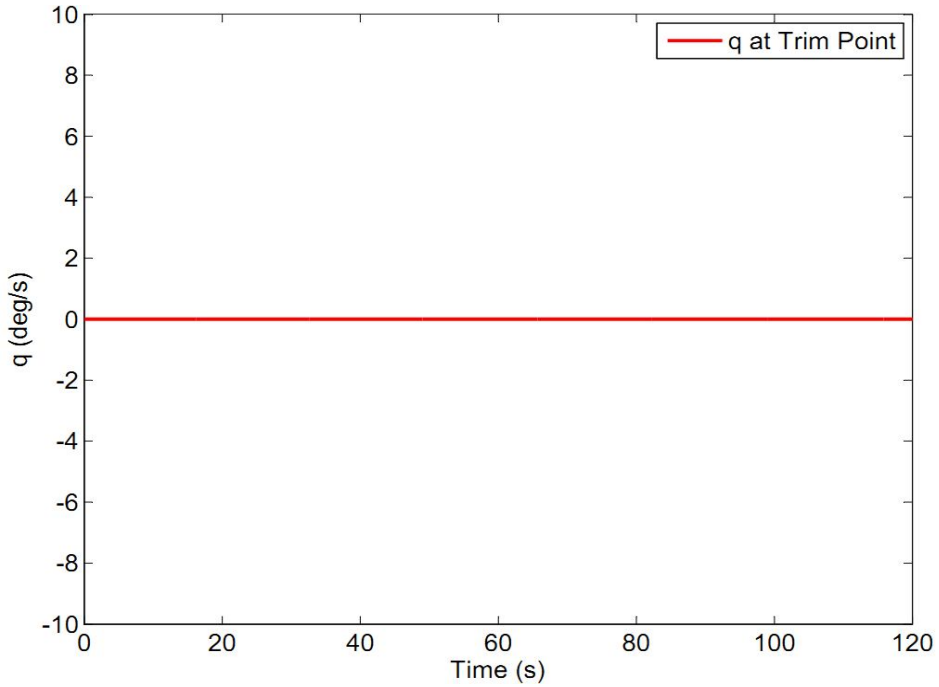

Figure 6.6 b: q (Rotation Rate around Y-Axis) at Trim Points

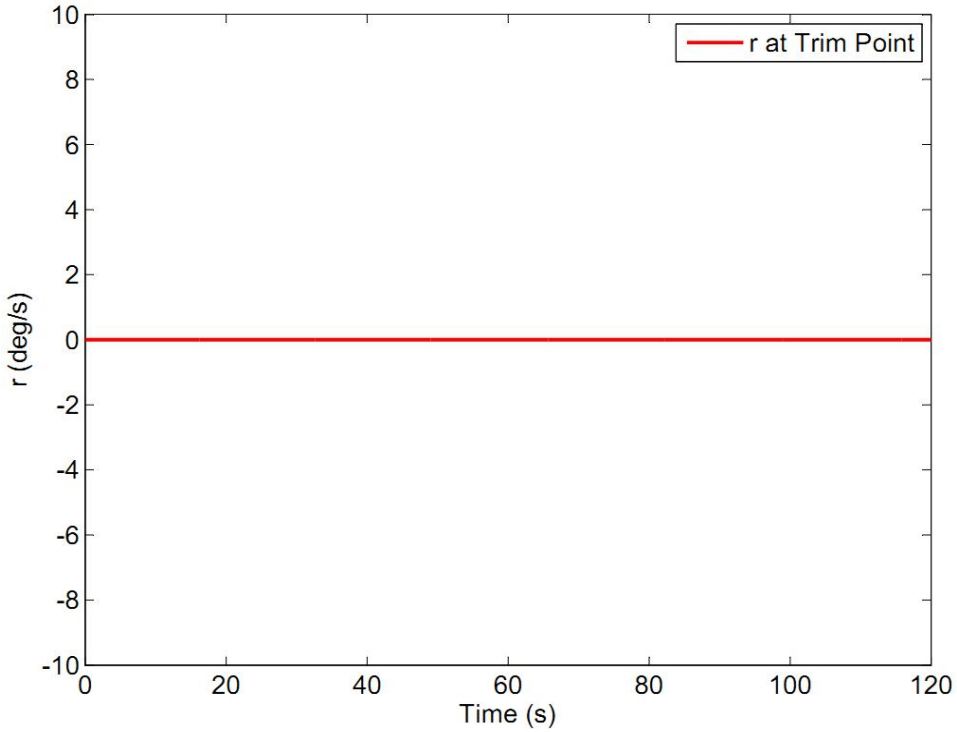

Figure 6.6 c: r (Rotation Rate around Z-Axis) at Trim Points

Figure 6.6 Trimmed point verification

After trimming the WIG craft, it is linearized using Matlab utility "Linear System Analysis".

6.4 Linear WIG Model

State space representation is widely used for designing control systems, especially in modern control theory. Similarly, for modeling, simulation and control analysis of WIG, state space representation is used.

$$\begin{aligned} \dot{x} &= Ax + Bu \\ y &= Cx + Du \end{aligned} \qquad (6.1)$$

Following states are used as "system states"; linear velocities along axes (u, v, w), speed V, angle of attack (α), side slip angle (β), yaw, pitch, roll rates (p, q, r), yaw, pitch roll angles (ϕ, θ, ψ), position in fixed Earth frame (x, y, H). The same states are used for autopilot design.

$$x = [V, \alpha, \beta, p, q, r, \phi, \theta, \psi, x, y, H\ (u, v, w)]' \qquad (6.2)$$

Different outputs can be defined; here, the output is defines as the states

$$y = [V, \alpha, \beta, p, q, r, \phi, \theta, \psi, x, y, H, (u, v, w)]' \qquad (6.3)$$

The following initial conditions X_0 (trim conditions) and initial input (U_0) are used:

$$X_0 = [30, -0.003, -0.009, 0, 0, 0, 0, 0.18, 0, 0, 0, 1]^T$$

$$U_0 = [0.05, 0.008, 0, 0, 1, 1, 0, 0, 0, 0, 0, 0]^T$$

Another set of initial conditions are:

$$X_0 = [30, -0.0075, -0.009, 0, 0, 0, 0, 0.08, 0, 0, 0, 1\ 0]^T$$

$$U_0 = [0.05, 0.008, 0, 0, 1, 1, 0, 0, 0, 0, 0, 0]^T$$

With the help of MATLAB utility "Linear System Analysis", the following state space representation (A, B, C, D) is found.

1. For the case; $V = 30\ m/s$ and $h = 1\ m$:

A=

$$\begin{bmatrix} -0.105 & 6.32 & 0.598 & 0.0064 & -0.674 & -0.019 & 0 & -9.38 & -0.085 & 0 & 0 & 0.0002 \\ -0.208 & -23.81 & 0.0613 & 0.009 & 0.701 & 0 & 0 & -0.095 & 0 & 0 & 0 & 0 \\ 0 & -0.546 & 2.13 & -0.023 & -0.0002 & -0.902 & 0 & -0.003 & 0.303 & 0 & 0 & 0 \\ 0 & -0.308 & -26.18 & -13.96 & 0.163 & 5.057 & 0 & 0 & 0 & 0 & 0 & 0 \\ 0 & -47.6 - & 0.996 & 0 & -28.74 & -1.64 & 0 & 0 & 0 & 0 & 0 & 0 \\ 0 & 0.322 & 4.3 & -1.01 & 0.875 & -2.23 & 0 & 0 & 0 & 0 & 0 & 0 \\ 0 & 0 & 0 & 0 & 0 & 1.045 & 0 & 0 & 0 & 0 & 0 & 0 \\ 0 & 0 & 0 & 0 & 1 & 0 & 0 & 0 & 0 & 0 & 0 & 0 \\ 0 & 0 & 0 & 1 & 0 & 0.305 & 0 & 0 & 0 & 0 & 0 & 0 \\ 0.956 & 8.76 & 0.26 & 0 & 0 & 0 & 0.273 & -8.76 & -0.081 & 0 & 0 & 0 \\ -0.01 & 0 & 30 & 0 & 0 & 0 & 28.7 & 0 & 0.01 & 0 & 0 & 0 \\ 0.92 & -28.7 & 0.08 & 0 & 0 & 0 & 0 & 28.7 & 0.261 & 0 & 0 & 0 \end{bmatrix}$$

B=

$$\begin{bmatrix} -0.0056 & 0.0231 & 1.373 & -4.04 & 2.221 & 2.221 & 0 & 0 & 0 & -1 & 0.0091 & 0.0003 \\ -1.713 & 0 & 0 & -5.9 & 0 & 0 & 0 & 0 & 0 & 0 & 0 & -0.0333 \\ 0 & -0.082 & 0.3211 & -0.0012 & 0.0007 & 0.0007 & 0 & 0 & 0 & -0.0003 & -0.0323 & 0 \\ 0 & -41.35 & 6.519 & 0 & -0.2834 & 0.2834 & 0 & 0 & 0 & 0 & 0 & 0 \\ -152.06 & 0 & 0 & 32.23 & 0 & 0 & 0 & 0 & 0 & 0 & 0 & 0 \\ 0 & 3.426 & -19.7 & 0 & 1.521 & -1.521 & 0 & 0 & 0 & 0 & 0 & 0 \\ 0 & 0 & 0 & 0 & 0 & 0 & 0 & 0 & 0 & 0 & 0 & 0 \\ 0 & 0 & 0 & 0 & 0 & 0 & 0 & 0 & 0 & 0 & 0 & 0 \\ 0 & 0 & 0 & 0 & 0 & 0 & 0 & 0 & 0 & 0 & 0 & 0 \\ 0 & 0 & 0 & 0 & 0 & 0 & 0.956 & 0 & 0.29 & 0 & 0 & 0 \\ 0 & 0 & 0 & 0 & 0 & 0 & 0 & 1 & 0 & 0 & 0 & 0 \\ 0 & 0 & 0 & 0 & 0 & 0 & 0.2918 & 0 & -0.96 & 0 & 0 & 0 \end{bmatrix}$$

$$C = [I]_{12\times 12}$$

$$D = [0]$$

Above representation is given as an example. In a similar way, system has been linearized for different trim points; characteristics can be found and be analyzed for controller design and other purposes.

6.5 Lateral Dynamics

Lateral states are

$$x = \begin{bmatrix} \beta \\ p \\ r \\ \phi \end{bmatrix}$$

Lateral state matrix A is shown for the case where aileron is the input versus Phi angle as the output. This case is shown just as an example to have an idea about the characteristics of the lateral system.

$$A_{lat} = \begin{bmatrix} -2.12 & -0.0232 & -0.902 & 0.303 \\ -26.18 & -13.62 & 5.05 & 0 \\ 4.28 & -1.01 & -2.23 & 0 \\ 0 & 1 & 0.305 & 0 \end{bmatrix}$$

Table 6.1 shows the characteristics of A_{lat}:

Table 6.1 A_{lat} Characteristics

Poles	Damping	Frequency
-0.021	1	-0.021
-2.25+2.58j	0.657	3.42
-2.25+2.58j	0.657	3.42
-13.5	1	13.5

In the similar way, for each SISO (or MIMO) system, characteristics can be found and system can be analyzed for controller design.

6.6 Longitudinal Dynamics

Longitudinal states are

$$x = \begin{bmatrix} \alpha \\ q \\ \theta \end{bmatrix}$$

Some other states like linear velocity along x-axis can also be added here. Longitudinal state matrix A is shown for the case where elevator is the input versus theta angle is the output. This case is shown just as an example to have an idea about characteristics of the longitudinal system.

$$A_{long} = \begin{bmatrix} -23.8 & 0.701 & -0.095 \\ -47.606 & -28.7 & 0 \\ 0 & 1 & 0 \end{bmatrix}$$

Table 6.2 below shows the characteristics of A_{long}:

Table 6.2 A_{long} Characteristics

Poles	Damping	Frequency
-0.006	0.8	-0.00633
-26.3+5.24j	0.981	20.8
-26.3-5.24j	0.981	20.8

In the similar way, for each SISO (or MIMO) system, characteristics can be found and system can be analyzed for controller design.

6.7 Comparison of Flight with and Without GE

This section provides a comparison of the effect of GE during vehicle motion. Power consumption has been calculated for a specific distance travelled by the vehicle. Power is the product of thrust and velocity over that period of travelling.

$$Power\ (Watts) = Thrust\ (Newton) \times Velocity(m/s) \qquad (6.4)$$

In the first example, the vehicle is moved at 1000 m in exactly x-axis direction while the height was kept around 1 m, so that the vehicle can utilize full ground effect. Y-axis distance was kept zero. Initially power consumption increases exponentially and reaches its maximum value and then consumption remains at constant rate until it reaches its target. Power consumption graph is shown Figure 6.7, after some scaling.

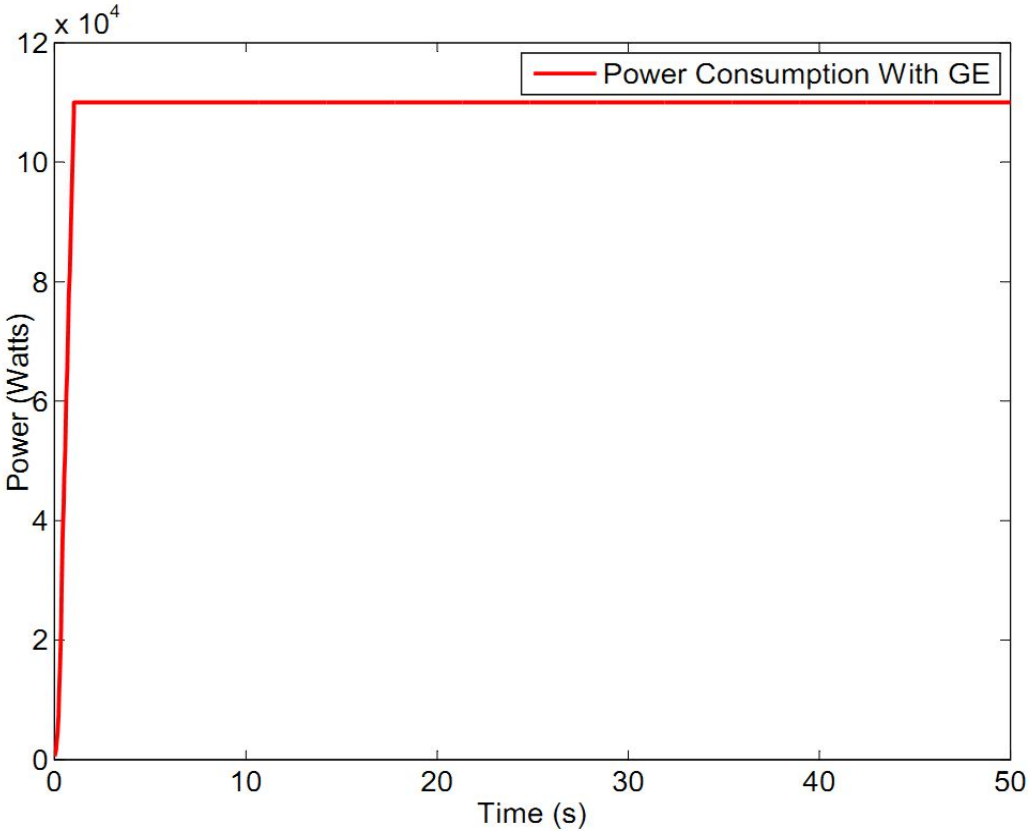

Figure 6.7: Power Consumption with GE

Total power consumed can be calculated by:

$$P = \int_0^{50} P.\, dt \qquad (6.5)$$

and it is found as 5437300 watts.

On the other hand, vehicle is moved again keeping the same conditions (travelling 1000 m along x-axis, with y-axis distance being zero) while, this time height (altitude) is kept 10 m, so that vehicle moves out of ground effect. Power consumption is shown in Figure 6.8.

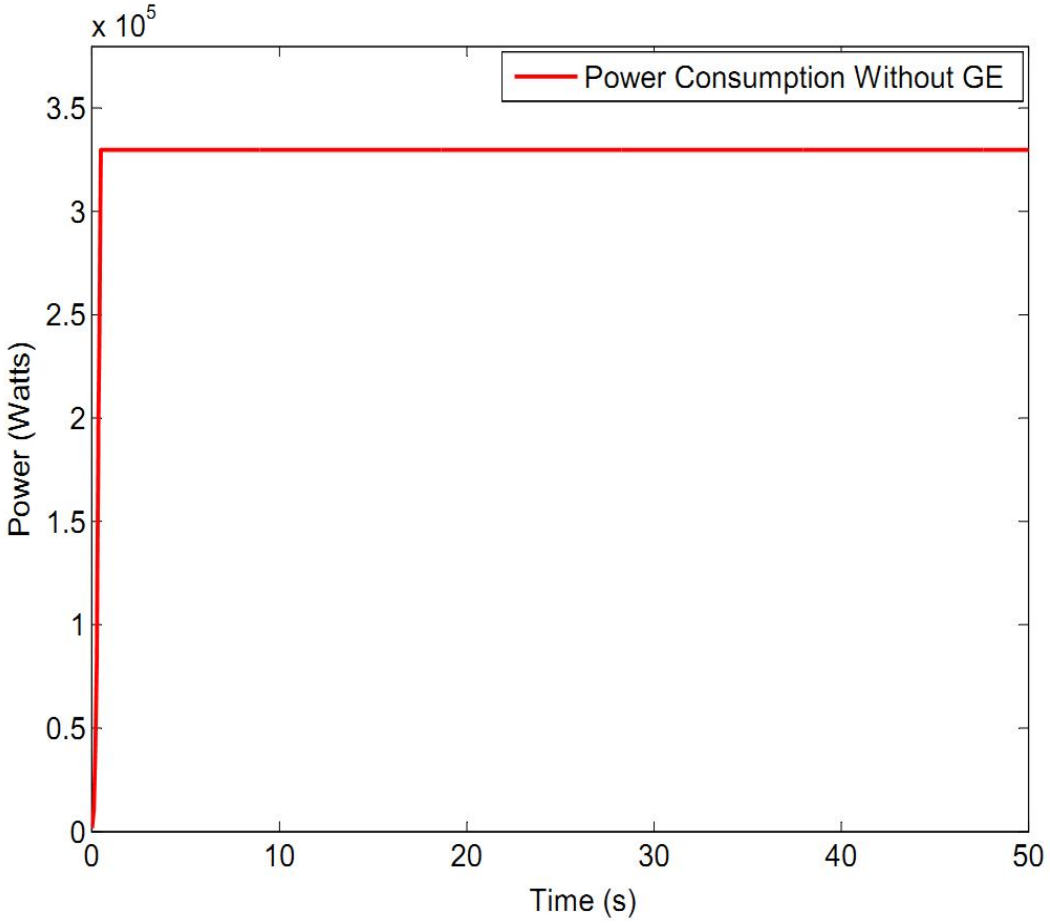

Figure 6.8: Power Consumption without GE

In this case, consumed power is found as 163970000 $watts$. So, it clearly shows that power consumption is about 3.025 times more without ground effect than with ground effect.

Similar graphs are shown in Figures 6.9 a & b to describe the change in lift and drag with height. As vehicle gains on altitude, it loses advantages of ground effect. These figures are obtained when vehicle moves along just Z axis on altitude, from 0 to 45 m. Figure 6.9 (a) shows change in lift which is at maximum level at 0 altitude and then decreases exponentially from the start and become almost constant when the vehicle is in steady flight and out of ground effect. Almost opposite case is seen for the drag

shown in Figure 6.9 (b). These results are scaled to show the difference in a better way.

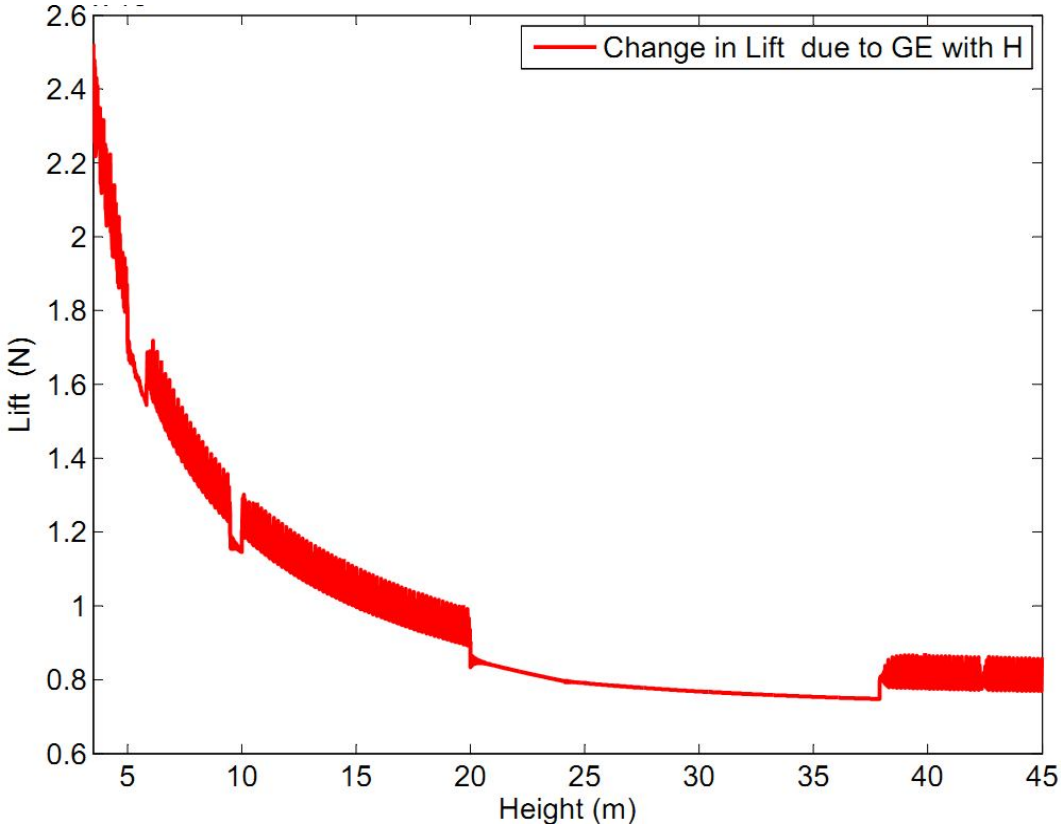

Figure 6.9 a: Change in Lift with Altitude from Simulation (Scaled)

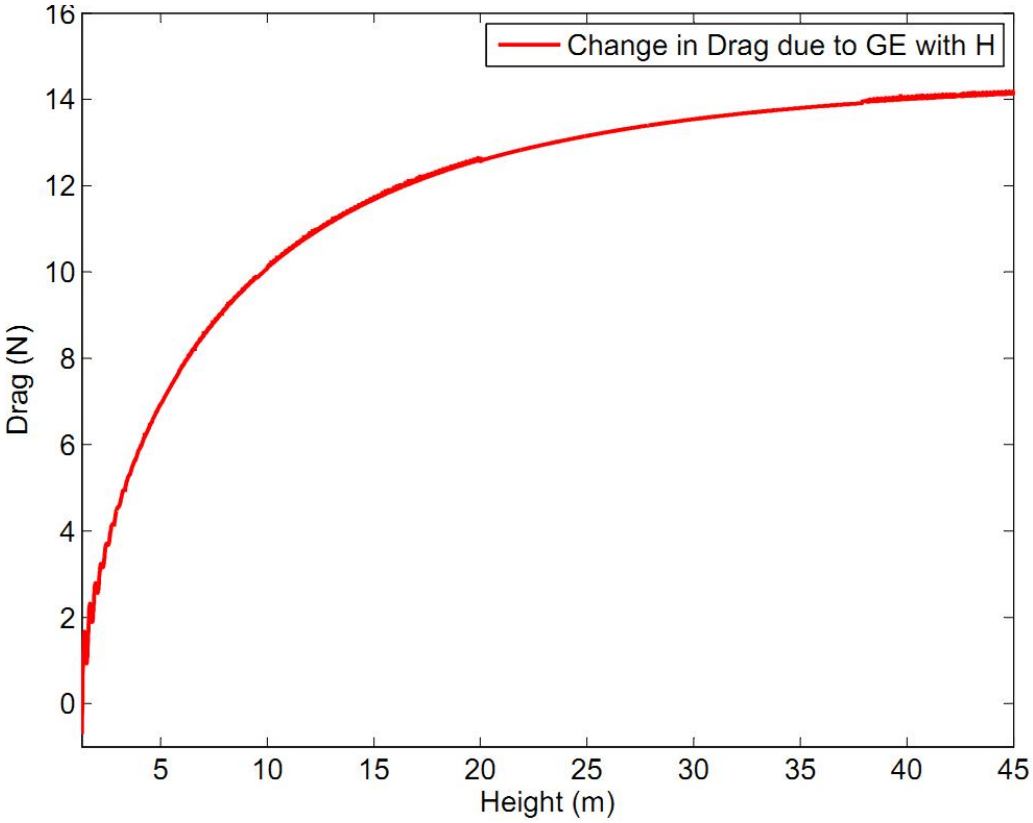

Figure 6.9 b: Change in Drag with Altitude from Simulation (Scaled)

CHAPTER 7

CONTROLLER DESIGN

7.1 Autopilot

Autopilot is designed to perform the following two functions.

1. Controller: Development and implementation of the forces and moments to the craft, to move it to a stable state. Restore and regulate it within allowable constraints.

2. Guidance: To determine the path or other control parameters, wrt. some reference, for the vehicle to follow. So, it can follow a desired trajectory autonomously, to reach its destination.

Autopilot can be divided into inner and outer loops. The control function is fulfilled by the inner loops which control the symmetric (longitudinal like pitch attitude) and asymmetric (lateral like roll attitude) parts of the aircraft. These longitudinal and lateral attitude control commands are created by the outer loops, which guide the vehicle, equipped with the inner loops, so that it can follow a desired flight path. Chapter 7 is about the first part “Controller” and the next chapter describes the guidance part.

Chapter 7 is about controller design for pitch, yaw, roll, speed and altitude hold. Here classical approach is used for controller design. PID controllers are developed and implemented. They are discussed in detail with results in the following sections.

7.2 Theory of PID Controller

In classical theory of controller design, a closed loop feedback controller is used to stabilize the states of a dynamical system. This method uses system dynamics and its frequency analysis for the development of controller. In feedback loop systems, system dynamics, sensors and actuators are involved in the design process. The process is explained in Figure 7.1. Feedback is taken to reduce the effect of noises, disturbances and uncertainty on the system and to reduce them to a minimum level [47].

Closed loop feedback control systems have many advantages over the open loop systems, such as:

- Systems become more stable even in the presence of disturbances.
- Avoid uncertainty.
- Improve system characteristics and make its response better.

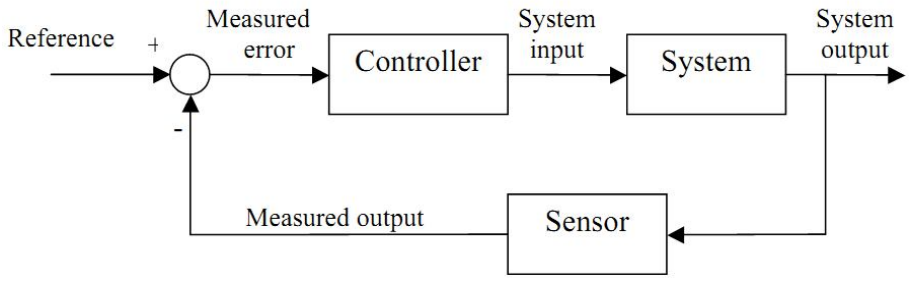

Figure 7.1 General Structure of a Feedback Loop System [47]

Most commonly used controller is PID controller, which is simple in its structure and nature. It consists of three parts: proportional (P), integral (I) and derivative (D). Due to its feasibility and practicality it is widely used everywhere in industry [46]. The controller has the transfer function:

$$G_{PID} = K_p + K_i/s + K_d s \qquad (7.1)$$

where K_p, K_i and K_d are controller gains.

In the time domain, it is defined as:

$$u(t) = K_p\left(e(t) + \frac{1}{T_i}\int_0^t e(\tau)d\tau + T_d\frac{de(t)}{dt}\right) \qquad (7.2)$$

Here *e(t)* is the error to be minimized with input u(t) while other terms shows proportional gain K_p, integral time T_i and derivative time T_d. As it is shown, *u(t)* is basically a linear combination of error *e(t)* with its proportional gain, integral and derivative time.

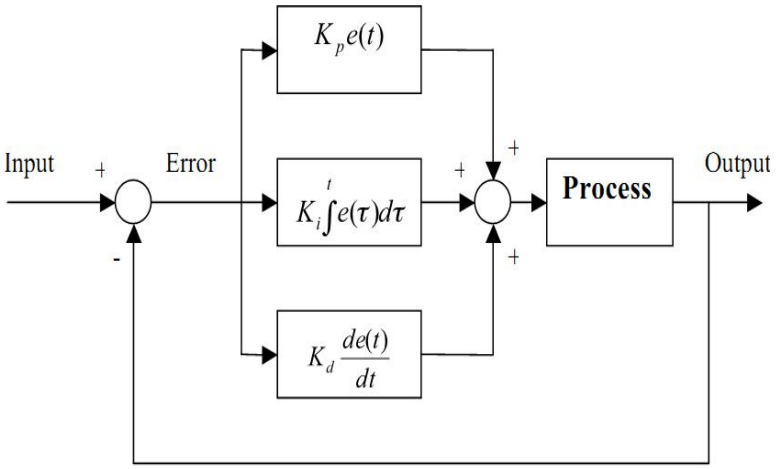

Figure 7.2 PID General Structure (Discrete Time) [48]

PID is basically a combination of PI and PD. PD is for high frequency control and PI is for low frequency handling. Because of its effectiveness in both regions it is very efficient for transient and steady state responses.

Large proportional gain makes the rise time smaller, so, it enables the system to reach steady state in a short time, but reduces its value; therefore can never eliminate the steady state error (to make it to zero). It also helps to reject noise at high frequencies. Therefore the integral term is added, which means placing a zero at the origin, so it drives the system like having infinite gain at zero frequency, in literal meaning. In other words, in the complex plane, this placement of pole to the origin makes the

steady state error to become zero under the step input. On the other hand, derivative term improves stability, settling time and overshoot. This edition of derivative term makes the system very sensitive to noise and disturbances, even sometimes it may cause amplification of them. In fact, derivative means making system proper by adding a zero(s) to the numerator of the transfer function; therefore derivative term alone cannot be used. It has limitations in its practical use, either. Therefore, when derivative term (gain) is estimated, generally it is decreased to a small positive term ε, rather than using its real calculated value to reduce its disadvantages. More details can be found in [49], [50].

That is the reason of why usually PI controllers are used and they are sufficient for simple systems (like first order systems or systems with easier requirements). When systems are complicated and of higher orders, then PID controllers are used. The references [51], [52] cover the details of PIDs, their merit and demerits and how to develop and implement them.

7.3 Tuning

Currently a number of techniques are available for determining (proportional–integral–derivative) controller gains. Ziegler-Nichols initially devised rules for tuning PID controllers. [53] describes Ziegler-Nichols tuning rule for PID controllers. [54] shows structure and further tuning rules for internal model control (IMC)-PID tuning. Within time many other techniques were developed, but [53] provides most of the comprehensive tools. Here, tuning is done after analyzing system dynamics and structure of the control and other available parameters. Their performance varies from system to system and on operation conditions. IMC and direct synthesis proved to be better in performance. [55] uses iterative feedback tuning (IFT) method, also known as the non-parametric method based on frequency response. In [56] different techniques are evaluated on the basis of performance, robustness and sensitivity. It also provides a range of stability of related controller, references, specifications and features etc. Now even auto-tuning techniques are available; for example some are mentioned in [57].

7.3.1 Method for Tuning

In this study, tuning is done with the help of Matlab initially; then tuning is done manually for better results. As was mentioned in Chapter 6, first, the system is trimmed at different points with the help of “trim function” and then it is linearized at those trim points and state space representations are found by “Linear System Analysis” tool of MATLAB. After that, controller gains (Kp, Ki and Kd) are determined for the linear systems by “PID tuning” utility in Matlab. These gains are used for the nonlinear system as the initial set and further manual tuning and modifications were made on the basis of improving responses.

7.4 Setting up System and Defining Problem

System settings include:

- Online Instrumentation for measurements of the states and O/Ps.
- Actuators as system drivers.
- Modeling of the system including all factors.
- Control criteria and standards.
- Controller for the system.
- Simulation and evaluation of the controller performance on the basis of the defined criterion.
- Analysis of transient and steady state errors.
- Elimination of noises and disturbances.
- Sensitivity of the system with respect to certain angles.

In this study, the following criteria are considered:

- It will be tried to keep overshoot as minimum as possible (around < 10%) since it causes thrusters to push the vehicle in wrong directions and also draw higher current. This is not good in terms of energy loss and endurance.

- Steady state error should be very small (for example, around < 3.5%), since, if it remains large for a long time, then it can cause variations in the whole course of operation.
- Rise and settling times will also be tried to be as small as possible within feasible ranges, so that system can become stable at its earliest. Their value also depend on system (specific variables to be controlled) and flight operation conditions.

7.5 Command Filter

Command filters are used to match the "dynamics (of change) in command" to the dynamics of system, so that abrupt changes can be handled carefully and completely. Its purpose is to smooth the input signals so that system can follow it without saturation. For example, if there is some sudden change in system command like step command, it means rate of change is infinite, and accordingly, control surfaces like elevator or others can get saturated; so the command filter will be very useful to tackle such situations. For details, see [59].

Figure 7.3 Command Filter [59]

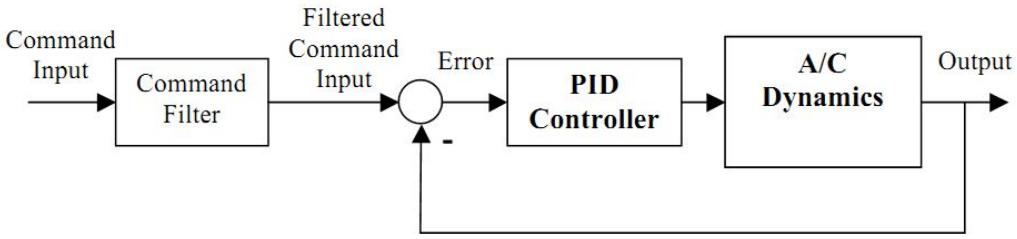

Figure 7.4 System Structure with Command Filter [59]

A low pass, second order filter as the command filter is used whose general transfer function is given below:

$$\frac{\omega_n^2}{s^2+2s\xi\omega_n+\omega_n^2} \qquad (7.3)$$

7.6 Signal Limiter

Command filters are used for the movements and rates of change in control surfaces and avoid saturation of the actuators. As was mentioned in Section 7.5, certain situations can cause saturation or even in some cases whole vehicle can become unstable and control can be lost over the system, resulting in the destruction of the vehicle. To avoid such undesirable situations, it is important to limit the system physically and virtually so that such situations cannot occur even in malfunctioning. It is not only good for virtual control, but it is very beneficial, when it comes to hardware. Here limiters are used for bounding the elevators and ailerons. In certain situations limiters are used to define upper and lower limits for pitch, yaw, roll angles and their rates of change.

7.7 Onboard Instrumentation

Online instrumentation (measurement and determination of different states) is very important for proper guidance and control (G&C) of the vehicle. Here everything is

expected to be measured with respect to the inertial frame (Fixed Earth Frame). Dynamics of inertial sensors, like accelerometers and gyros, with a high bandwidth is usually neglected. These sensors are modeled as simple gains [58]. The following sensors are expected to be available on board of the WIG:

1- INS: Since it is expected that we know the position of the vehicle at every instant, an inertial navigation system (INS) must be present in the vehicle on board. It is used to determine the position and orientation, automatically and independently. IMU unit usually involves three orthogonal accelerometers, and three orthogonal gyros (usually rate-gyros). They provide accelerations, and upon whose integrations, positons and rotation rates and Euler angels are determined.

2- GPS: Precise position and position rate can also be determined by the global positioning system (GPS).

3- Barometer, altimeter and other similar sensors can also be used to determine pressures, altitude.

In the following sections controller implementations will be discussed.

7.8 Pitch Attitude Hold

The pitch controller or pitch attitude hold (PAH) mode is the basic longitudinal autopilot mode; it controls the pitch angle theta (θ), if its value differs from the desired reference value, by applying appropriate deflections of the elevator (δ_e). Pitch controller can be implemented either by single loop (only one single loop from theta to deflection) or two loops (one inner of pitch rate q, and one outer of pitch angle itself), are used to design the controller. Normally, the PAH mode serves as the inner loop for the altitude hold and other longitudinal controllers.

The pitch angle θ is fed back to the system, to keep the pitch angle at the desired value. A proportional, integral and derivative controller is used, to make sure that no steady-state error will remain. Block diagram in Figure 7.5 shows the structure of PAH.

As was mentioned in Section 7.3.1, initial values for controller gains were determined on the basis of linearized systems. Those values are used initially and they are further tuned with the PID tuner for the nonlinear system and finally they are manually tuned for final values. Initial values found were $K_{\mathrm{p}} = -8$, $K_i = -0.6$, $K_d = 0.003$ and these values were further improved after some tuning to $K_{\mathrm{p}} = -10.3$, $K_i = -1$, $K_d = 0.0053$ for the outer loop.

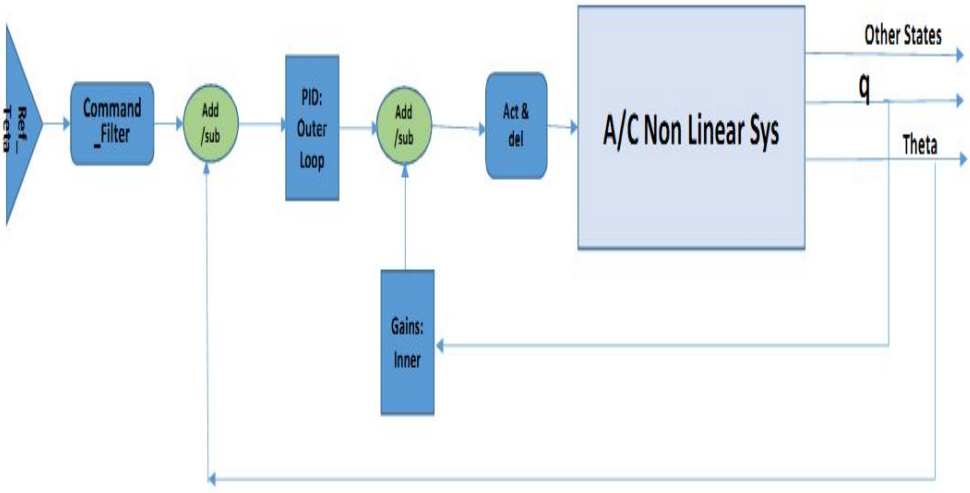

Figure 7.5 PAH Block Diagram

Performance of the controller is tested for the 6DOF nonlinear model of the WIG. Different inputs were given and response of the control system was tested. It gave satisfactory results. Figure 7.6 shows the results for different inputs.

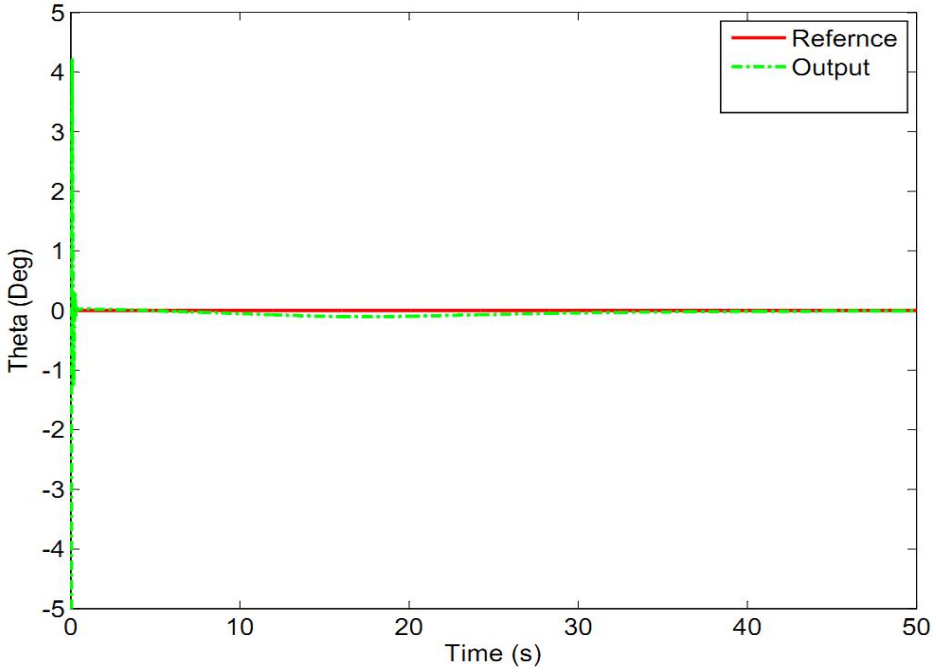

Figure 7.6 a: PAH Response Example 1

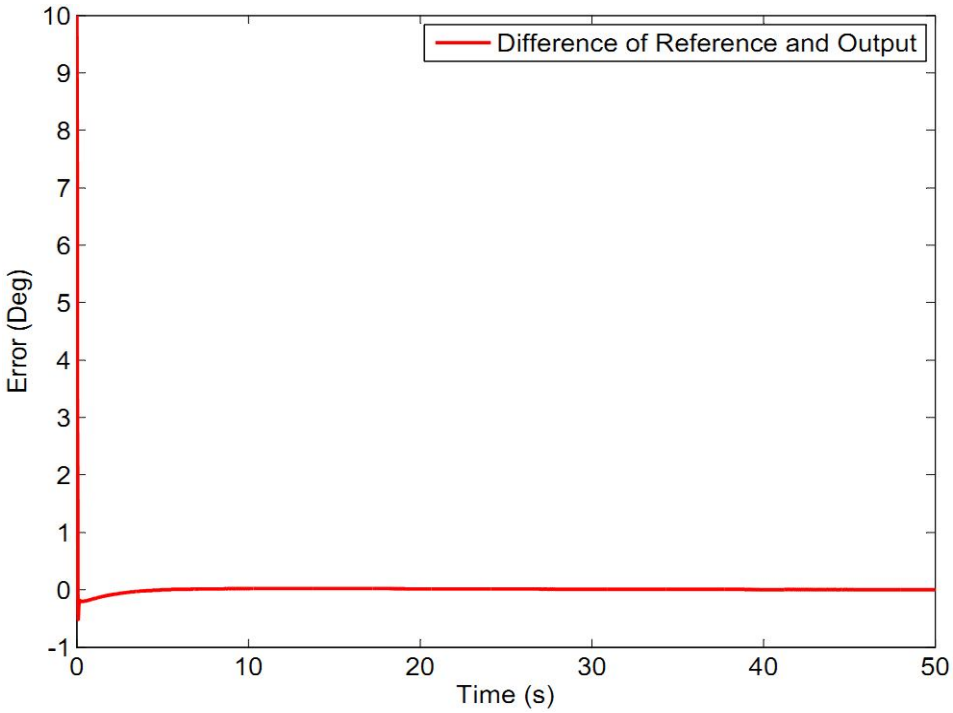

Figure 7.6 b: Error in case of PAH Example 1

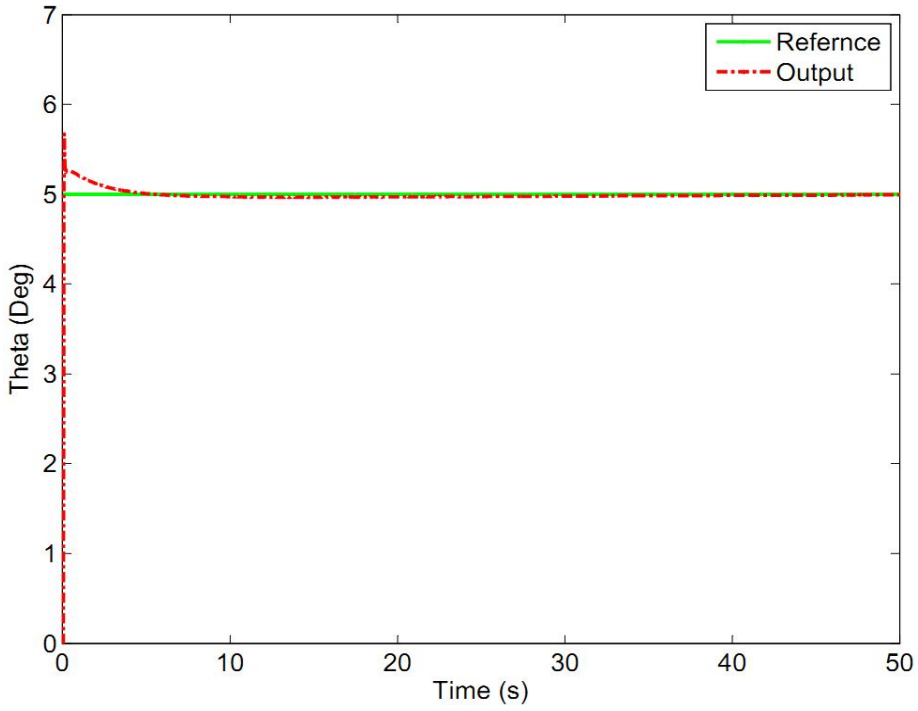

Figure 7.6 c: PAH Response Example 2 (Without Command Filter)

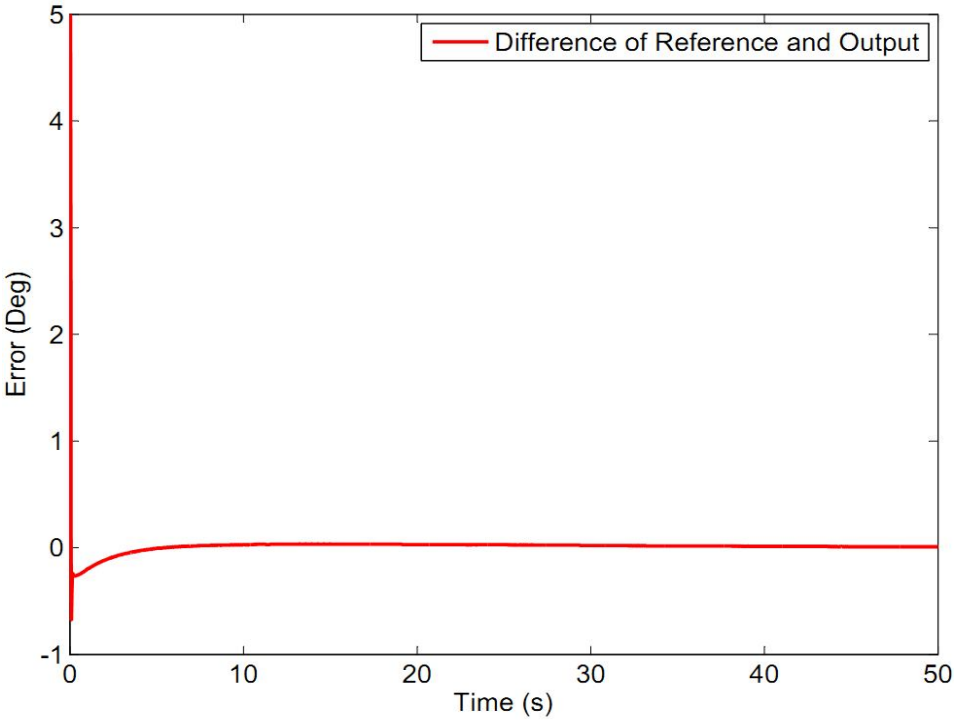

Figure 7.6 d: Error in case of PAH Example 2

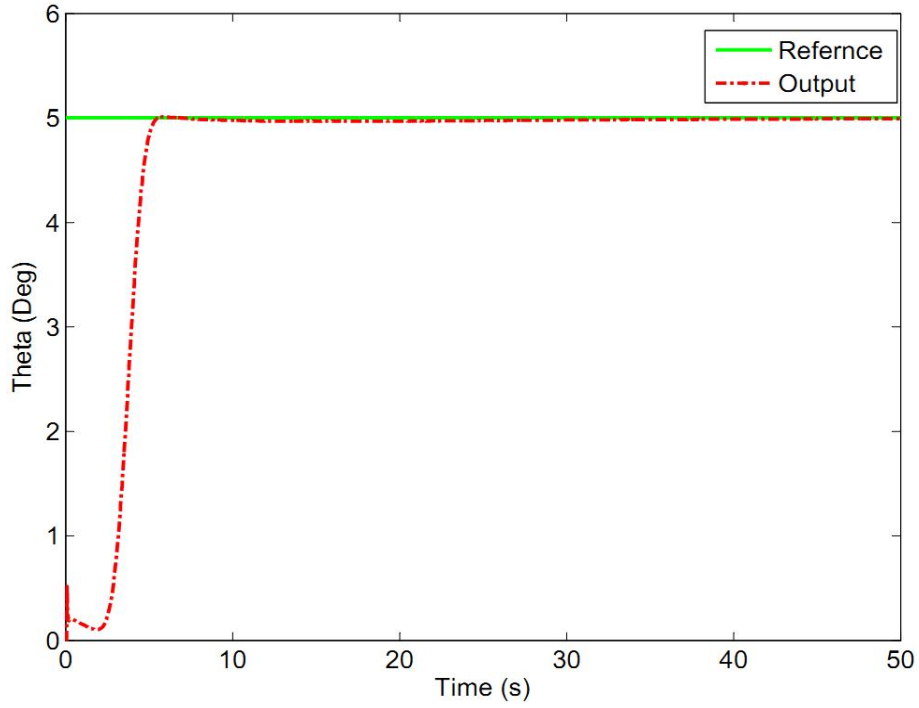

Figure 7.6 e: PAH Response Example 3 (With Command Filter)

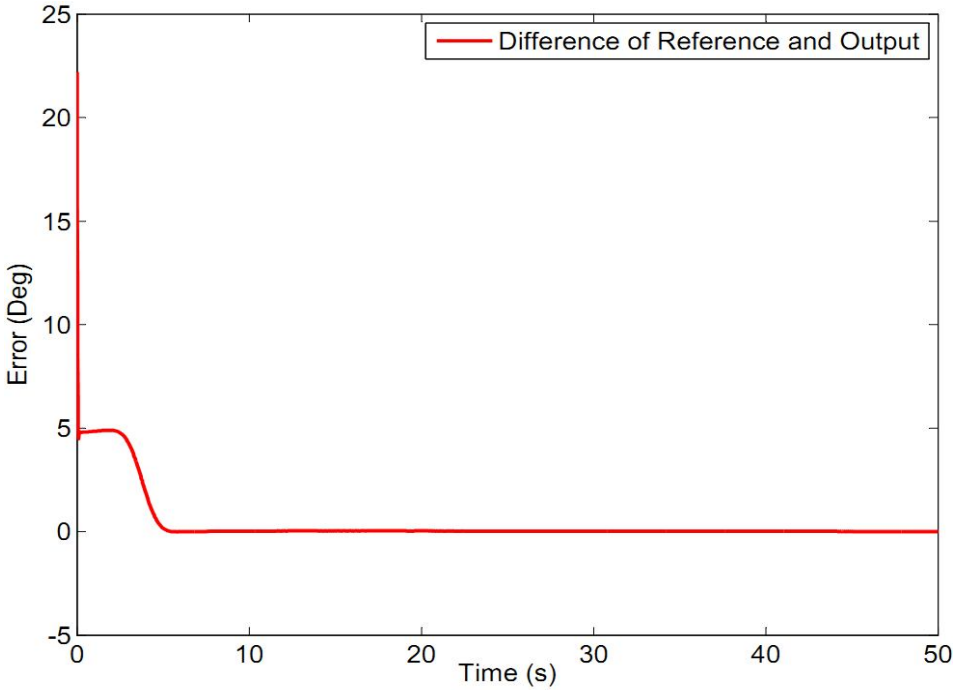

Figure 7.6 f: Error in case of PAH Example 3

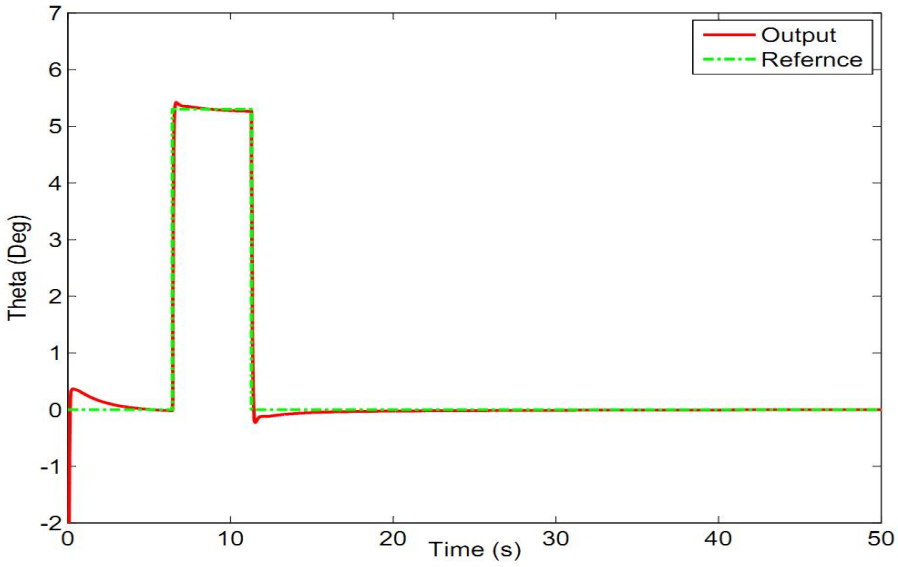

Figure 7.6 g: PAH Response Example 4 (Without Command Filter)

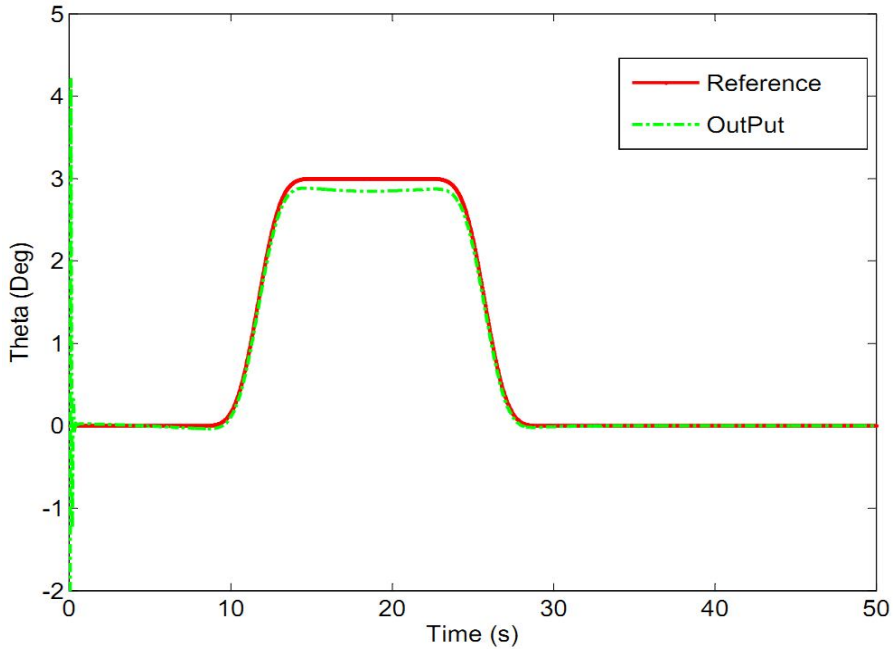

Figure 7.6 h: PAH Response Example 4 (With Command Filter)

Figure 7.6 PAH Responses to Different Inputs

7.9 Roll Attitude Hold

The roll controller or roll attitude hold (RAH) mode is the basic lateral autopilot mode; it controls the roll angle (ϕ), if its value differs from the desired reference value, by applying appropriate deflections of the aileron (δ_a). Roll controller can be implemented either in single loop (only one loop from phi angle) or two loops (one inner of roll rate p and one outer for phi angle itself) are used in the design of the controller. Normally, the RAH mode serves as the inner loop for the other lateral controllers.

The angle ϕ is fed back to system, to keep the phi angle at a desired value. Again proportional, integral and derivative controllers are used, to make sure that no steady state errors will remain. Block diagram in Figure 7.7 shows the structure of RAH.

As was mentioned in Section 7.3.1, initial values for controller gains were determined on the basis of linearized systems, and those values are used as initially and they are further tuned with PID tuner for the nonlinear system and finally it was manually tuned for final values. Initial values found were $K_{\mathrm{p}} = -35.3$, $K_i = -25$, $K_d = 0.003$ and these values were further improved after some tuning to $K_{\mathrm{p}} = -40$, $K_i = -30$, $K_d = 0.001$ for the outer loop.

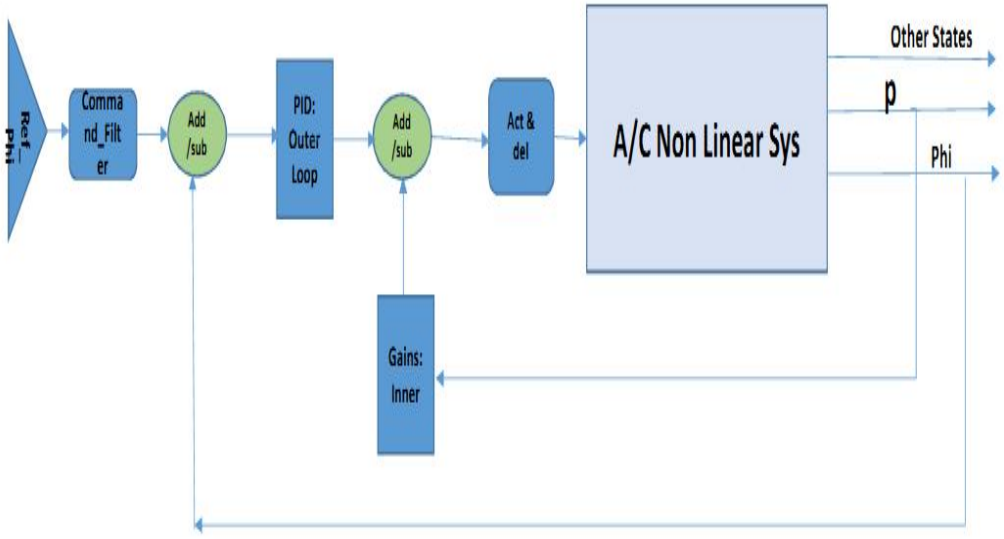

Figure 7.7 RAH Block Diagram

Performance of the controller is tested for the 6DOF nonlinear model of the WIG. Different inputs were given and response of the control system was checked. It gave satisfactory results. Figure 7.8 shows the results for different inputs.

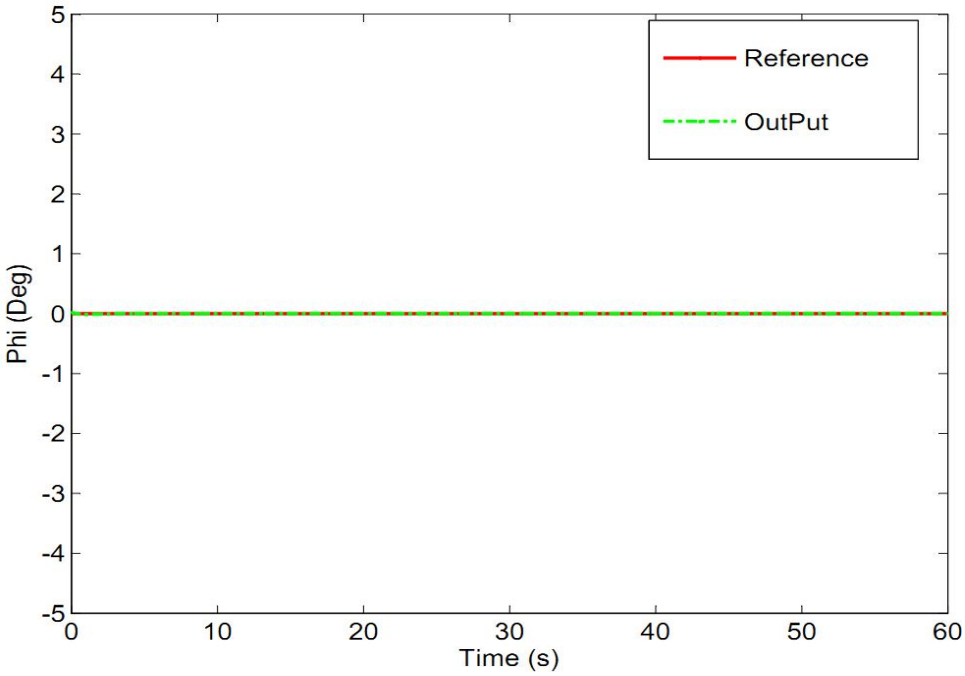

Figure 7.8 a: RAH Response Example 1

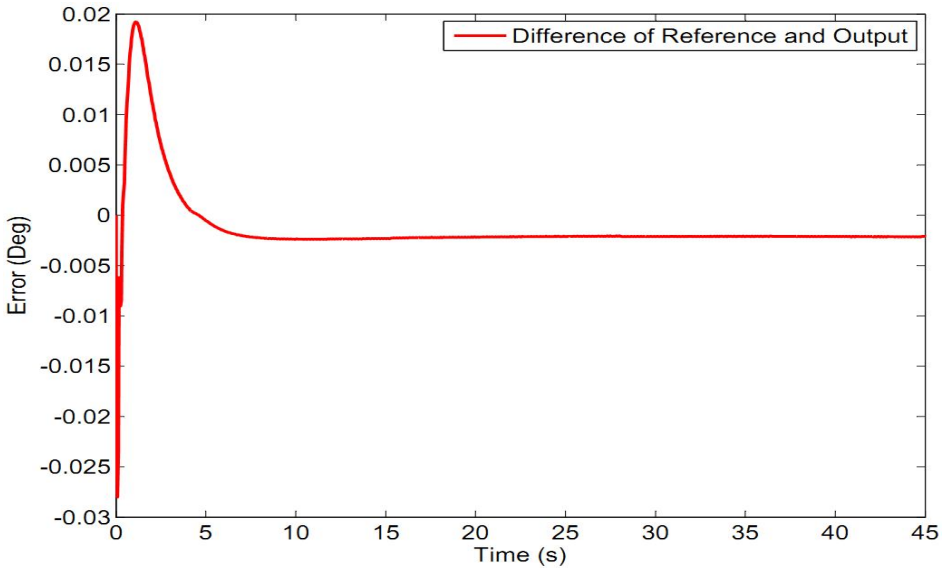

Figure 7.8 b: Error in case of RAH Example 1

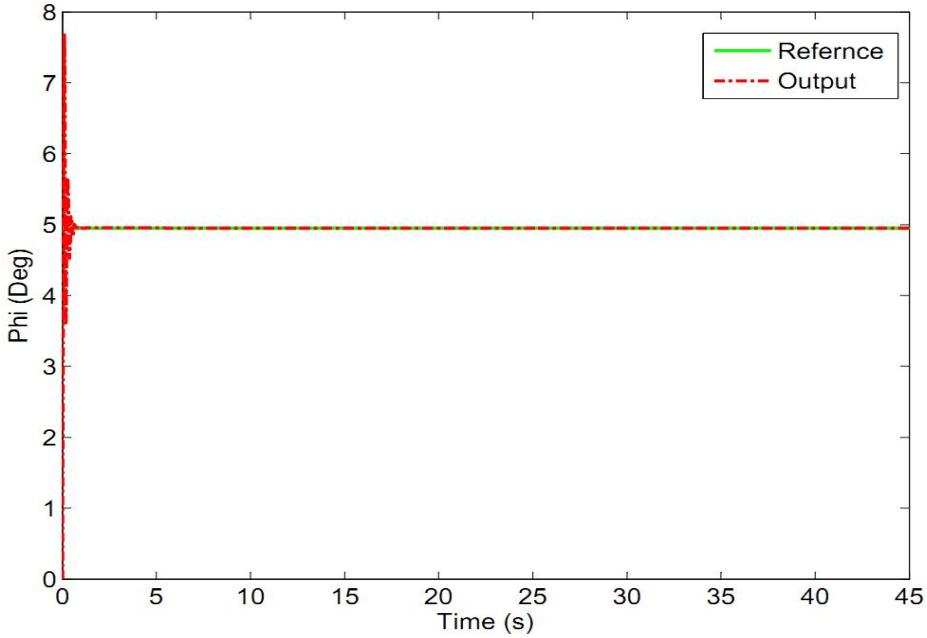

Figure 7.8 c: RAH Response Example 2 (Without Command Filter)

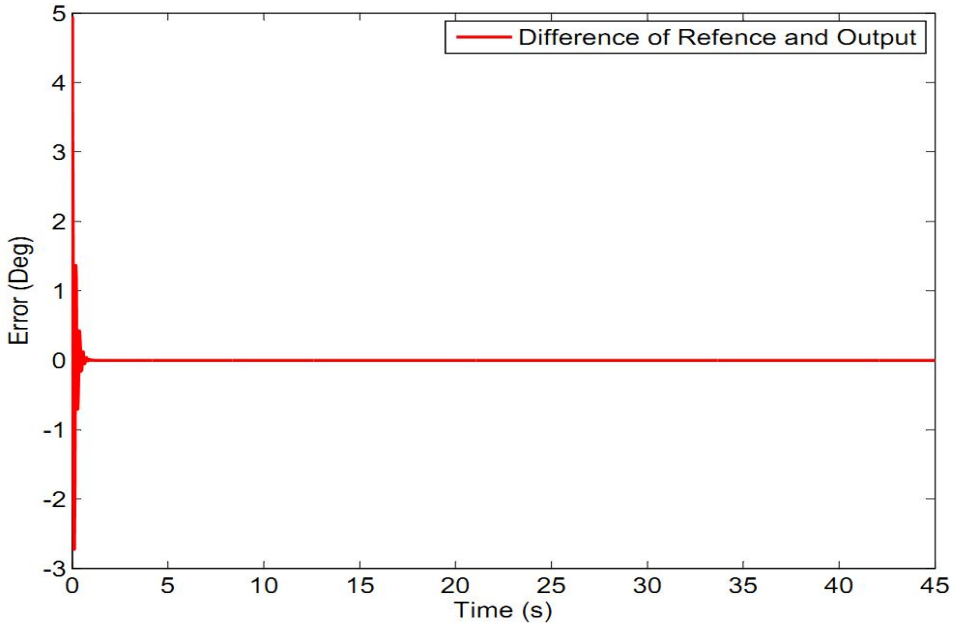

Figure 7.8 d: Error in case of RAH Example 2

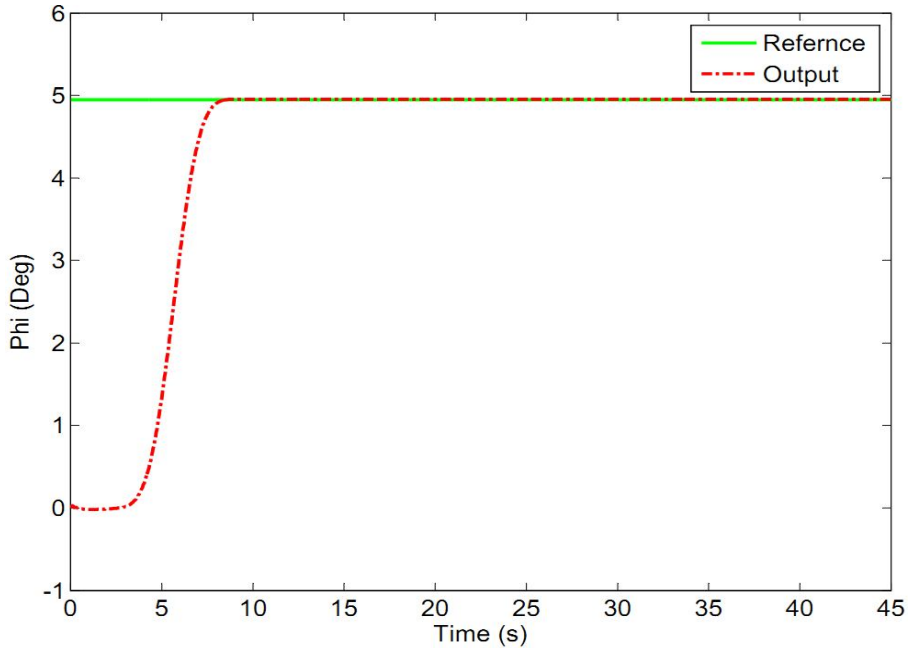

Figure 7.8 e: RAH Response Example 3 (With Command Filter)

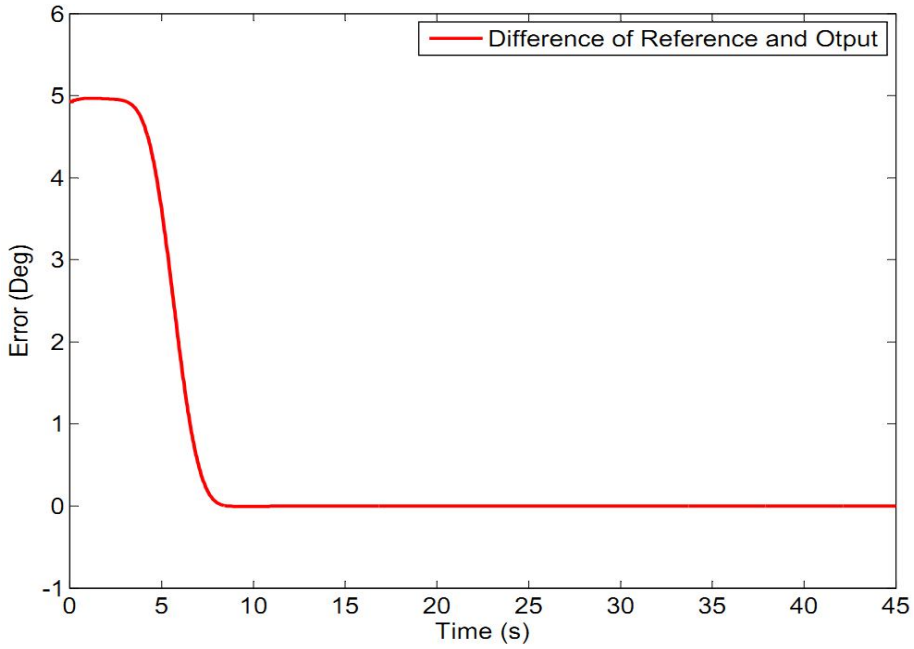

Figure 7.8 f: Error in case of RAH Example 3

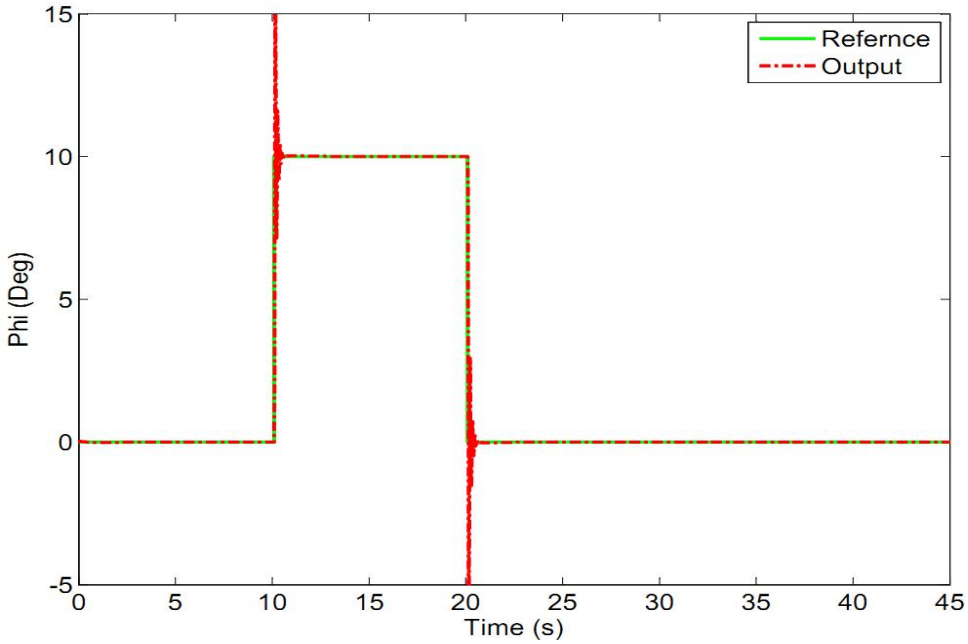

Figure 7.8 g: RAH Response Example 4 (Without Command Filter)

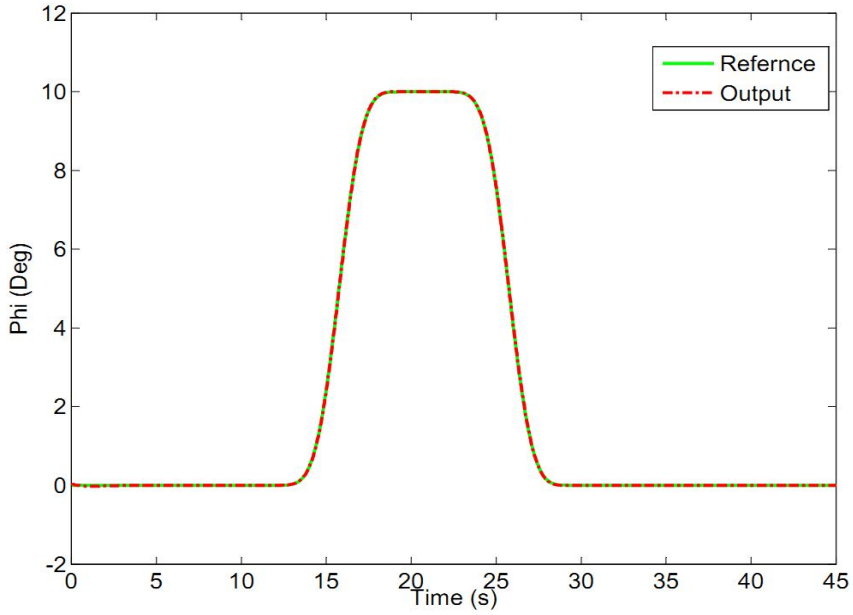

Figure 7.8 h: RAH Response Example 5 (With Command Filter)

Figure 7.8 RAH Responses to Different Inputs

7.10 Speed Controller

It was mentioned in the modeling part that vehicle speed has three components u, v, w. Although these three components can be controlled separately, here controller is developed for the overall vehicle speed.

For speed control, in the same way as before, speed is fed back to adder/subtracter, which inputs the difference of its reference speed and the current speed (error), to the controller.

Two thrusters (right and left) are used as the propulsion (forward) source. The force produced by them is directly proportional to the thrust force and in fact, directly proportional to the speed of the vehicle. It controls the speed, although it can have different effects on different (three) components of the speed. Equation 7.63, again mentioned below shows effects of thrust force directly in x direction.

$$T = F_b = \sum_i^n F_i \begin{bmatrix} 1 \\ 0 \\ \alpha_m \end{bmatrix}$$

It is the reason that only a single loop is enough for the speed controller. Even the same controller is sufficient for right and left parts, because they have the same contribution to thrust force. Its block diagram is shown in Figure 7.9.

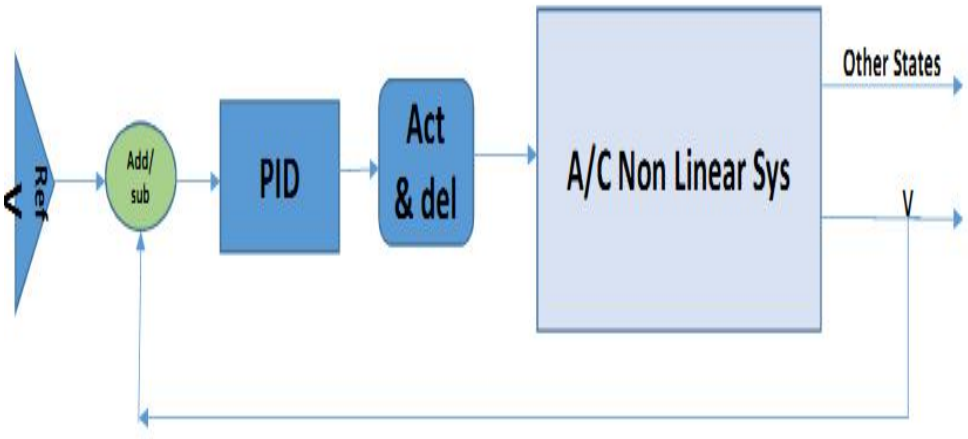

Figure 7.9 Speed Controller Block Diagram

Initial values found were $K_p = 1$, $K_i = 1$, $K_d = 0.0123$ and these values were further improved after some tuning, to $K_p = 1.5$, $K_i = 1.5$, $K_d = 0$.

Different inputs were given and response of the control system was checked. It gave satisfactory results. Figure 7.10 shows the results for different inputs.

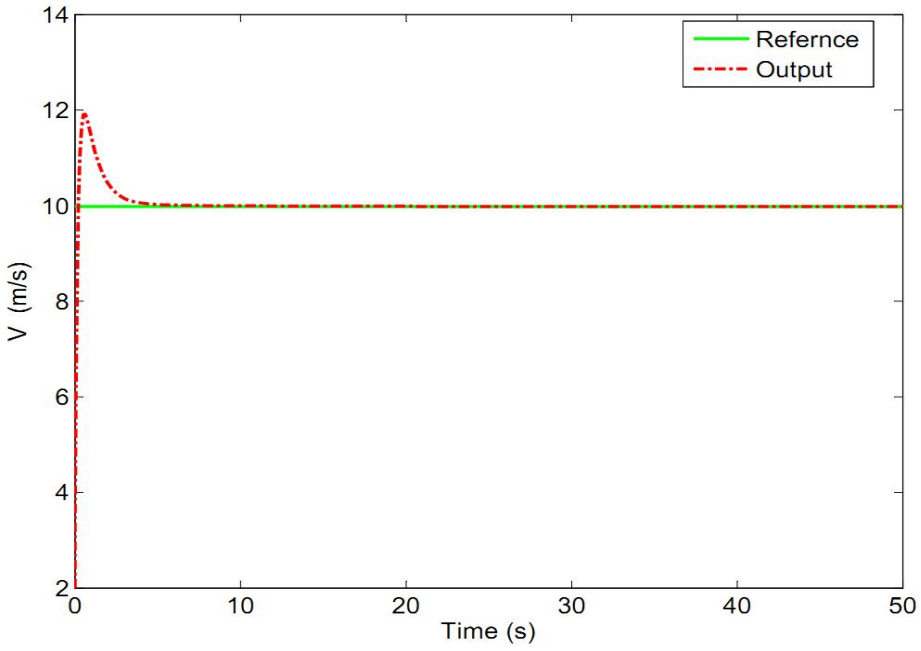

Figure 7.10 a: Speed Controller Response Example 1

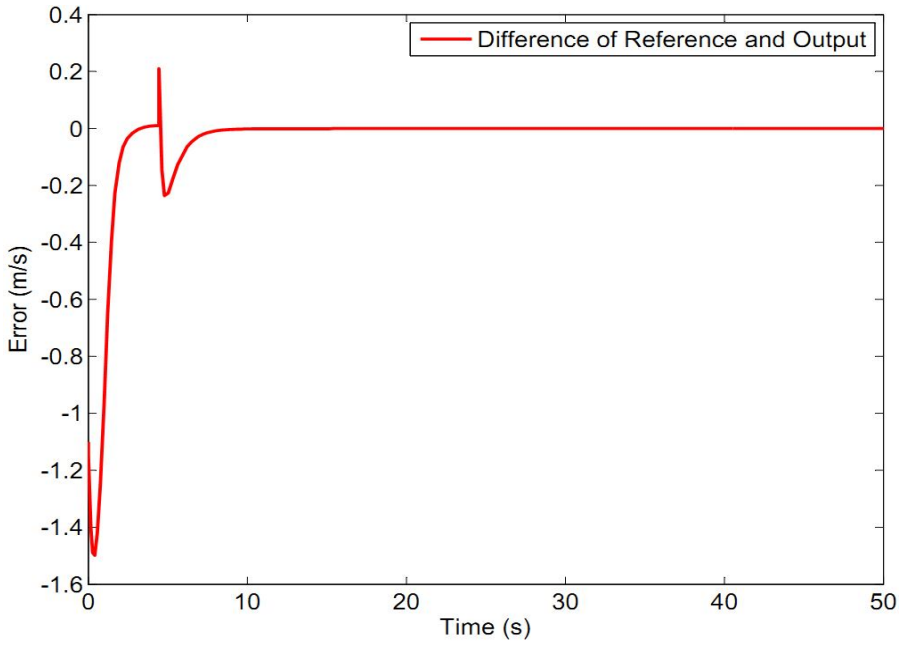

Figure 7.10 b: Error in case of Speed Controller Example 1

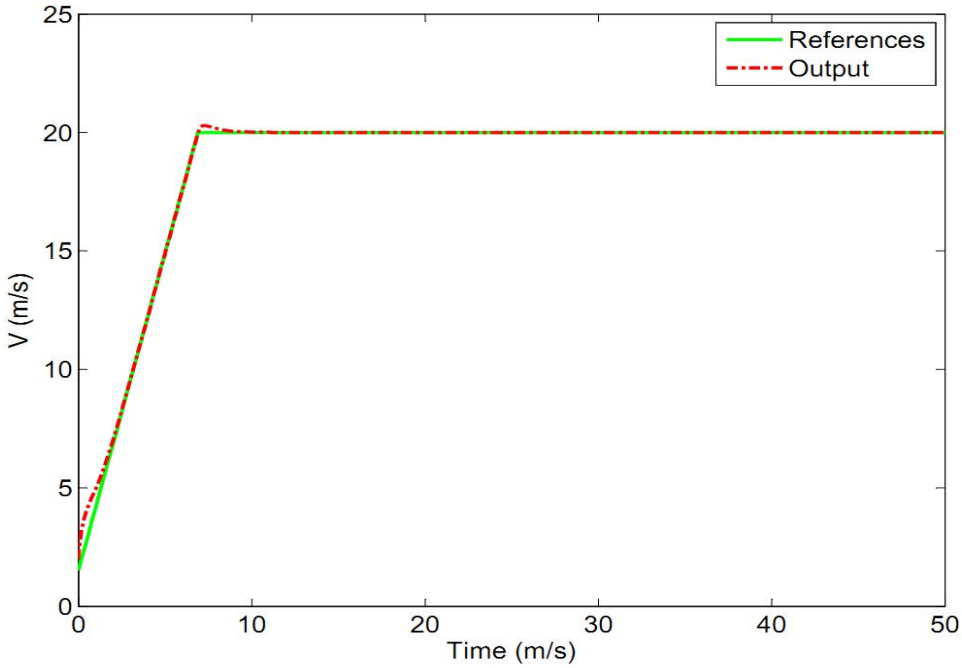

Figure 7.10 c: Speed Controller Response Example 2

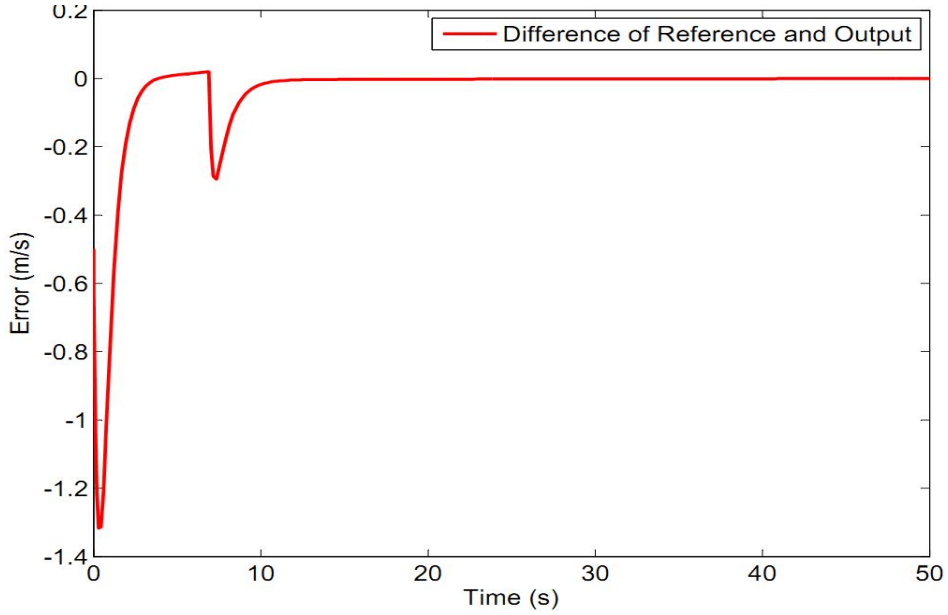

Figure 7.10 d: Error in case of Speed Controller Example 2

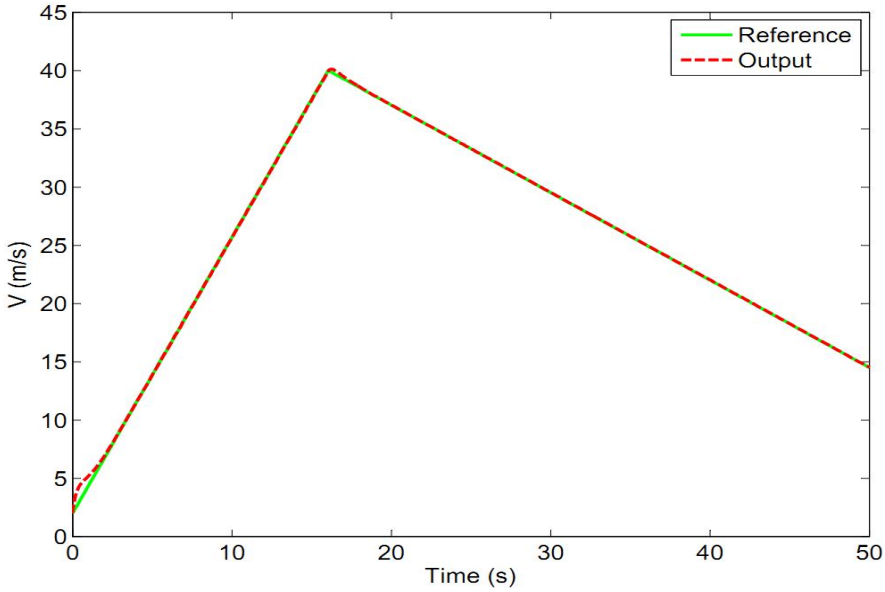

Figure 7.10 e: Speed Controller Response Example 3

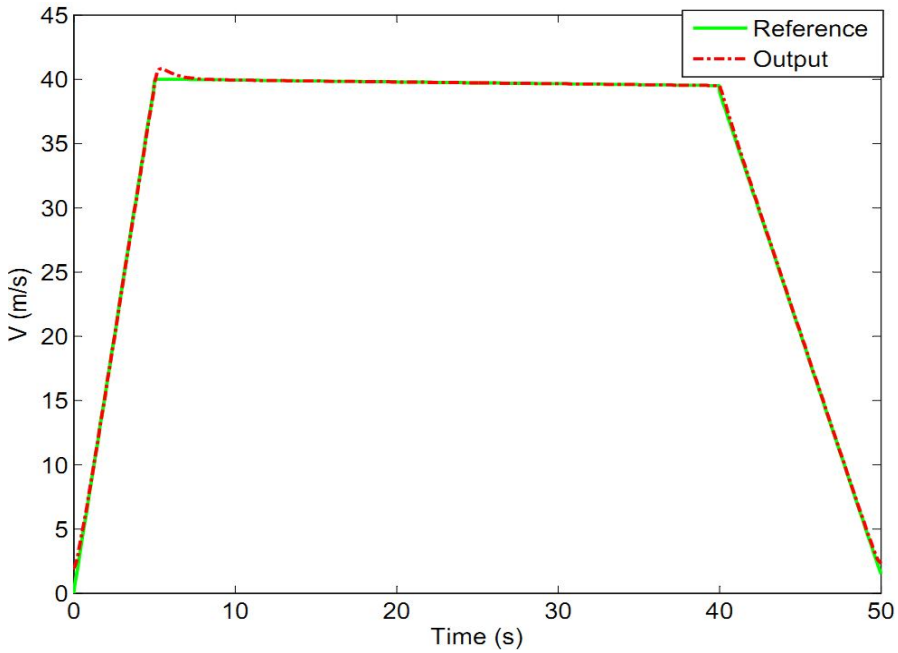

Figure 7.10 f: Speed Controller Response Example 4

Figure 7.10 Speed Controller Responses

7.11 Yaw Angle (Heading) Controller

The yaw angle or heading control maintains a specific direction for the vehicle. It controls the yaw angle psi (ψ) by applying appropriate force with the help of propellers, if its value differs from the desired reference value. Only for the heading control, controller is designed with a simple single loop, but with two separate controllers. Only psi (ψ) is fed back, but two separate controllers are used; one for the right propeller and one for the left propeller control. When it is desired to turn it to right, left controller becomes more effective and right propeller becomes less effective or zero or negative, depending upon the conditions. Similarly, for turning left, right controller becomes more effective, and left propeller becomes less effective, zero or negative depending upon the conditions. The yaw rate (r) can be used as the inner feedback loop, but it can work perfectly without the inner loop. Section 5.3.3 describes it in mathematical terms. Explicitly, the resultant action is shown in the equation below.

$$M_b = \sum_i^n M_{Fi} \left(z_b - x_b \alpha_m\right) \begin{bmatrix} 0 \\ 1 \\ 0 \end{bmatrix}$$

Figure 7.11 shows block diagram structure of the design. The values found are: values for the right PID controller were $K_{\mathrm{p}} = 25$, $K_i = 20$, $K_d = 0.0$ and for the left controller were $K_{\mathrm{p}} = -15$, $K_i = -20$, $K_d = 0.0$.

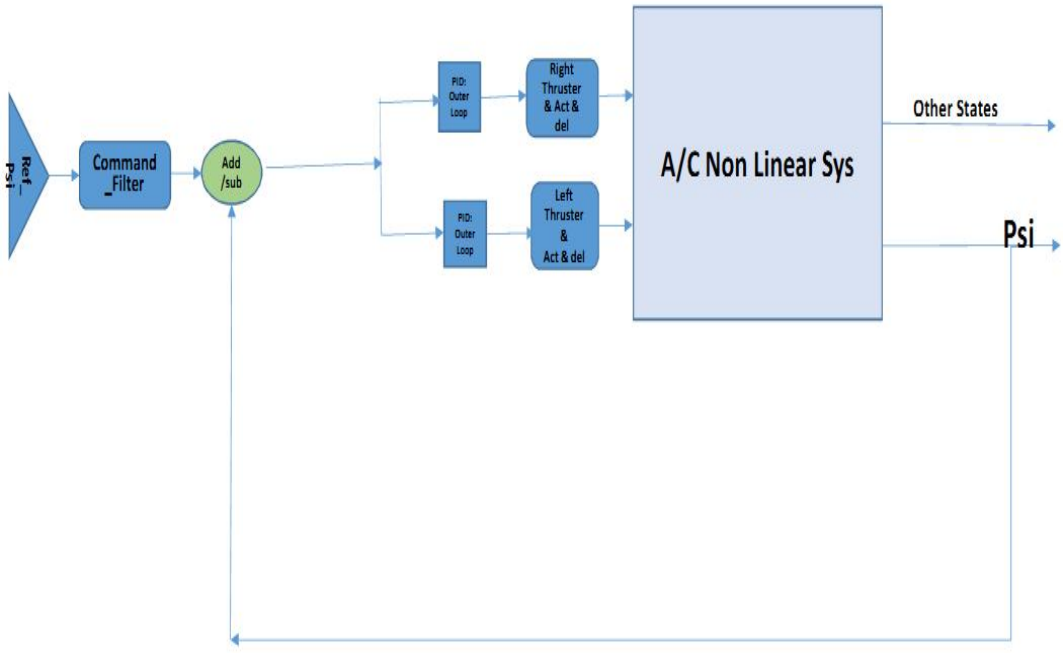

Figure 7.11 Heading Controller Block Diagram

Different inputs were given and response of the control system was checked. It gave satisfactory results. Figure 7.12 shows the results for different inputs.

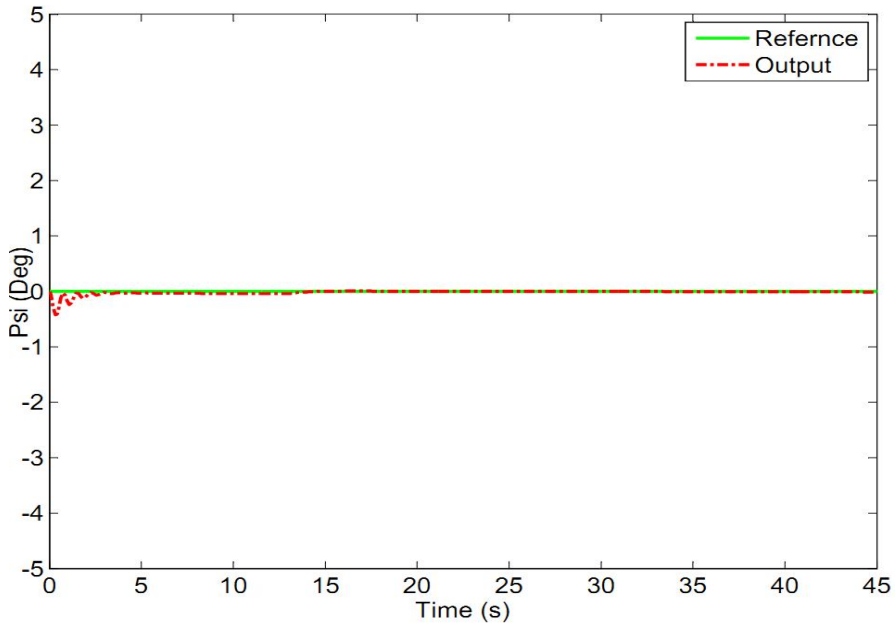

Figure 7.12 a: Heading Controller Response Example 1

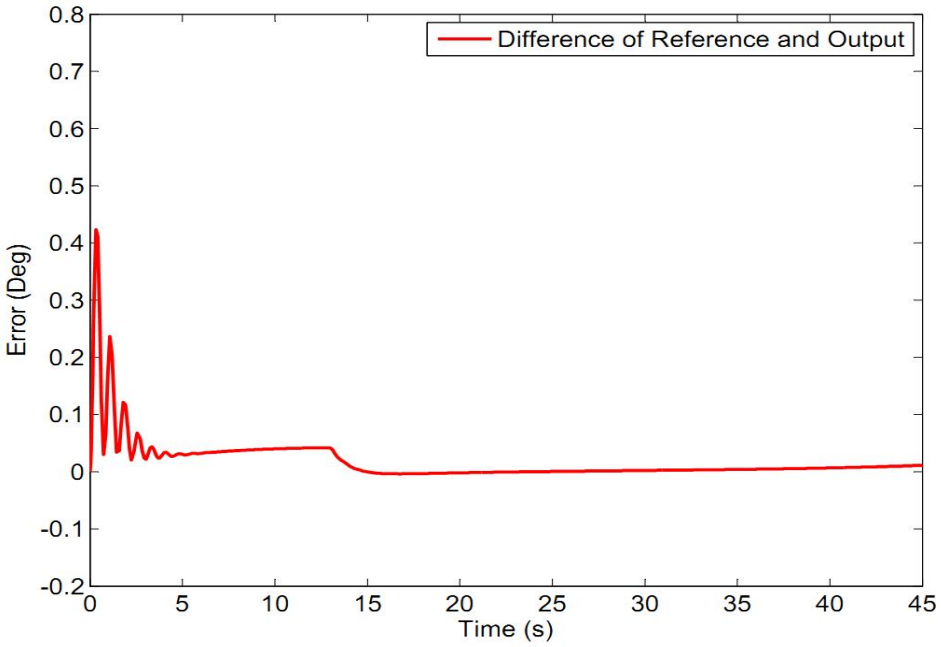

Figure 7.12 b: Error in case of Heading Controller Example 1

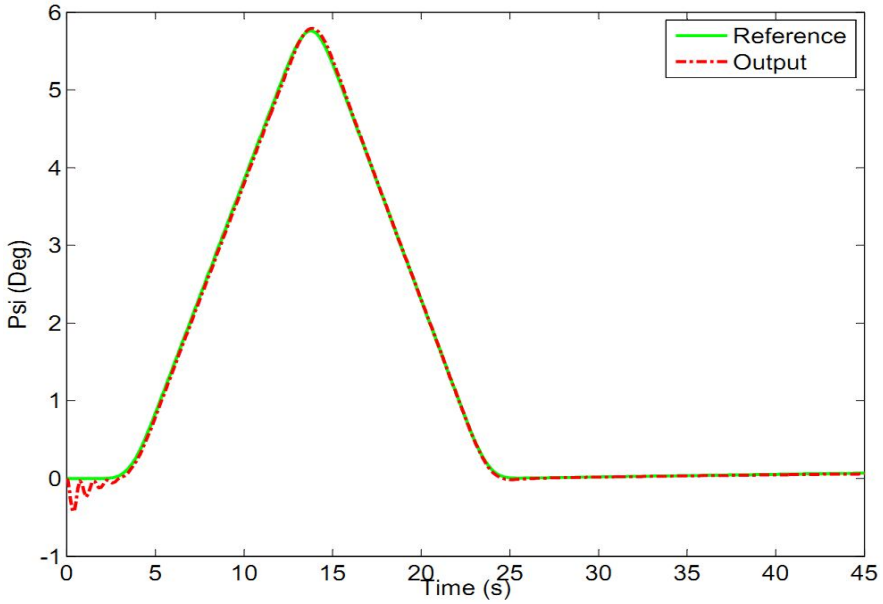

Figure 7.12 c: Heading Controller Response Example 2 (With Command Filter)

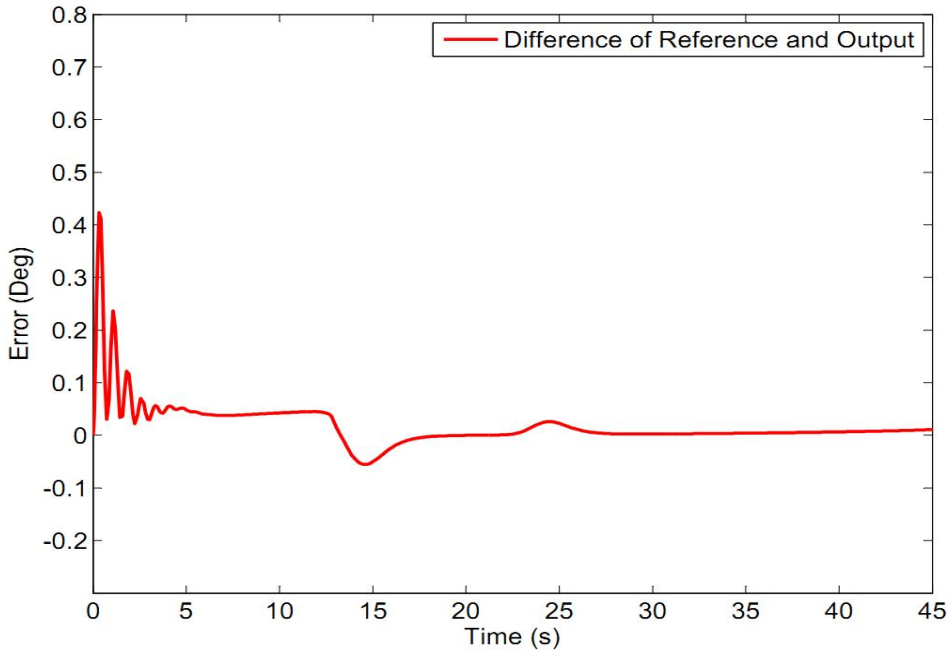

Figure 7.12 d: Error in case of Heading Controller Example 2

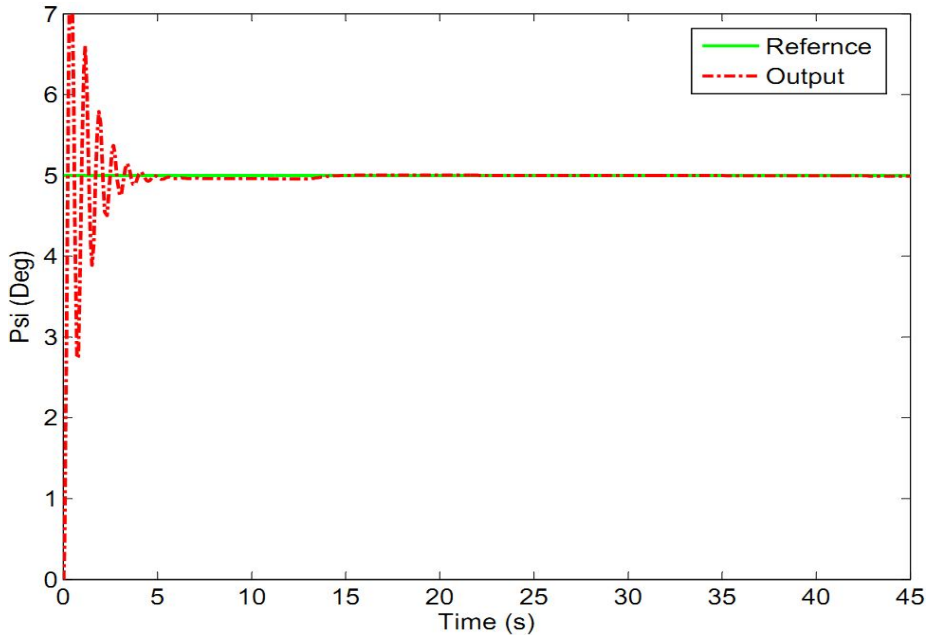

Figure 7.12 e: Heading Controller Response Example 3 (Without Command Filter)

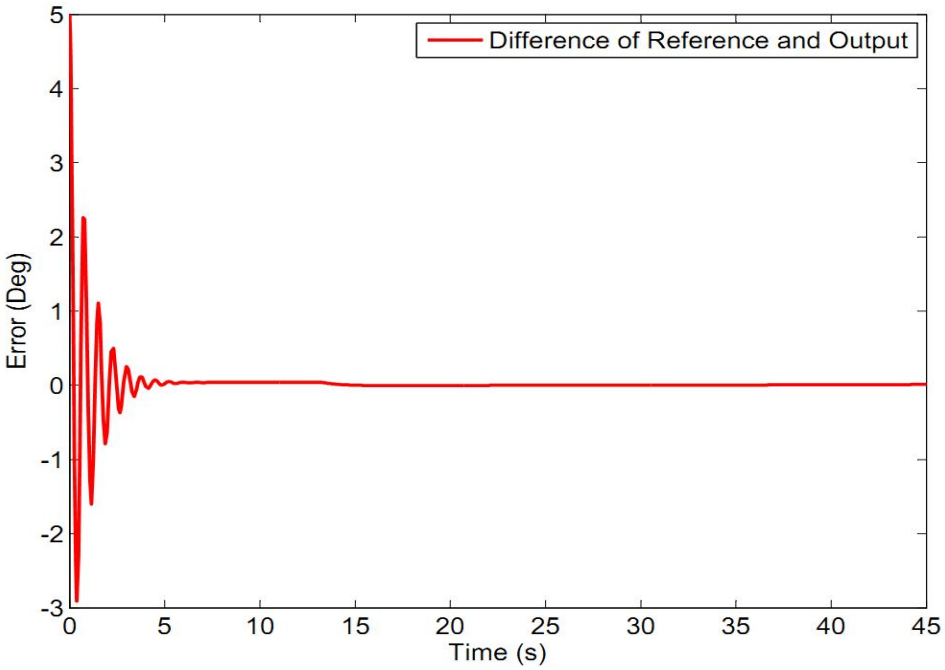

Figure 7.12 f: Error in Case of Heading Controller Example 3

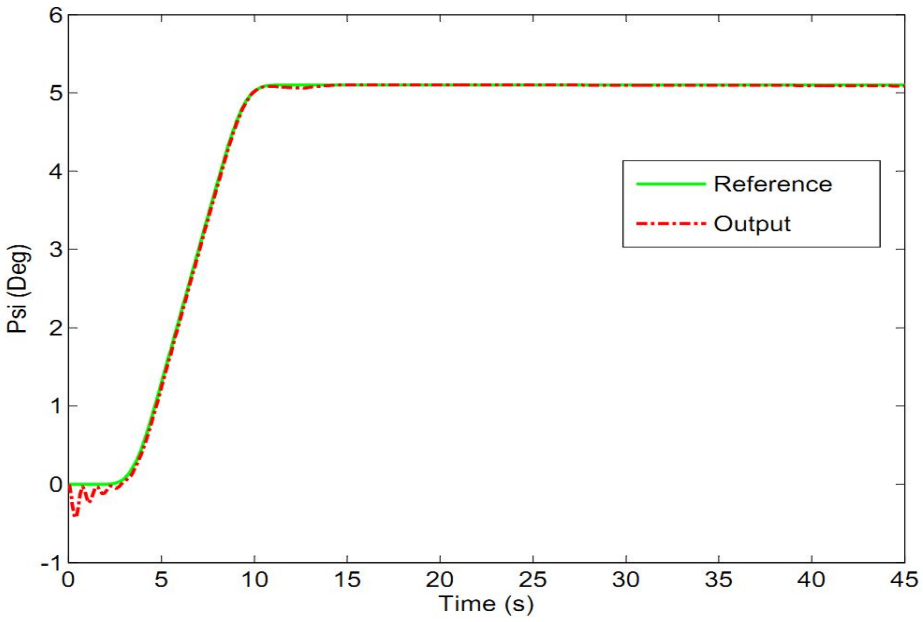

Figure 7.12 g: Heading Controller Response Example 4

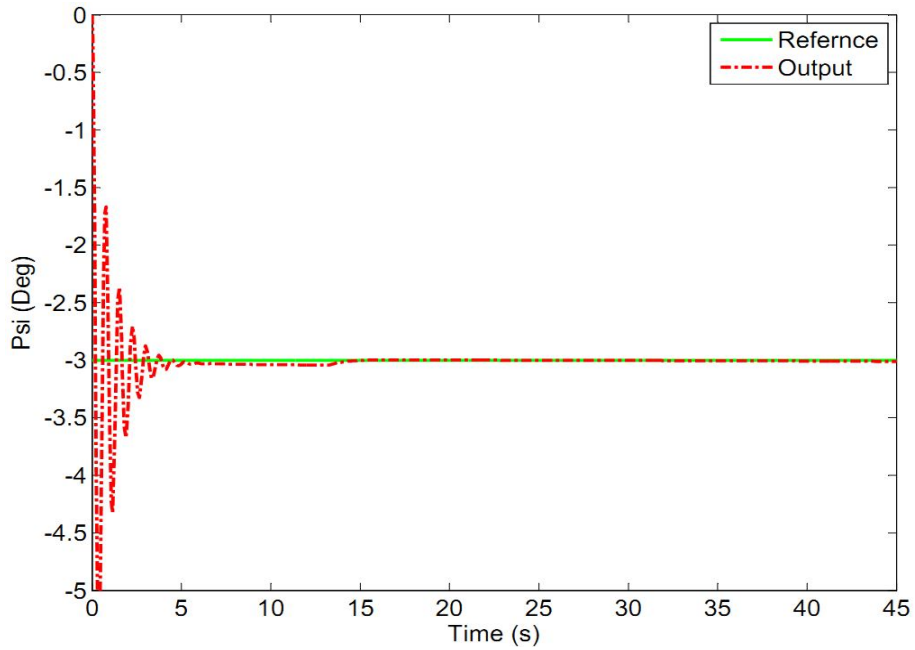

Figure 7.12 h: Heading Controller Example 5

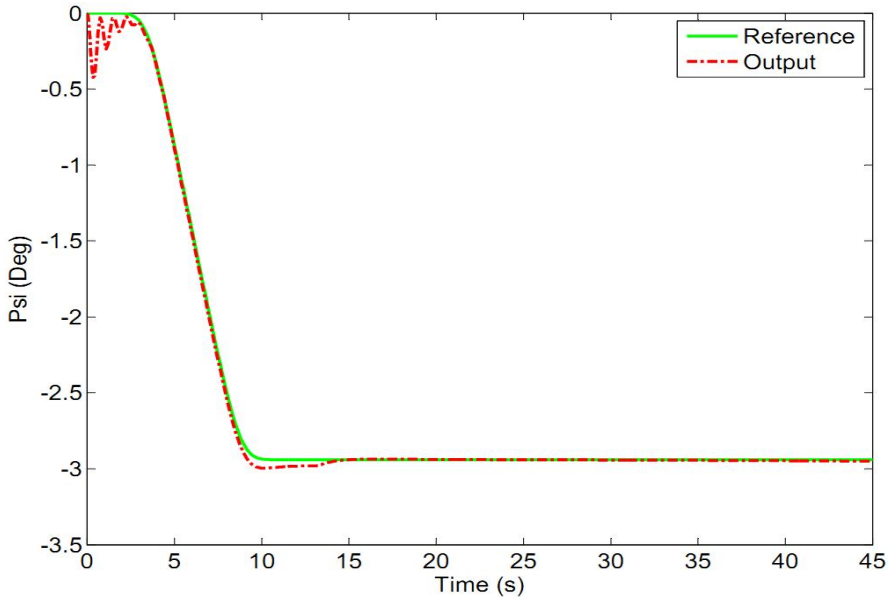

Figure 7.12 i: Heading Controller Example 6

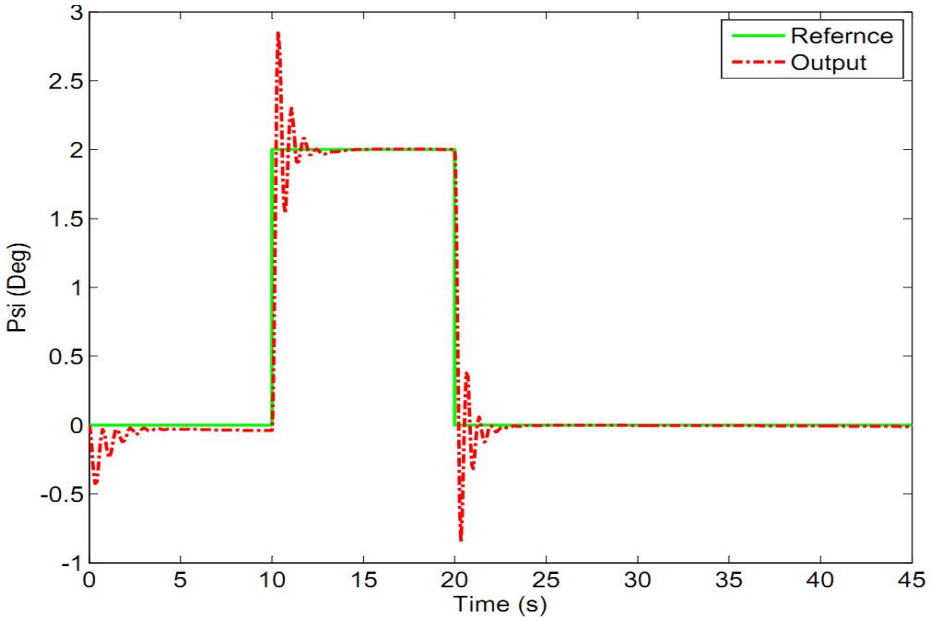

Figure 7.12 j: Heading Controller Example 7

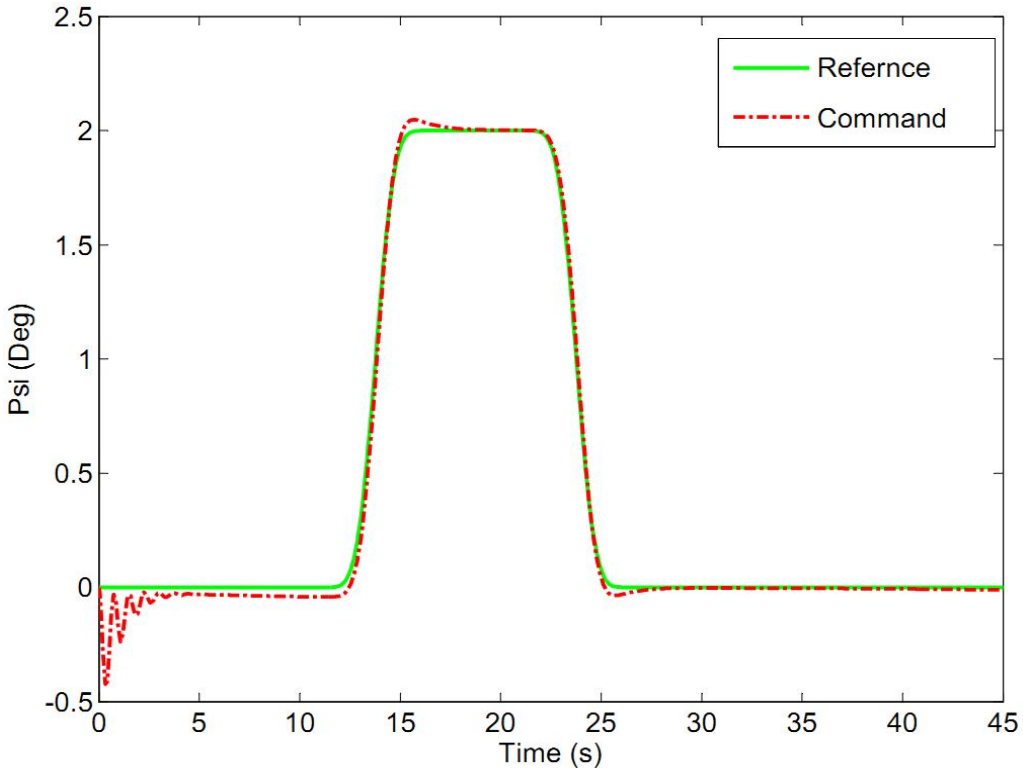

Figure 7.12 k: Heading Controller Example 8

Figure 7.12 Heading Controller Testing Examples

Although heading controller alone can work properly, this perfection is only for controlling the heading, since the same propellers are also working for speed (thrust). So, even though this design is good for direction control, it can have adverse effects on the velocity of the vehicle, at the same time. Like if it is turning in one direction, since one thruster gets slower or less efficient, it will certainly lower the forward speed. In order to tackle this situation, a third controller with an inner velocity control loop can be used to control the speed and heading at the same time. This case is considered in the next session.

7.12 Speed and Heading Autopilot

As was mentioned before, if a single loop is used for the heading controller only, it will affect the speed of the vehicle, since the same thruster are controlling the speed which are used for the heading control, which may be undesirable in certain situations. So, to avoid this situation, double loop (one inner and one outer loop) are used for the speed and heading controller at the same time. Inner loop is for speed; it is fed back and accordingly, the difference with reference speed is input to the speed controller and the yaw angle is fed back and its difference with the reference acts as the input to both left and right thruster controllers, separately. Inner loop (speed loop) acts very fast while the heading controller is acting as the outer loop and is comparatively slower. So, three controllers are used, one for the right thruster, second one for the left thruster and third for the speed, in two loops. This design was implemented, as shown in Figure 7.13, and worked perfectly for both heading and speed controllers at the same time. Now, when the vehicle turns in a certain direction, one thruster gets slower for the turning moment, the other thruster becomes faster, for the compensation of the speed loss and results in quick turning.

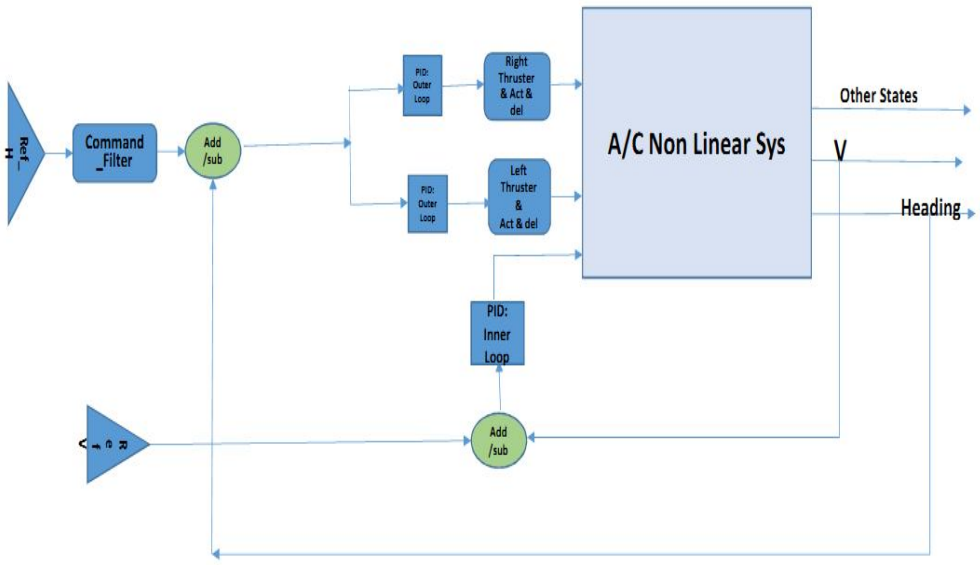

Figure 7.13 Heading-V Controller Block Diagram

1. Only Forward Command: For such situations, right and left thrusters operate at the same speed (rpm) and they push the vehicle forward in the same direction without any moment from thrusters (since they are produce equal and opposite thrust, cancelling the moment of the other one). Their heading change is associated with the commanded force direction.

2. When Only Heading (Yaw Moment) is Commanded: For such situations, right and left propellers (thrusters) work at the same rpm, but in opposite directions. Direction of propellers changes, accordingly as the commanded yaw moment changes.

3. Both Yaw Moment and Forward Thrust are Commanded: The situation becomes very interesting when both yaw moment and forward movement are commanded at the same time. Now thrusters operate at different rpms. For instance, when it is required the craft to turn around in a circle in some direction such as clockwise, than the rpm of the left must be greater than the right one. Mathematically, this relation can be expressed as follows.

$$T1\ rpm\ (Left) = F$$

$$T2\ rpm\ (Right) = F - \Gamma F$$

$$0 < \Gamma < \text{const}$$

where V and const. are the parameters depending on different specifications of the propellers like weight and efficiency factor, diameter (dia) of the circle. In this example the dia of the circle is inversely proportional with the propeller weight.

Figure 7.13 shows the block diagram structure of the design. The values found were $K_p = 24$, $K_i = 19$, $K_d = 0.0$ for the right psi controller, and $K_p = -16$, $K_i = -21$, $K_d = 0.0$ for the left controller, and for speed (V) controller gains were $K_p = 1$, $K_i = 1$, $K_d = 0.0$.

Different inputs were given and response of the control system was checked. It gave satisfactory results. Figure 7.14 shows the results for different inputs.

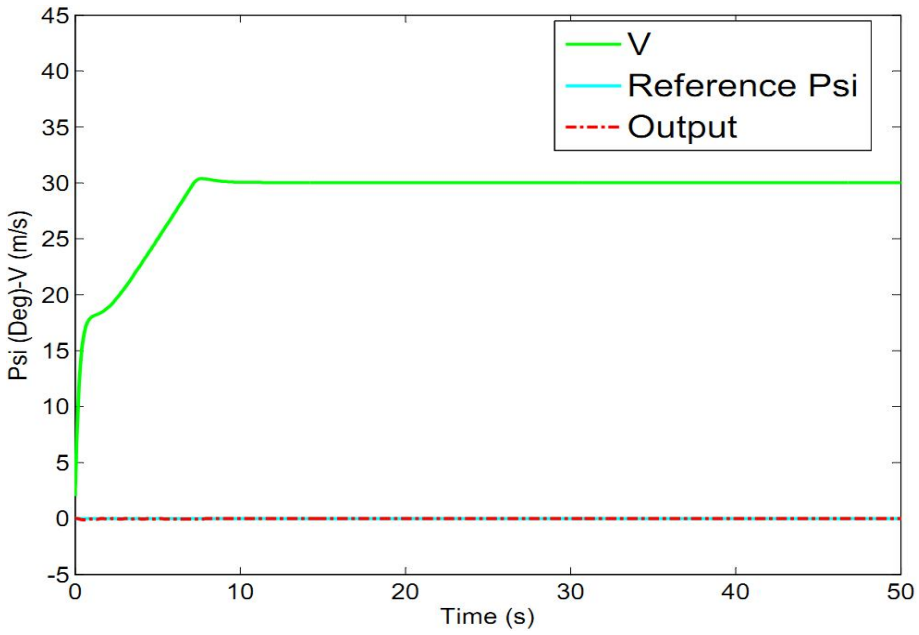

Figure 7.14 a: Psi-V Autopilot Response Example 1

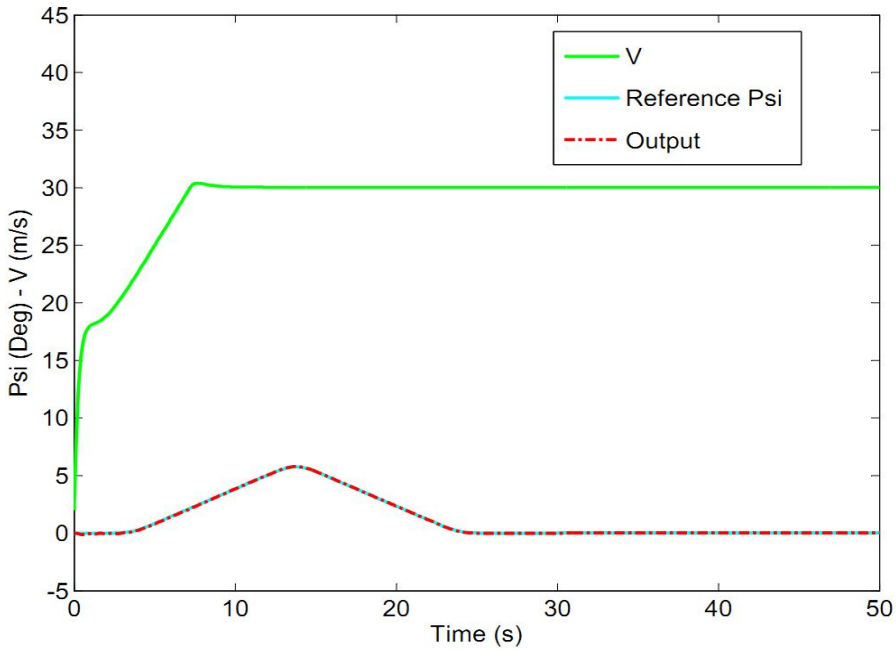

Figure 7.14 b: Psi-V Autopilot Response Example 2

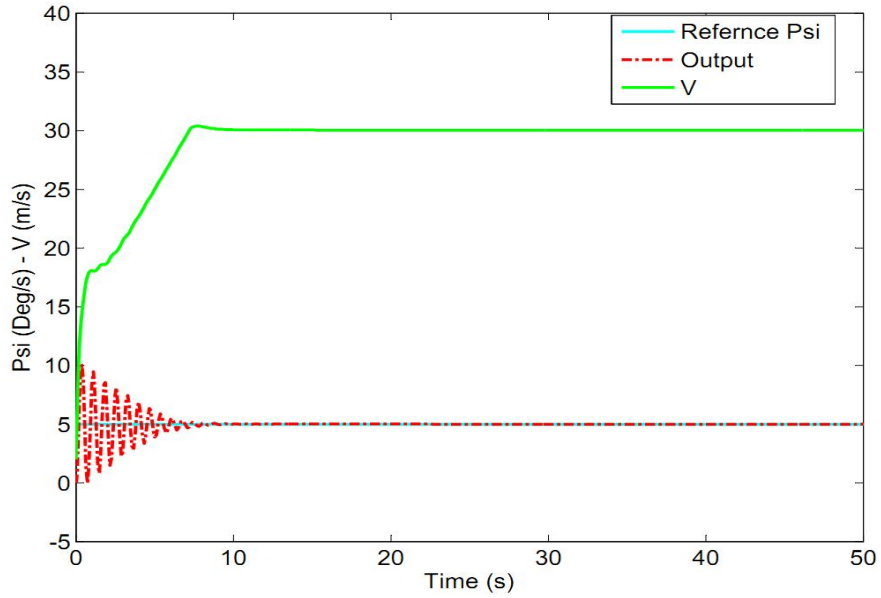

Figure 7.14 c: Psi-V Autopilot Response Example 3 (Without Command Filter)

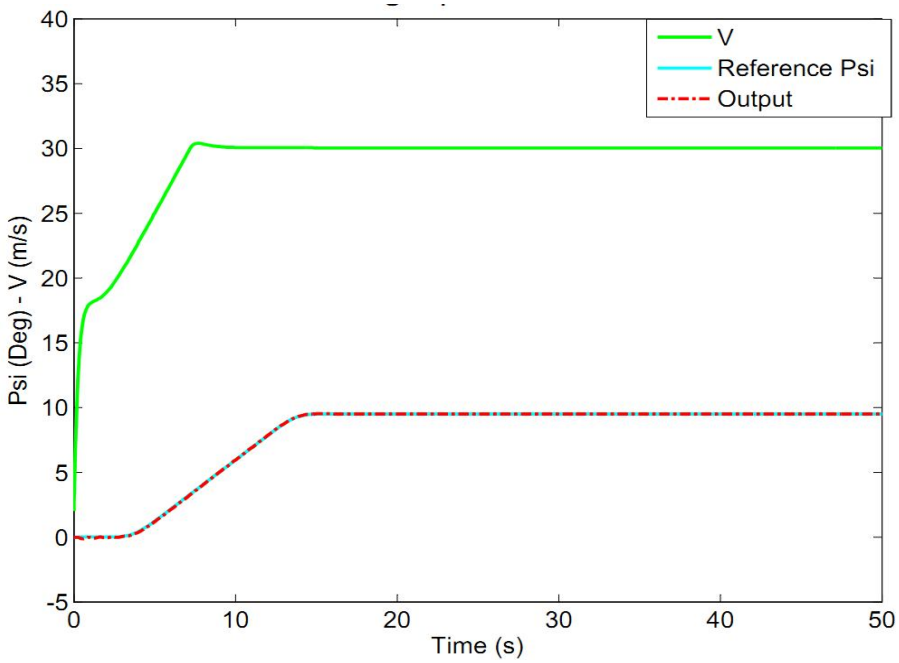

Figure 7.14 d: Psi-V Autopilot Response Example 4 (With Command Filter)

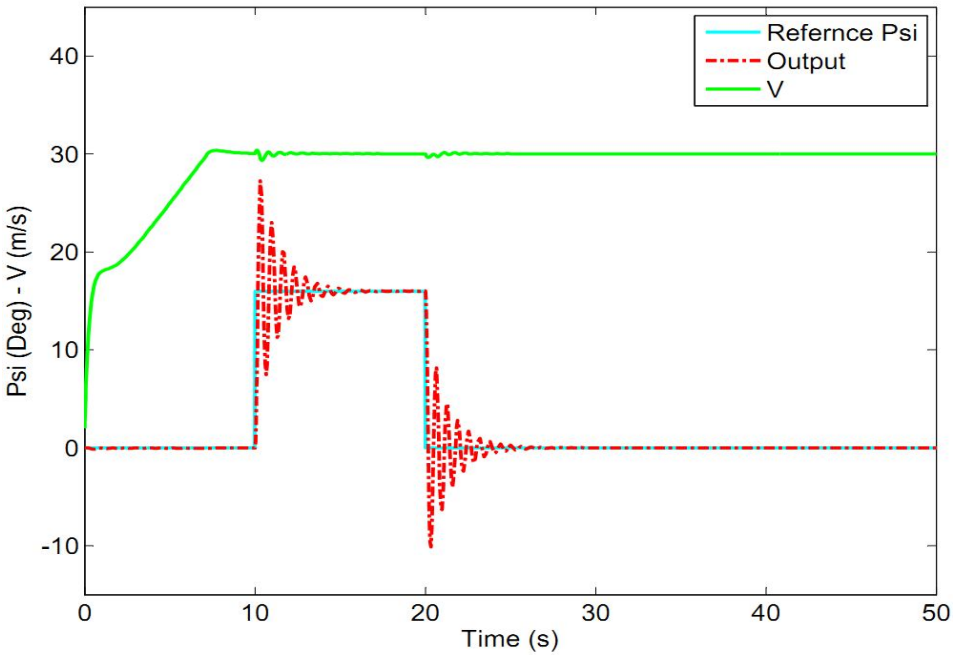

Figure 7.14 e: Psi-V Autopilot Response Example 5 (Without Command Filter)

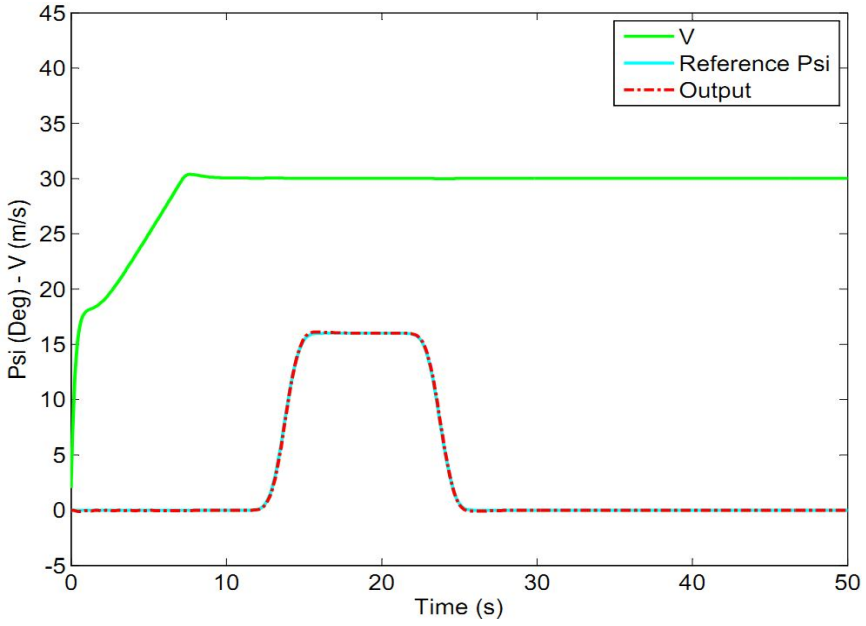

Figure 7.14 f: Psi-V Autopilot Response Example 6 (With Command Filter)

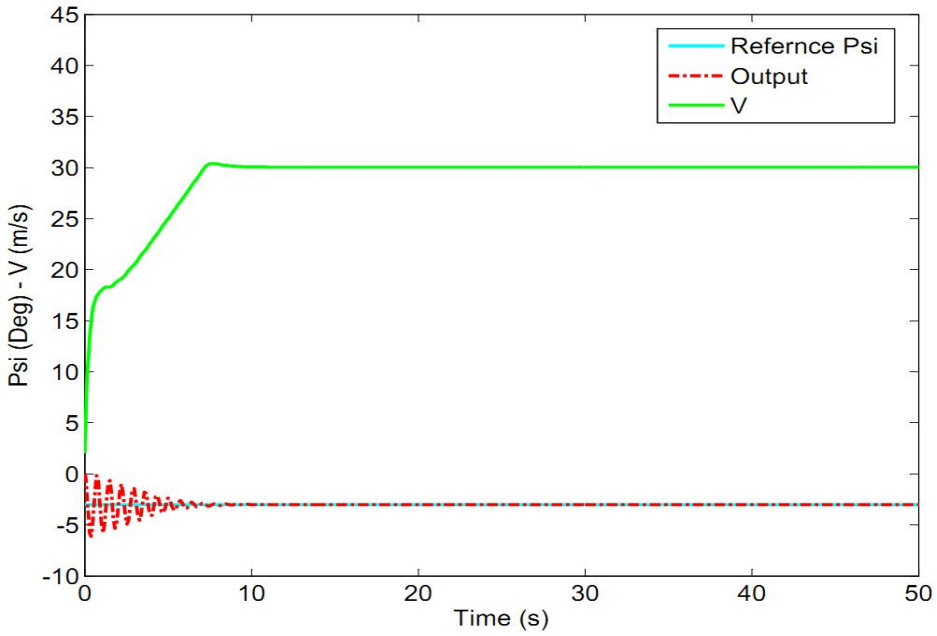

Figure 7.14 g: Psi-V Autopilot Response Example 7 (Without Command Filter)

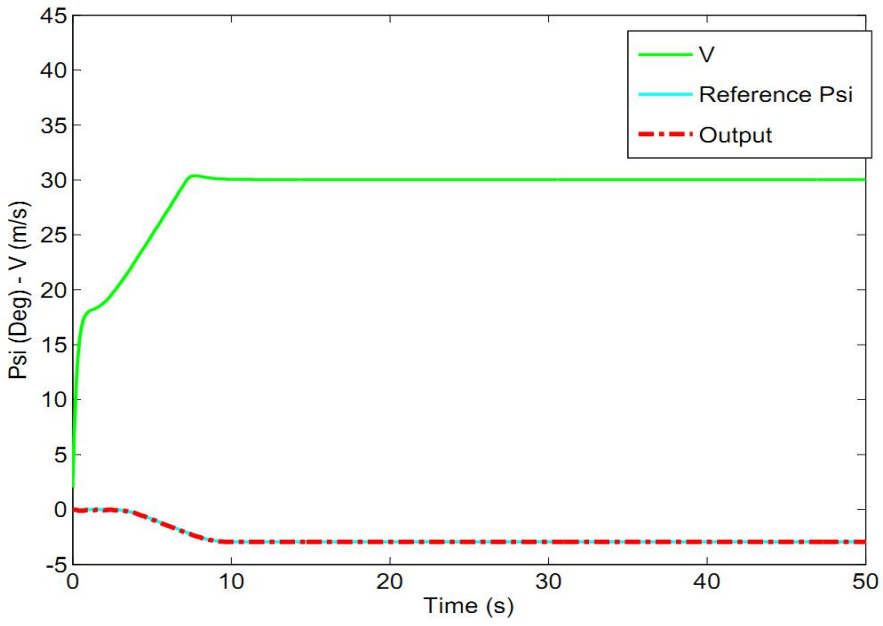

Figure 7.14 h: Psi-V Autopilot Response Example 8 (With Command Filter)

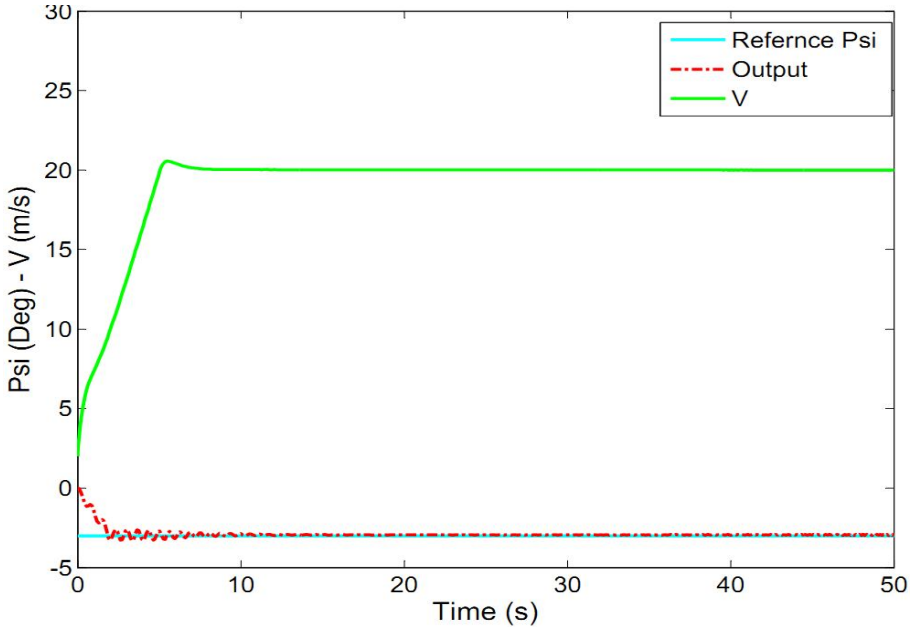

Figure 7.14 i: Psi-V Autopilot Response Example 9 (Without Command Filter)

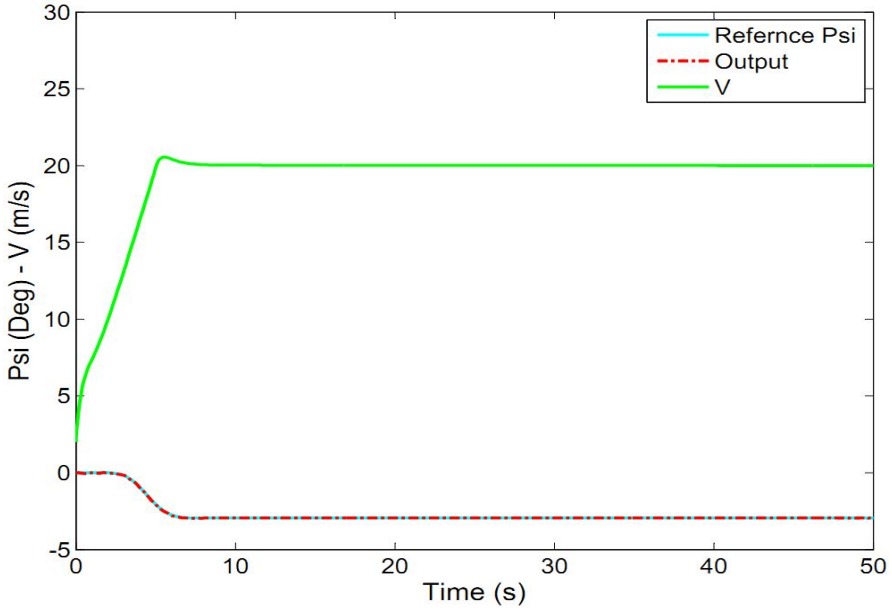

Figure 7.14 j: Psi-V Autopilot Response Example 10 (With Command Filter)

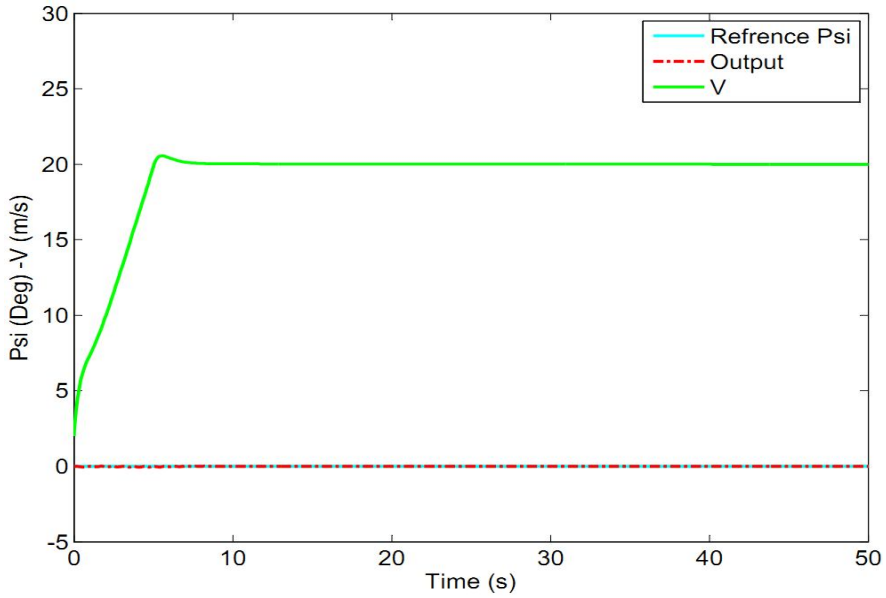

Figure 7.14 k: Psi-V Autopilot Response Example 11

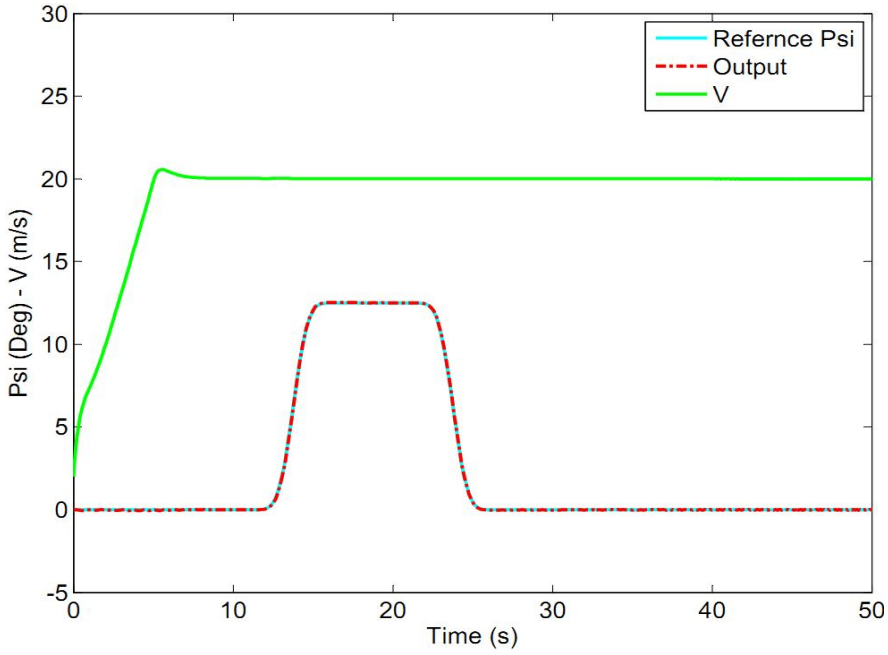

Figure 7.14 l: Psi-V Autopilot Response Example 12 (With Command Filter)

Figure 7.14 Speed and Yaw Autopilot Responses

7.13 Height Hold Controller

Since WIG vehicles are designed to get benefit from GE, they are kept at low heights (low level flight). Flight height (altitude) is the key to determine that either craft is in extreme ground effect or normal GE or out of GE, so height controller is of prime importance.

Design of altitude controller as shown in Figure 7.15, is little bit complicated; it uses different loops. The innermost and the most (important) loop is the PAH loop, because it is one of the main factors for controlling the altitude of the vehicle. Rate of change of altitude ($\dot{H}$) is also fed back. Height hold controller is not only controlling the altitude, but it is also important for other flight conditions and stability purposes. Speed controller loop is also used as the third inner loop.

For each loop, the difference of its reference value with the current state is fed to the respective controller as input. Overall design was efficient enough, because even at low altitude, when system is most sensitive to disturbances, it showed good performance.

Figure 7.15 shows the block diagram of the design. The controller gain values found were $K_{\mathrm{p}} = 0.05$, $K_i = 0.05$, $K_d = 0.0$ for speed (V), and $K_{\mathrm{p}} = -0.1$, $K_i = -0.001$, $K_d = 0.0$ for $\mathrm{H_{dot}}$ and $K_{\mathrm{p}} = -6$, $K_i = -1.2$, $K_d = 0.005$ for H (altitude) controller.

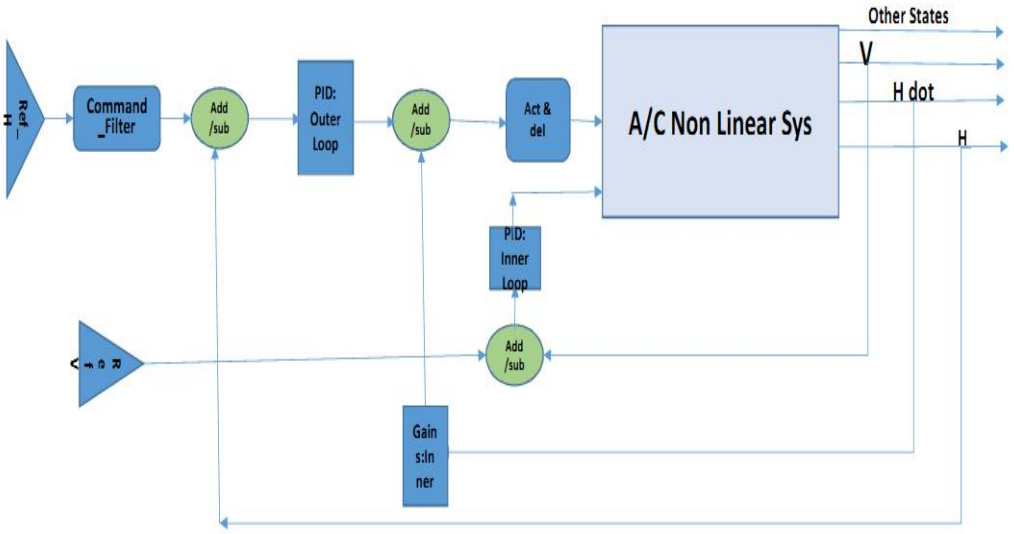

Figure 7.15 Block Diagram for Altitude Controller

Different inputs were given and response of the control system was tested. It gave satisfactory results. Figure 7.16 shows the results for different inputs.

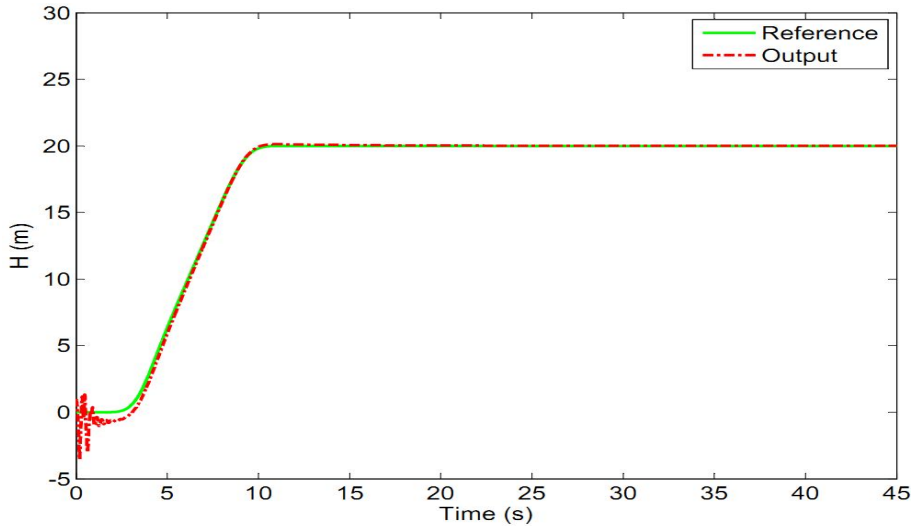

Figure 7.16 a: Altitude Controller Response Example 1 (With Command Filter)

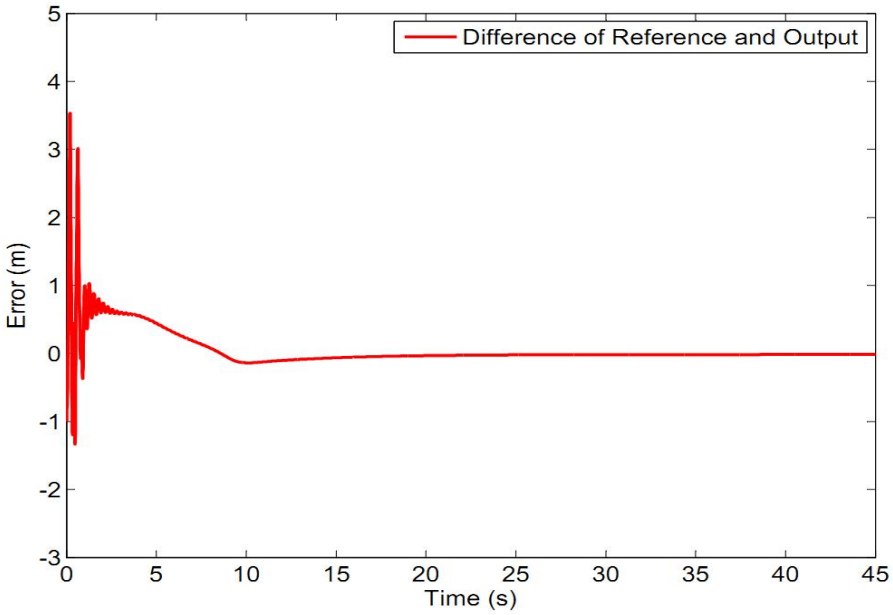

Figure 7.16 b: Error in case of Altitude Controller Example 1

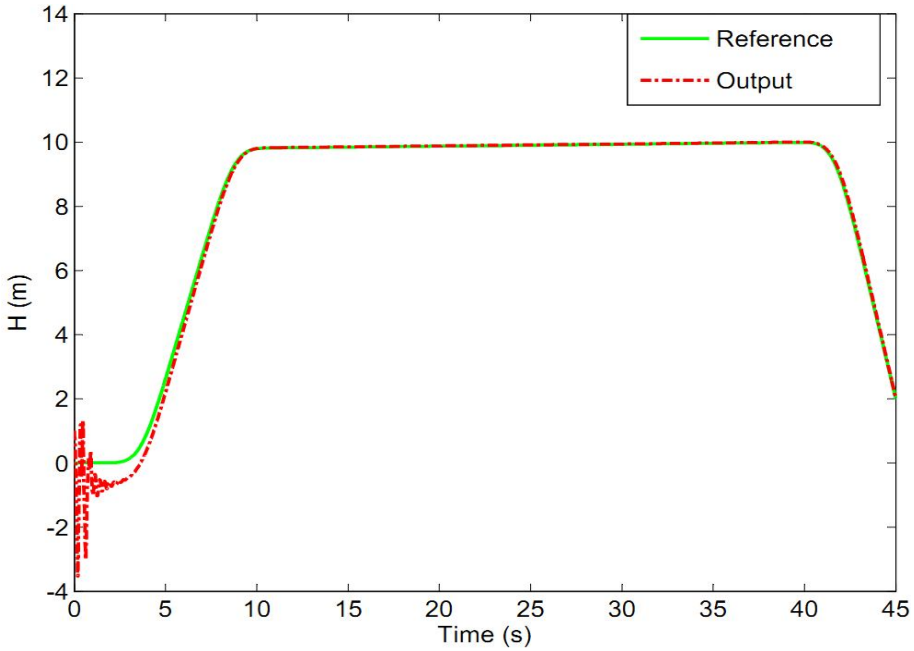

Figure 7.16 c: Altitude Controller Response Example 2 (With Command Filter)

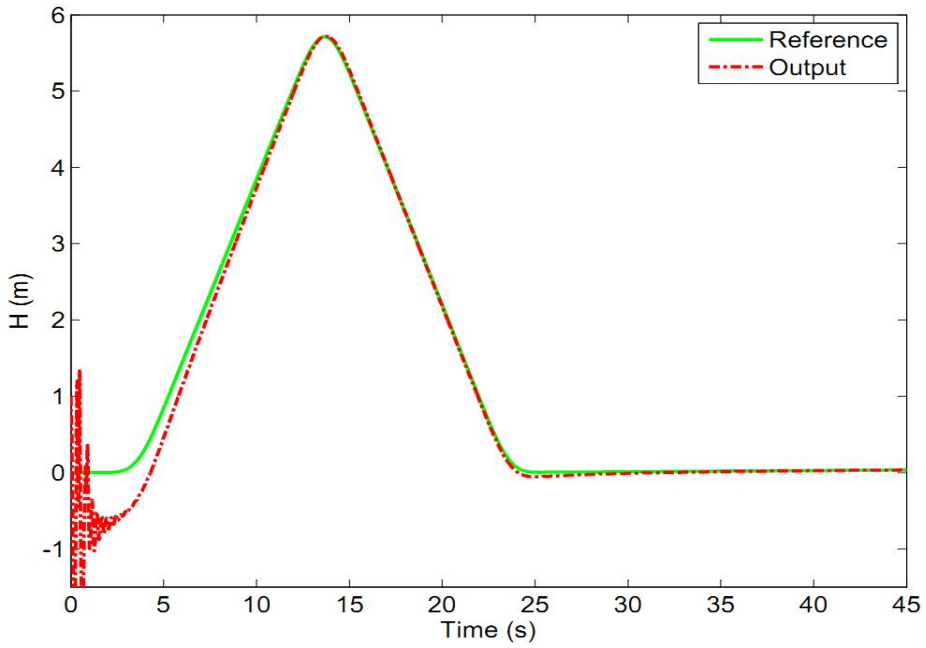

Figure 7.16 d: Altitude Controller Response Example 3 (With Command Filter)

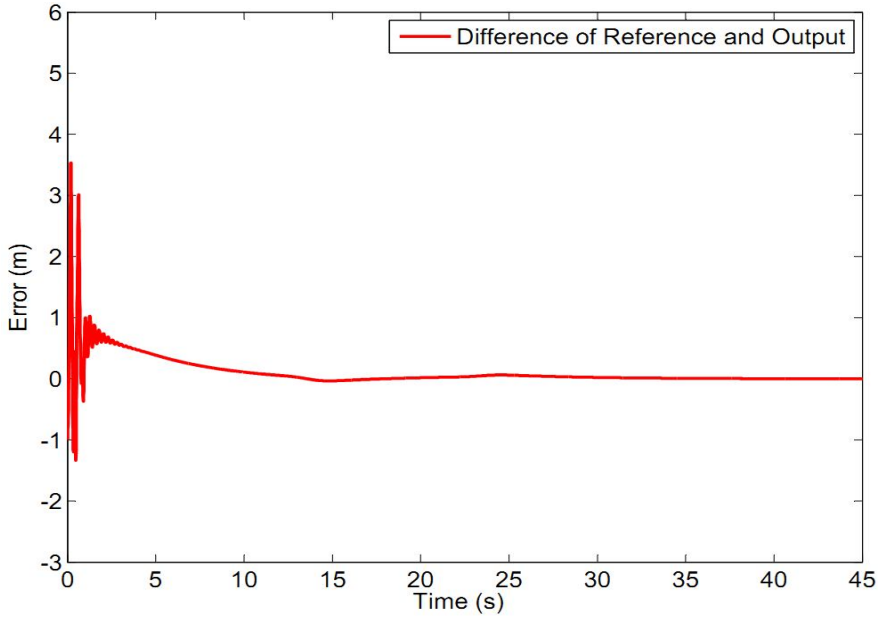

Figure 7.16 e: Error in case of Altitude Controller Example 3

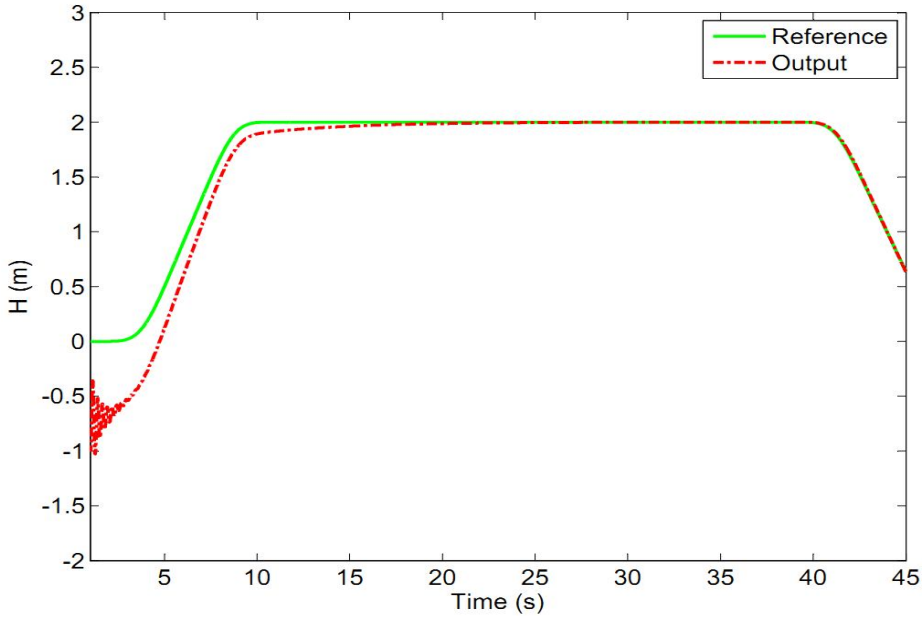

Figure 7.16 f: Altitude Controller Response Example 4 (With Command Filter)

Figure 7.16 Altitude Hold Mode Responses

CHAPTER 8

GUIDANCE

This last chapter is about the development and implementation of a guidance algorithm for WIG vehicles. It can be considered as the second part of the autopilot development. It determines the reference values for the controllers to follow. Usually guidance is implemented in two parts separately, one for the horizontal plane plane (XY plane) and one for the vertical plane (XZ plane). Here, guidance is implemented only for the horizontal plane (heading) so that it can reach any point independently in XY plane. Guidance is done by line of sight through Way Points (WPs). It can also be implemented for the vertical plan on the basis of the same principles, but there is no need for it because WIG is a special craft and it will stay at a low altitude, so it will just cause computational delay, because any kind of flight operation can be accomplished without it. It is been discussed in detail in this chapter. In this regard references [60], [62] and [63] are useful.

8.1 Brief Introduction and Different Available Techniques

Guidance is the method (algorithm) used to pilot (navigate) the vehicle from one state (position) to another. It is called the pilot of the aircraft, when controls are added; it becomes the “AUTOPILOT”. Guidance takes information and data from sensor and navigation, and processes this data and determines where it is at the moment and where to head for the target to reach.

Many different kinds of guidance techniques and algorithms are available, and their selection depends on the dynamics of system and requirements of the operation. These techniques can be broadly divided into two main categories:

i- Online

ii- Offline

In offline methods, all autopilot commands and information are already generated and available before the flight. Fully defined path is there, during operation or flight, it just sufficient to follow the given path. But in online guidance, some information like way point vectors are already available, but it makes use of the current position and available data to find its target and destination step by step, during the flight. After having current information about the system and target position, guidance system generates commands for the controller, to be executed by the autopilot. In any case, guidance serves the controller by generating references for it.

Guidance input can be in the form of speed, pitch, altitude and yaw commands. Since autopilot realizes commands from the guidance, guidance outputs should be appropriate and feasible. The relations between different parts are shown below.

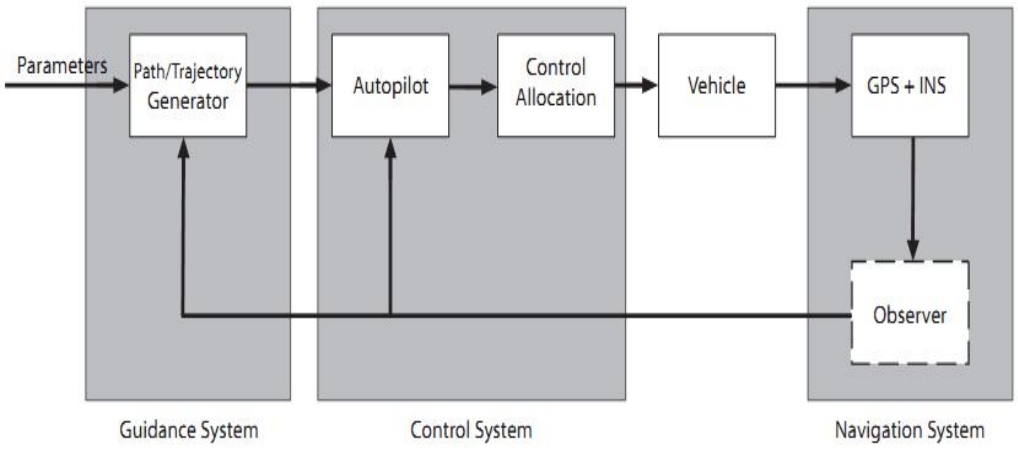

Figure 8.1 GNC Blocks [60]

Some of the available techniques are given below:

- Way Point Guidance by Line-of-Sight (LOS).
- Lyapunov Based Guidance.
- Electromagnetic Guidance.
- Vision Based Guidance.
- Guidance Using Magnetometers for Cable Tracking.
- Guidance Using Chemical Signals.
- Proportional Navigation Guidance (PNG) for AUVs.

It is a common practice to generate a path or trajectory, separately for horizontal (yaw) and vertical (pitch) planes, for unmanned vehicles to follow. Horizontal guidance, which is usually used for finding the heading, destination, masking, obstacle avoidance and threat avoidance, will be mainly focused here. Vertical guidance is for maintaining the height, which is not critical for WIG because it always flies at low altitudes. Even when the vehicle is a small scale craft, it will remain below or within the chord length for getting maximum advantage of GE. So our major concern is the horizontal plane or heading guidance. Here, the method of "Way Point Guidance by LOS" has been adopted.

8.2 Way Point Guidance by Line-of-Sight (LOS)

Way point guidance by LOS is the most commonly used method, since it is easy and simple in structure to implement and very little computation is required. It is usually used for marine vehicles, but is valid for all kinds of unmanned vehicles. In this method, path or trajectory, to be followed, is marked into many points known as Way Points (WPs).

8.2.1 Way Points

These waypoints are defined in a special order (usually sequentially) and form a desired path. They may be defined by their coordinates (x_i, y_i, z_i) or some other parameters like speed at that specific way point, and radius of acceptance can also be added into the description of way points (x_i, y_i, z_i, V_i, R_i), depending on the algorithm and design requirements. These WPs are given before the flight; in other words aircraft knows the positions of the way points before the flight, and it is supposed to follow them one by one and in order (sequentially). When vehicle comes close (within specified accepted range) to a way point, it is considered as the current point and next way point (WP) is activated as the target (to be followed). In this way it follows all WPs one by one until it reaches its destination.

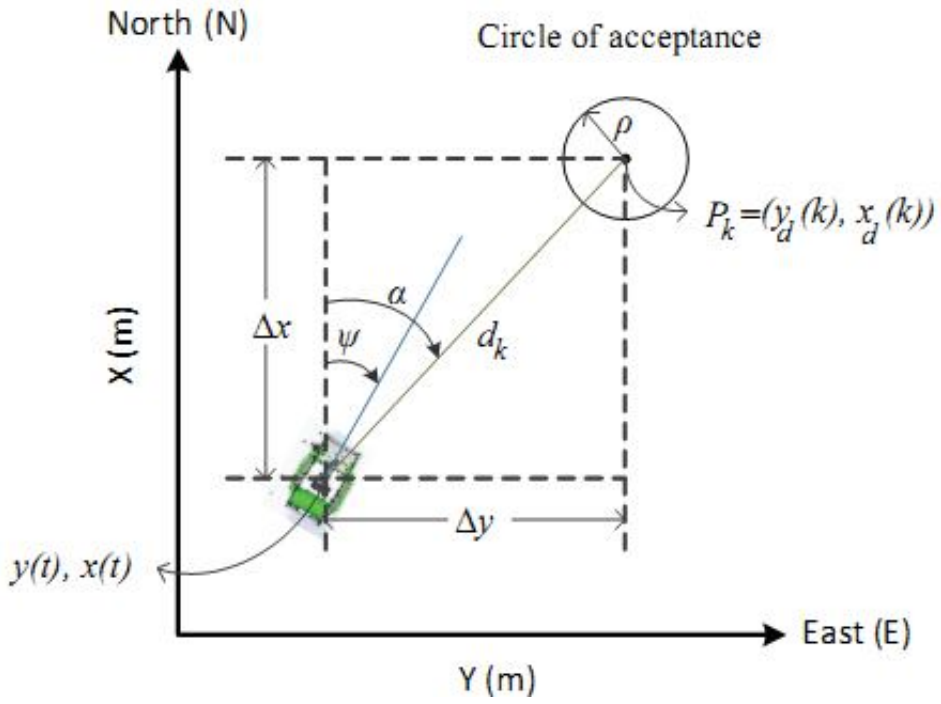

Figure 8.2 Way Point Guidance Overview [44]

8.2.2 Line of Sight Algorithm

Line of sight is generally referred as the straight line between two points. Idea is to define a LOS point between two consecutive WPs. Usually the first point is the current WP like P_k and the next point can be either a point (known as LOS set point), or in some cases, it can be the next WP, P_{k+1}. This vector, from the vehicle's current position to LOS set point, is the LOS vector and it becomes the course of the craft. There are different ways for finding this set point, but the method which is adopted in this study is called "Enclosure Circle Method". In this enclosure based technique, a radius R, encircling the vehicle, is drawn to find the set point (LOS set point). This, LOS set point, is chosen from one of the two intersection points, which are formed on the straight line between the point Pk and Pk+1, where this circle cuts it. This selection depends on the orientation of the way point. In this way, vehicle is moving from point Pk to Pk+1, by these set points. It is explained in detail in [60] and [61].

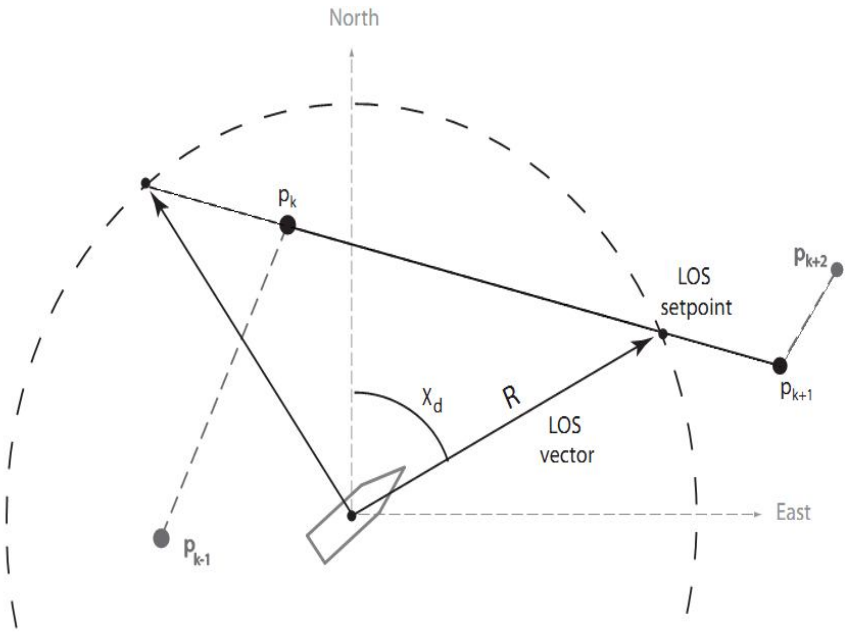

Figure 8.3 Enclosure Circle Method to Find LOS Set Points [45]

Derivation of its equations is very simple. Assuming that currently it is at position p(t) = [x(t), y(t)]' and the set point is found as [x(los), y(los)]', then simply by using the trigonometric relations

$$\tan(\chi_d(t)) = \frac{\Delta y(t)}{\Delta x(t)} = \frac{y_{los} - y(t)}{x_{los} - x(t)} \qquad (8.1)$$

So, the heading angle can be found as

$$\chi_d(t) = atan2\,(\,y_{los} - y(t), x_{los} - x(t)\,) \qquad (8.2)$$

8.2.3 Following LOS by Enclosure

Assume that current position of vehicle is at p(t) = [x(t),y(t)]' and consider a circle of radius R. Assuming R is large enough, it intersects the line between P_k and P_{k+1} at two points, as shown in Figure 8.3. The purpose is to drive the vehicle (velocity) to the chosen auxiliary (set point) [x (los), y (los)]', so that the difference (error) can be made zero between these two points. This position (orientation) of the set point [x(los), y(los)]', can be determined using trigonometric equations. One of these two points is chosen as the next way point.

The derivation of these formulae is given in [60], [62].

$$y_{los} = \frac{\Delta y}{\Delta x}(x_{los} - x_k) + y_k \qquad (8.3)$$

$$a = 1 + \left(\frac{\Delta y}{\Delta x}\right)^2$$

$$b = -2x(t) - 2x_k\left(\frac{\Delta y}{\Delta x}\right)^2 + 2y_k\left(\frac{\Delta y}{\Delta x}\right) - 2y(t)\left(\frac{\Delta y}{\Delta x}\right)$$

$$c = x(t)^2 + y(t)^2 + x_k^2\left(\frac{\Delta y}{\Delta x}\right)^2 + y_k^2 - 2y_k x_k\left(\frac{\Delta y}{\Delta x}\right) + 2y(t)x_k\left(\frac{\Delta y}{\Delta x}\right) - 2y(t)y_k - R^2$$

(8.4)

Now, one of the solutions is to be chosen from the two; this is done on the basis of its distance from the target point. As it is obvious, the one which is closer to the target

way point (next WP) will be chosen. If the vehicle has not yet reached the radius of acceptance, selection criterion is as follow:

$$\begin{aligned} x_{los} &= \frac{-b+\sqrt{b^2-4ac}}{2a} && if\ \Delta x > 0 \\ x_{los} &= \frac{-b-\sqrt{b^2-4ac}}{2a} && if\ \Delta x < 0 \end{aligned} \qquad (8.5)$$

If $\Delta x = 0$, then,

$$x_{los} = x_k = x_{k+1}$$

$$y_{los} = y(t) + \sqrt{R^2 - (x_{los} - x(t))^2} \qquad \text{if } \nabla y > 0$$

$$y_{los} = y(t) - \sqrt{R^2 - \left(x_{los} - x(t)\right)^2} \qquad \text{if } \nabla y < 0 \qquad (8.6)$$

After having the orientation of the set point [x(los), y(los)], heading angle can be calculated from Equation 8.2.

8.2.4 Switching From One Way Point to Another

As was described before, the strategy adopted here is such that all WPs are followed one by one, until the vehicle reaches its destination. Vehicle follows these WPs sequentially; when it is on its course, one of the WP which is within the radius of acceptance (current WP) is active and the next is the target. When it reaches the next one, it becomes active and the point after the next one is set as the target. This switching between WPs (from one to another) is very important and is the basic step in vehicle motion. For this purpose a circle of acceptance is assigned to each WP, so that when the vehicle comes within that radius (circle) of acceptance, it becomes current position and the next one is set as the target. From onboard navigation (instrumentation) system, current position p(t) = [x(t), y(t)]' is available all the time. So, it can be easily checked that whether the vehicle is within the radius of acceptance or not, from

$$(x_{k+1} - x(t))^2 + (y_{k+1} - y(t))^2 \leq R_{k+1}^2 \qquad (8.7)$$

In Equation 8.7, target WP is considered at p(k+1) = [x(k+1), y(k+1)]' εR^2 and the current p(t) = [x(t), y(t)]'εR^2 represents the position of the vehicle at time t. There are different ways and criterion to determine the radius of acceptance. These WPs are generally in proper order such that once vehicle enters the radius of acceptance of the targeted WP, P_{k+1}, the next P_{k+2} from the list will be set as the target. To avoid deceleration and other problems, special precautions or care is to be taken for the last WP. In real life, it is usually switched to manual pilot a bit before reaching the final WP, so that it can be stopped properly, [60] and [63].

8.2.5 Missed Waypoint Detection

When vehicle bypasses the radius of acceptance of a WP, that one is called as a missed WP. There can be various reasons for this missing, such as disturbances, noise or vehicle dynamics and maneuverability. This missing causes the consumption of extra time and energy. To avoid this, its detection is important. The simple strategy to detect this missing is the check on the range between the vehicle and WP. It is obvious that range should always be decreasing between the craft and the target point, if it is approaching in the right direction. But if range starts increasing, it means a WP has been missed. So, if the range starts to increase, it means that a WP is missed and an alternative strategy must be adopted.

8.2.6 Speed Check

It is also a wise strategy to specify the speed of the vehicle for each WP for making sure about feasibility of the path and to avoid acceleration and inertia problems, especially when turns are sharp. This speed check can be determined on the basis of WPs positions and distance and angle of sharpness towards the next WP. Here, desired speed has been set as a function of angle between the previous P_{k-1}, the current P_k and the next P_{k+1} WPs, [60] and [64]. Consider the Equation 8.8:

$$\alpha_k = atan2(\|u_k \times u_{k+1}\|, u_k \cdot u_{k+1}) \qquad (8.8)$$

where u_k = [x(k), y(k)]' and u_{k+1} = [x(k+1), y(k+1)]'. So, the reference or desired velocity can be expressed as:

$$v_{ref}(\alpha_k) = v_{min} + (v_{max} - v_{\min})e^{-\frac{\alpha_k^2}{\sigma^2}} \qquad (8.9)$$

where v_{min} and v_{max} can be set an the upper and lower bounds.

8.2.7 Radius of Acceptance

Different methods have been defined to determine the radius of acceptance, such as the strategy just to take the radius of acceptance (RoA) to be between 1.5 to 3 times of the length of the vehicle. Sometimes it is determined on the basis of P_{k-1}, P_k and P_{k+1} points. Another way is to determine wrt. the turn radius (curvature of turn) for smooth turns as

$$R = \frac{V^2}{g \tan(\emptyset)} \qquad (8.10)$$

Another and one of the comprehensive ways, is to find this radius on the basis of angle between consecutive points.

$$R(\alpha) = R_{max} - (R_{max} - R_{min})e^{-\frac{\alpha^2}{\sigma_R^2}} \qquad (8.11)$$

This algorithm was chosen and it was implemented in the horizontal plane.

8.3 Implementation in YAW Plane

All of defined algorithms and formulations, in previous sections of Chapter 8, were implemented for the horizontal plane to find the reference yaw angle for the WIG vehicle. Exactly the similar approach can be implemented for the vertical plane, even for 3D motion of the vehicle. Here, for WIG, it has been implemented only for the

yaw plane, because of obvious reasons, that WIG will remain at low altitudes and it can even complete mission without vertical guidance. Vertical input can be manually adjusted since it is in a very narrow range.

Implementation was successful and it provided satisfactory results. Some of them are shown in the following figures:

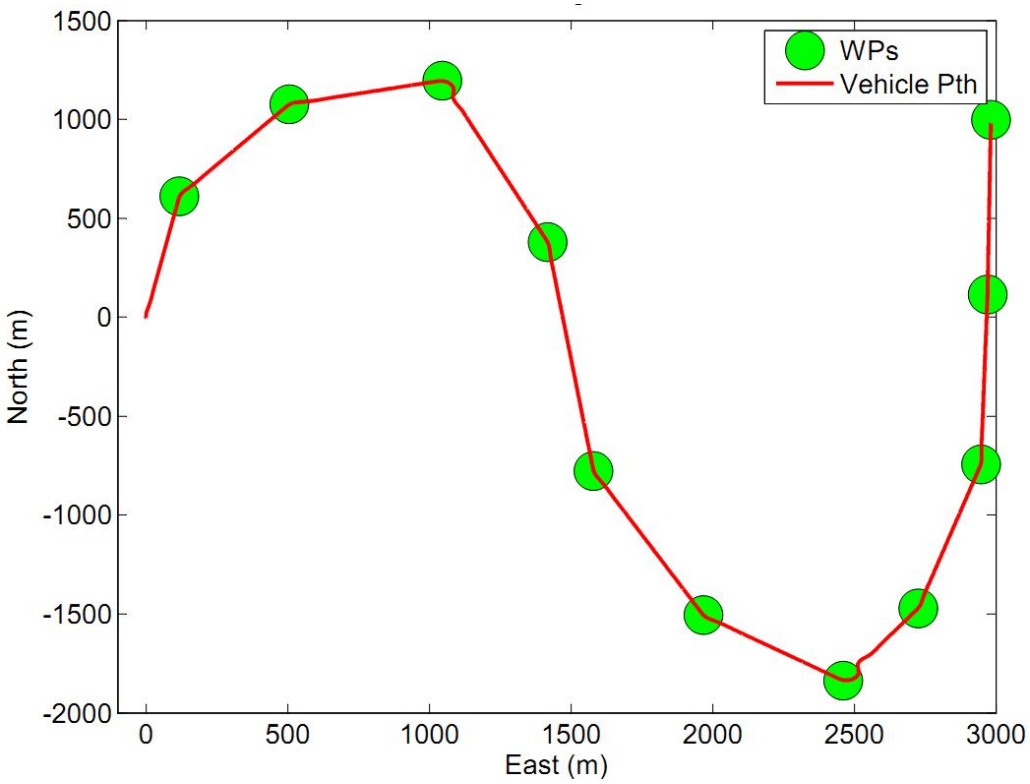

Figure 8.4 a: Guidance (Path Following) Example 1

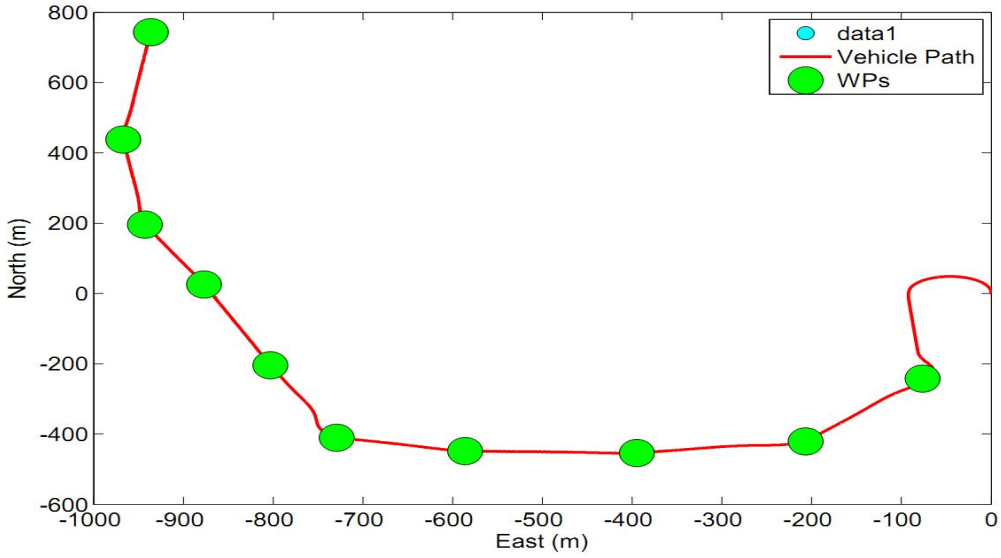

Figure 8.4 b: Guidance (Path Following) Example 2

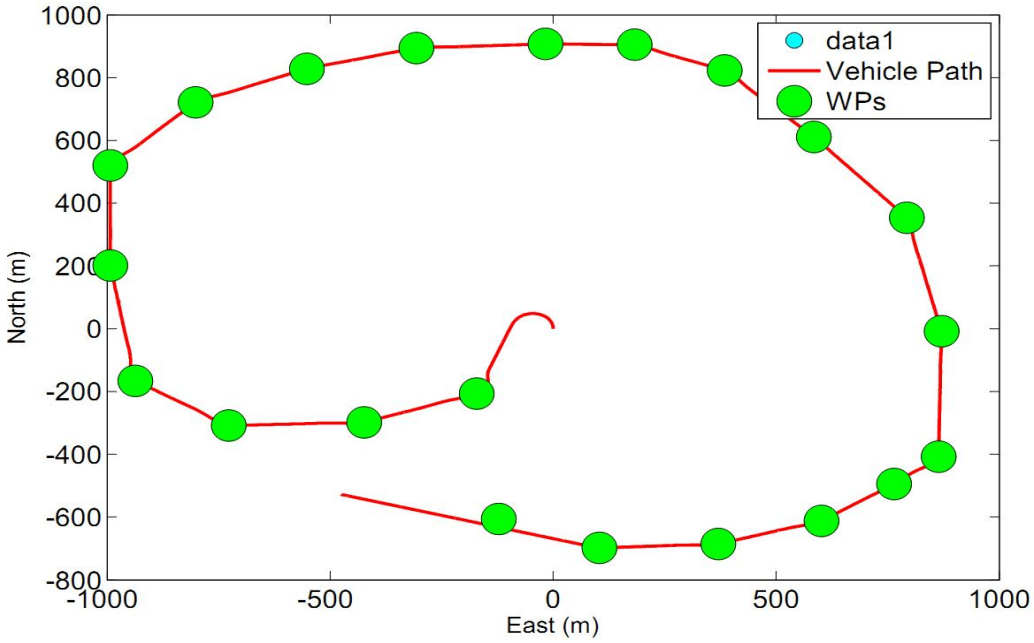

Figure 8.4 c: Guidance (Path Following) Example 3

Figure 8.4 Guidance (Path Following) Examples

CHAPTER 9

CONCLUSION/FUTURE WORK

In this part there are some conclusions and some recommendations are suggested after this experience of studying on WIG vehicles. The prime purpose was to model the ground effect in a unified way and design a controller for a WIG vehicle. WIG vehicles are more efficient vehicles than other aircrafts and surface vehicles. They have a vast scope of civil and military applications.

Initially different configurations/structures were chosen for vehicle design for its wing, horizontal and vertical stabilizers and fuselage. These selections were done after an extensive study of aerodynamics, so that GE can be utilized in a better way. After these selections, the geometrical design was implemented in Solidworks to have a better idea about vehicle body and to determine its geometric, mass and inertial elements. CAD design is also useful for determining its aerodynamics.

DATCOM was used for determining aerodynamics and stability derivatives for the WIG. Its outputs are given in the modeling parts of Chapter 5. Ground effect was studied in detail, its formulations were found for both span dominated and chord dominated GEs. These GE formulations were added in the vehicle model.

After the completion of determining GE study, its complete mathematical model was obtained. This model is a dynamical model with 6DOF. All external forces including aerodynamics, ground effect, propulsion and gravity and their moments were determined and were used for 12 ODEs of the state variables. These 12 ODEs describe the motion of the vehicle. Different atmospheric elements were also taken into account. This model was implemented in Matlab/Simulink. Matlab/Simulink provides

a good platform for the experimental work for design analysis. System was analyzed for different inputs. Open loop responses, with and without disturbances were checked. Different equilibrium points were determined using “trim function” and system was linearized around those trim points. This linearization was done using “Linear Analysis Utility”. This linear model can be used in different ways, for determining eigenvalues, obtaining the frequency response and for designing a controller.

Next, simple controllers were developed and implemented for pitch, yaw, roll, speed and altitude/attitude holds. PID controllers were used. Pitch and roll are controlled by elevators and ailerons, respectively, while speed and yaw are controlled by two thrusters. Pitch and roll controllers consist of two loops, one inner loop for their rate controls and one outer main loop for their angle controls, to follow a reference value. For speed control and heading (yaw) control separately, single loops are used. Since both are dependent on the same source, a controller for both of them together is also developed with a double loop, to control them (make them follow different reference values) at the same time. Similarly for altitude hold mode, three loops were used, one innermost loop for speed, second outer loop for H_{dot} (rate of change of height) and third, outermost loop for the altitude itself. These controllers were tested for different inputs and they provided excellent results.

Finally guidance was done by using LOS techniques through Way Points. These way points are defined before the flight and guidance algorithm is developed in such a way that vehicle can reach a target point autonomously by following those WPs sequentially. Guidance is designed for the horizontal frame only, since there is no need for vertical plane guidance in case of WIG. This study is finished with satisfactory results from the guidance part. All of this work was done in a virtual environment using Matlab/Simulink, since this vehicle has not been manufactured/fabricated yet.

Although the given task is achieved, still a lot needs to done for further development. Here are some suggestions/recommendations for future work. This work has only considered aerodynamic parts (as aircraft) with ground effect. One more feature which can be added in future is to deal with hydrodynamics; in this way the vehicle will be able to sail on the surface of sea. It means it can act as an aircraft and as a marine

vehicle at the same time. This design was done keeping in mind all these possibilities. That is the reason of why fuselage is based on “Catamaran Empennage Configuration” and winglets are also added at wingtips, because they provide a lift as well as thrust, when vehicle goes on the sea surface.

Other improvements that can be done later are verifying its aerodynamics by wind tunnel methods or by CFD. DATCOM, which was used here, provide a good initial value for aerodynamics and stability derivatives but there is always a need to modify them, which can be done after some experimental work or by using the techniques mentioned above.

Another thing that can be added is to replace these classical controllers with modern robust ones; because they are more effective in the presence of uncertainties and noise. In controllers, MIMO mode can also be added, so that all the states can be kept in control at the same time.

Finally it can be concluded that this study was a good start to provide a unified platform for small scale WIG vehicles, their autopilot development and testing its performance. WIGs or GEVs are useful vehicles and can fill the gap between aircrafts and marine vehicles. It is strongly recommended to extend this study to a further broader level and to bring it into practical uses.

REFERENCES

[1] http://www.ikarus342000.com/INTRO3.htm, (Last Accessed on August 10, 2015).

[2] C. Wieselsberger, “Wing Resistance near the Ground”, NACA TM No. 77, 1922.

[3] L. Prandtl, “The Induced Drag of Multiplanes”, NACA TM No.182, 1924.

[4] http://www.imo.org/en/Pages/Default.aspx, (Last Accessed on September 01, 2015).

[5] L. Bennet, A. Frank, R. Moreton, S. Wong, M. Thomas, R. Samuel, “Wing in Ground Effect (WIG) Aerodynamics”, M.Sc. thesis, The University of Adelaide, Australia, 2009.

[6] A.V. Nebylov, R. Alexander, S. Sukrit, "Comparative Analysis of Design Variants for Low Altitude Flight Parameters Measuring System", 17th IFAC Symposium for Automatic Control, part 1, vol. 17, pp. 663-668, 2007.

[7] http://www.hovercraft.com, (Last Accessed on July 01, 2015).

[8] S. Hirdaris, M. Guerrier, "Technology Developments in Ground Effect Craft", 2nd Annual Ship Tech Dubai Release, 8–9 November, 2009.

[9] L.Y. Young, "Speech at the Christening of the Wing-In-Ground Craft, Airfish 8-001", Harbor and Port Authority of Singapore Press Release for the Christening of M/V Airfish8, April, 2010.

[10] http://www.eng.nus.edu.sg/ero/news/index.php?id=718, (Last Accessed on June 06, 2015).

[11] http://www.wingship.com, (Last Accessed on June 07, 2015).

[12] K.V. Rozhdestvensky, "Wing in Ground Effect Vehicles", Progress in Aerospace Science, vol. 42, pp. 211-283, 2006.

[13] L. Yun, A. Bliault, J. Doo, "WIG Craft and Ekranoplan", Springer MARIC, vol. 1, 2010.

[14] J. Roskam, "Layout Design of Cockpit, Fuselage, Wing and Empennage: Cutaways and Inboard Profiles", Part 3, vol. 4, DAR Corporation Kansas, 2004.

[15] J. Roskam, "Preliminary Sizing of Airplanes", Part 1, vol.3, DAR Corporation Kansas, 2004.

[16] M.R. Ahmed, S.D. Sharma, "An Investigation on the Aerodynamics of a Symmetrical Airfoil in Ground Effect, Experimental Thermal and Fluid Science", The Scientific World Journal, vol. 1, no. 4898, pp. 47-54, 2004.

[17] http://airfoiltools.com/airfoil/details?airfoil=naca4412-il, (Last Accessed on January 12, 2015).

[18] D.E. Calkins, "Feasibility Study of a Hybrid Airship Operating in Ground Effect", Journal of Aircraft, vol. 14, no. 8, pp. 809-815, August 1977.

[19] R.C. Nelson, "Flight Stability and Automatic Control", McGraw-Hill, 2nd ed., 1998.

[20] H.H. Chun, C.H. Chang, “Longitudinal Stability and Dynamic Motions of a Small Passenger WIG craft”, Ocean Engineering, vol. 29, no. 10, pp. 1145-1162, August 2002.

[21] http://airfoiltools.com/airfoil/details?airfoil=n63012a-il, (Last Accessed on January 10, 2015).

[22] K.V. Rozhdestvensky, “Aerodynamics of a Lifting System in Extreme Ground Effect”, 1st ed., Springer Verilog, pp. 63-67 & pp. 263-280, 2000.

[23] J.D. Anderson, “Fundamentals of Aerodynamics”, 3rd ed., McGraw-Hill, 2001.

[24] C. Wieselsberger, “Wing Resistance near the Ground,” NACA TM No. 77, 1922.

[25] I. Tani, T. Masuo, S. Simidu, “The Effect of Ground on the Aerodynamic Characteristics of a Monoplane Wing”, Rep. No. 150, vol. 8, Aero. Res. Inst., Tokyo Imperial Univ., September 1937.

[26] I. Tani, H. Itokawa, T. Masuo, “Further Studies of the Ground Effect on the Aerodynamic Characteristics of an Aero Plane with Special Reference to Tail Moment”, Rep. No. 158, vol. 8, Aero. Res. Inst., Tokyo Imperial Univ., November 1937.

[27] J.W. Wetmore, L.I. Turner, “Determination of Ground Effect from Test of a Glider in Towed Flight”, NACA TM No. 01-ADA301227, 1949.

[28] M. LeSueur, “Ground Effect on the Take-Off and Landing of Airplanes”, NACA TM No. 771, 1935.

[29] L. Prandtl, “The Induced Drag of Multiplanes”, NACA TM No.182, 1924.

[30] R.V. Mises, “Theory of Flight”, Dover Publications, 1st ed., pp. 243, 1959.

[31] D.C. Richard, W.M. Olson, “Ground Effect Determination of a Piper Comanche”, AIAA Atmospheric Flight Mechanics Conference, vol. 1, no. 5316, pp. 178-193, 2003.

[32] N.D. En, N.G. Hean, Y.S. Quah, T.B. Whye, L. Gerarad, “Wing in Ground Effect (WIG) Vehicle”, Aeronautical Engineering Group, National University of Singapore 2001.

[33] Z. Zong, H. Liang, L. Zho, “Lifting Line Theory for Wing-In-Ground Effect in Proximity to a Free Surface”, Springer: Journal of Engineering Mathematics, vol. 74, no. 10, pp. 143-158, 2011.

[34] J.L. Boiffier, “The Dynamics of Flight: The Equations”, John Wiley & Sons, vol. 1, August 24, 1998.

[35] B. Etkin, “Dynamics of Flight; Stability and Control”, John Wiley and Sons, 2nd ed., 1982.

[36] P.H. Zipfel, “Modeling and Simulation of Aerospace Vehicle Dynamics”, AIAA Education Series, 2nd ed., 2007.

[37] E.L. Duke, R. Antoniewicz, D. Krambeer, “Derivation and Definition of a Linear Aircraft Mode”, NASA Science and Technical Information Division USA, reference no. 1207, 1988.

[38] http://www.pdas.com/datcom.html, (Last Accessed on December 12, 2014).

[39] Properties of the U.S. Standard Atmosphere 1976, http://www.pdas.com/atmos.html, (Last Accessed on November 19, 2014).

[40] H. Akimoto, S. Kubo, “Canard Type Wing-In-Surface-Effect-Ship”, International Journal of Aerodynamics: The 1st International Symposium on WIG Crafts Seoul, Korea, vol. 10, no. 55, pp. 55-65, 2005.

[41] G.H. Ng, “AM90 Wing in Ground (WIG) Aircraft-Aerodynamics”, M.Sc. thesis, National University of Singapore, 2005.

[42] P. Anna, “Robust Controller Design for a Fixed Wing UAV”, M.Sc. thesis, Middle East Technical University, September 2009.

[43] R. Marc, “Flight Dynamics and Control Analysis: A Simulink Toolbox”, Dutchroll Production Distributed via Internet, 2001.

[44] C.Y. Fırat, “Autopilot and Guidance Design for Mini ROV”, M.Sc. thesis, Middle East Technical University, September 2012.

[45] J.M. Tor, “Way Point Following Guidance Based on Feasibility Algorithms”, M.Sc. thesis, Norwegian University of Sciences and Technology, June 2011.

[46] L.P. Charles, R.D. Harbor, “Feedback Control Systems”, Prentice Hall, 1991.

[47] H. Özbay, “Introduction to Feedback Control Theory”, CRC Press, 1st ed., 2000.

[48] K.J. Astrom, T. Hagglund, “Advanced PID Control”, Dover Publication: International Society of Automation, 4th ed., 2006.

[49] D. Sellers, "An Overview of Proportional Plus Integral Plus Derivative Control and Suggestions for Its Successful Application and Implementation", ESL: International Conference for Enhanced Building Operations, May 2007.

[50] A. Visioli, “Practical PID Control”, Springer-Verlag: Advances in Industrial Control, 1st ed., 2006.

[51] J. Karl, T. Hagglund, “Advanced PID Control”, Dover Publication: International Society of Automation, 3rd ed., 2006.

[52] J. Karl, T. Hagglund, “Automatic Tuning of PID Controllers”, Dover Publication: International Society of Automation, 2nd ed., 1988.

[53] A. O’Dwyer, “Handbook of PI and PID Controller Tuning Rules”, Imperial College Press London, 2003.

[54] M. Morari, M. Zafiriou, E. Zafiriou, “Robust Process Control”, Prentice Hall, AlChe Journal, Facsimile ed., 1989.

[55] C. Yu, “Auto Tuning of PID Controllers: A Relay Feedback Approach”, Springer: International Journal of Adaptive Control and Signal Processing, vol. 14, 5th ed., 2006.

[56] J. Guillermo, D. Aniruddha, S.P. Bhattacharyya, “PID Controllers for Time-Delay Systems”, Birkhauser Boston, 1st ed., 2005.

[57] K.J. Astrom, T. Hagglund, “Advanced PID Control”, Dover Publication: International Society of Automation, 4th ed., 2006.

[58] P.H. Zipfel, “Modeling and Simulation of Aerospace Vehicle Dynamics”, AIAA Education Series, 2nd ed., 2007.

[59] G. Ellis, “Observers in Control Systems: A Practical Guide”, Academic Press, 2nd ed., 2002.

[60] T.I. Fossen, “Handbook of Marine Craft Hydrodynamics and Motion Control”, John Wiley & Sons Ltd., 1st ed., 2011.

[61] M. Caccia, “Autonomous Surface Craft: Prototypes and Basic Research Issues”, IEEE Control and Automation MED’06, 14th Mediterranean Conference, no. 1109, pp. 1–6, 2006.

[62] T.I. Fossen, M. Breivik, R. Skjetne, “Line-of-Sight Path Following of Underactuated Marine Craft”, IFAC Conference on Maneuvering and Control of Marine Crafts, pp. 244-249, 2003.

[63] J. Osborne, R. Rysdyk, “Waypoint Guidance for Small UAVs in Wind”, AIAA InfoTech: Aerospace Conference, no. 6561, pp. 1-12, 2005.

[64] C. Edwards, D. Penney, “Calculus”, Prentice Hall, 6th ed., 2002.